gear TECHNOLOGY®

AUG 2015

Gearing Up!

Get prepped with pre-show coverage of Gear Expo 2015 and the ASM Heat Treating Society Conference & Exhibition

The G 250 / G 450 can be easily equipped with various automation solutions

30

features

technical

Vol. 32, No. 6 GEAR TECHNOLOGY, The Journal of Gear Manufacturing (ISSN 0743-6858) is published monthly, except in February, April, October and December by Randall Publications LLC, 1840 Jarvis Avenue, Elk Grove Village, IL 60007, (847) 437-6604. Cover price $7.00 U.S. Periodical postage paid at Arlington Heights, IL, and at additional mailing office (USPS No. 749-290). Randall Publications makes every effort to ensure that the processes described in GEAR TECHNOLOGY conform to sound engineering practice. Neither the authors nor the publisher can be held responsible for injuries sustained while following the procedures described. Postmaster: Send address changes to GEAR TECHNOLOGY, The Journal of Gear Manufacturing, 1840 Jarvis Avenue, Elk Grove Village, IL, 60007.

NILES
ZE 800
NILES

R&P
PM 750

gear TECHNOLOGY

Vol. 32, No. 6

departments

Cover photo courtesy of the COBO Center

THE GEAR INDUSTRY'S INFORMATION SOURCE

www.geartechnology.com

Buyers Guide: Recently Added

The *Gear Technology* Buyers Guide is your fastest way to find information on gear industry product and services vendors. Check back often, because we're always improving the site and adding new companies to the listings:

MILES

This Month's Highlighted Topics:

Every month we feature two topics from our extensive archive of 31 years of back issues. On the home page you can find a sampling of these key topics, along with links to the archive. Stop by *geartechnology.com* to see this month's featured topics:

- **Gear Noise**
- **Lubrication**

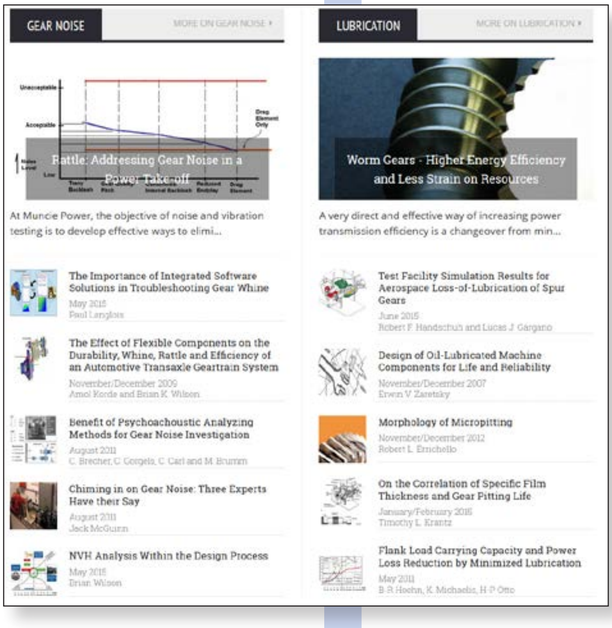

Upcoming Webinar

3M gear TECHNOLOGY LIEBHERR

Register today for 3M's upcoming webinar on advanced grinding technologies. This webinar, presented by *Gear Technology*, will also feature a presentation by Dr. Andreas Mehr of Liebherr Verzahntechnik. The webinar takes place Tuesday, September 22 at 11:00 a.m., but if you sign up now, you'll get an automatic reminder e-mail prior to the event.

www.geartechnology.com/3MWebinar

Stay Connected

Follow us on Twitter
twitter.com/#!/Gear_Technology

Connect with us on LinkedIn
www.linkedin.com/groups/Gear-Technology-Magazine-3893880

Subscribe Online
www.geartechnology.com/subscribe.htm

gear TECHNOLOGY

RANDALL PUBLICATIONS LLC
1840 JARVIS AVENUE
ELK GROVE VILLAGE, IL 60007
(847) 437-6604
FAX: (847) 437-6618

EDITORIAL

Publisher & Editor-in-Chief
Michael Goldstein
publisher@geartechnology.com

Associate Publisher & Managing Editor
Randy Stott
wrs@geartechnology.com

Senior Editor
Jack McGuinn
jmcguinn@geartechnology.com

Assistant Editor
Erik Schmidt
erik@geartechnology.com

News Editor
Alex Cannella

Editorial Consultant
Paul R. Goldstein

Technical Editors
William (Bill) Bradley, Robert Errichello, Octave Labath, P.E., John Lange, Joseph Mihelick, Charles D. Schultz, P.E., Robert E. Smith, Mike Tennutti, Frank Uherek

DESIGN

Art Director
David Ropinski
dropinski@geartechnology.com

ADVERTISING

Associate Publisher & Advertising Sales Manager
Dave Friedman
dave@geartechnology.com

Materials Coordinator
Dorothy Fiandaca
dee@randallpublications.com

China Sales Agent
Eric Wu, Eastco Industry Co., Ltd.
Tel: (86)(21) 52305107
Fax: (86)(21) 52305106
Cell: (86) 13817160576
eric.wu@eastcotec.com

ON-LINE

Digital Content Manager
Kirk Sturgulewski
kirk@geartechnology.com

CIRCULATION

Circulation Manager
Carol Tratar
subscribe@geartechnology.com

Circulation Coordinator
Barbara Novak
bnovak@geartechnology.com

RANDALL STAFF

President
Michael Goldstein

Accounting
Luann Harrold

BPA WORLDWIDE℠ BUSINESS

For the Last 60 Years, We've Never Stopped Learning

Searching for a higher gear-producing IQ? Make the smart choice today.

Your trusted source for 60 Years

FOREST CITY GEAR

11715 Main Street, Roscoe, IL 61073
815-623-2168
www.forestcitygear.com

Smart Move!

GEAR EXPO 2015
THE DRIVE TECHNOLOGY SHOW™

Booth #1826

Experts Work Here

Publisher & Editor-in-Chief
Michael Goldstein

Our goal at *Gear Technology* for the past 31 years has been to bring you the best possible technical information about gear manufacturing. We serve as the industry's educational resource, explaining the technology not only so that you can understand it, but also so that you can make use of it in your gear-related business.

We're serious about making sure that information is reliable, accurate and up-to-date. That's why we have our technical articles reviewed by experts before we publish them. We rely heavily on our roster of technical editors, all of whom have decades of experience solving gear related problems, teaching gear-related classes and seminars, and working with the AGMA to write the standards we all rely upon. Our authors and contributors are without a doubt among the most knowledgeable people in the gear industry. In short, when you're reading *Gear Technology*, you can be sure that you're reading the work of experts.

Nowhere is that more true than in our "Ask the Experts" column. Last issue we announced that we'll be hosting a live, in-person version of that column in our booth (#2030) at Gear Expo in October. We've lined up a panel of experts who should be able to answer almost any question you might have related to gears. So far, those experts include:

- **Dr.-Ing. Nicklas Bylund**, Sandvik Coromant, Manager Engineering Competence Center
- **Dr.-Ing. Andreas Mehr**, Liebherr Verzahntechnik, Technology Development, Grinding and Shaping
- **Dr. Hartmuth Müller**, Klingelnberg, Chief Technical Officer
- **John O'Neil,** Star SU, Engineering Manager-Gear Tools
- **Chuck Schultz,** *Gear Technology* technical editor and Principal, Beyta Gear Service
- **Dr. Hermann J. Stadtfeld**, Gleason Corporation, VP Bevel Gear Technology/R&D
- **Prof. Dr.-Ing. Karsten Stahl**, Technical University of Munich, Head of the Gear Research Center (FZG)
- **Frank Uherek**, Rexnord, Principal Engineer, Gear Engineering Software Development

I'm sure you'll recognize many of these names as regular contributors both to *Gear Technology* and the industry. We're in the process of finalizing the roster and expect another expert or two to round out the panel before the show.

We've tried to organize topics that will be of greatest interest to the largest number of visitors. There will be four sessions at our booth, with appropriate experts sitting on the panel in each session:

- GEAR GRINDING — Tuesday, October 20, 10:30 a.m.
- CUTTING TOOLS — Tuesday, October 20, 2:00 p.m.
- GEAR DESIGN — Wednesday, October 21, 10:30 a.m.
- ASK ANYTHING — Wednesday, October 21, 2:00 p.m.

I encourage all of you to take advantage of this tremendous opportunity. Go to Gear Expo, visit Booth #2030, and make use of the expertise we've assembled. Nowhere else can you get your gear-related questions answered in person by the foremost experts in the industry.

We will be video recording the sessions and making them available online after the show, so even if you aren't able to attend Gear Expo, you can still participate. In fact, we invite all of our readers to submit their challenging gear manufacturing problems to us now, for our expert panel. We'll get your questions answered either as part of the live event or as part of our ongoing column in the magazine. Either way, everybody benefits. Please send your questions to Jack McGuinn, Senior Editor (*jmcguinn@geartechnology.com*) or use the "Ask the Expert" link on our home page to submit your question online.

We're looking forward to seeing the experts answer your questions at the show.

Michael Goldstein

P.S. When you go to *www.geartechnology.com*, type "basics" in the search box to see a wide variety of articles from our archive that demonstrate the educational focus that's been our hallmark for more than 31 years.

Sourcing Gears and Gear-Related Products? Check Your TCO

Total Cost of Ownership Shows that Reshoring Can Be Good for the Gear Industry

Harry Moser

Reshoring offers an opportunity for increased domestic gear production. Reshoring is growing at a steady pace in most industries, and is particularly strong in the gear intensive industries such as automotive, aerospace and construction equipment (Table 1). This article provides background on the overall trend and tools for the gear buyer and the gear producer to make the offshore vs. domestic decision. The same logic and tools apply to all countries. Many companies are adopting a localization strategy, producing locally most of what is consumed in each country or region. So, for international readers, the recent U.S. experience is a model that can be adopted locally.

The Reshoring Initiative presented to the AGMA and ABMA Annual Meeting on May 1, 2015, and administered a poll asking attendees: "In the past 3 years have you or your customers relocated jobs back to North America?" Fifty-four percent of attendees replied "Yes." We have not seen such a high response in any other of the hundreds of industry groups we have addressed. The positive response is highly relevant to the Initiative's primary goal: to eliminate the U.S. manufactured goods trade deficit of $500 to $600 billion/year.

AGMA provided a spreadsheet prepared by IHS Economics from data supplied by AGMA, the U.S. Census Bureau and U.S. government foreign trade data. We concluded that in 2014 domestic gear production, excluding automotive gears, equaled about 70% of the domestic consumption of gears. Balancing the U.S. trade deficit in gears would increase domestic gear production by approximately 50%.

Table 1 Reshored Jobs and Company Numbers by Industry

INDUSTRY	JOBS	COMPANIES
Transportation Equipment	13823	33
Electrical Equipment, Appliances, Components	9240	58
Computer/Electronic Products	3483	25
Machinery	2860	20
Apparel/Textiles	2154	46
Fabricated Metal Products	1721	39
Food	1628	9
Wood Products	1028	18
Medical Equipment	738	17
Hobbies	723	29
Construction	577	4
Plastic/Rubber Products	470	16
Castings	57	8
Non-Metallic Mineral Products	12	1
Primary Metal Products	0	5
Chemicals & Energy	0	1 each
Other: Agriculture, Environmental, Tools, Research & Services, Home & Kitchen, Office	1016	24

Source: Reshoring Initiative Library published case studies as of 12/31/14

Background and Drivers of the Trend

In 2014 more than 60,000 manufacturing jobs were brought to the United States by reshoring and foreign direct investment (FDI) combined, representing a 400 percent increase since the height of the offshoring trend around 2003, and the first net positive job number in decades (Table 2).

Overall there are three main drivers of the reshoring trend. First are rising offshore wage rates. Second is an increased recognition of the previously ignored costs, risks and strategic impacts of offshoring. This recognition is enabled by the use of the refined metrics of total cost of ownership (TCO) to quantify these factors. Third is a reduction of costs through sustainable strategies such as design for manufacturability, innovation, automation and lean.

Using TCO is the first step a company should take when evaluating sourcing options. TCO is defined as the total of all relevant costs associated with making or sourcing a product domestically or offshore. TCO includes current period costs and best estimates of relevant future costs, risks and strategic impacts. TCO analysis helps companies objectively quantify, forecast and minimize total cost. It takes into account transportation costs, travel expense and time, carrying cost of inventory, warranty, IP loss, impact on product innovation, and many other factors such as those associated with the risk of supply chain shocks or disruptions caused by natural disasters, political unrest and dock slow-

Table 2 The Bleeding Has Stopped

	Manufacturing Jobs/Year		
	2003	2014	% Change
New Offshoring	~150,000*	30,000- 50,000*	-70%
New Reshoring & FDI	12,000*	60,000**	+ 400%
Net Jobs Gained	~-140,000	~+10,000	N/A

* Estimated ** Calculated

downs. It also helps to forecast the future impact of wage and currency changes.

Much of companies' efforts to deal with complex global supply chains is eliminated or drastically reduced by reshoring. Longer-term forecasting, monitoring of suppliers and regulatory compliance offshore is found to be waste when measured against the use of proven, local suppliers.

The not-for-profit Reshoring Initiative offers the free TCO Estimator, available on reshorenow.org. The initiative offers many resources to help companies make sourcing decisions (Table 3). Reshoring tools can also be used by gear salesmen to convince customers of the benefit of sourcing domestically, especially for custom gears.

Table 3 Resources available to readers

- Calculate TCO with the Total Cost of Ownership Estimator, a free online tool to help evaluate sourcing alternatives and to make a case when selling against offshore competitors (*www.reshorenow.org/tco-estimator/*).
- Watch an in-depth webinar on reshoring and TCO (*www.youtube.com/watch?v=uAh7FBZu2xA*).
- Visit our Reshoring Library (*www.reshorenow.org/library/*), which contains 2,400+ linked articles on reshoring. Data from these articles can be accessed and sorted through the advanced search function.
- Have a story to tell? Submit your reshoring success story on our Case Studies feature (*www.reshorenow.org/case-studies/*). All valid cases will be posted, and we will send the submitter a *Manufacturing is Cool* T-shirt -Made in USA of U.S. cotton.
- Use our Economic Development Program to strengthen your region by replacing imports with local production (*http://reshorenow.blogspot.com/2014/12/reshoring-initiatives-economic.html)*.
- See our Blog for recommendations on skilled workforce development in your area (*http://reshorenow.blogspot.com/2014/02/the-reshoring-initiative-offers-skilled.html*).
- We also track reshoring and nearshoring in Mexico and Canada and cooperate with many other countries in their efforts to be more self-sufficient.

Below are some examples of gear makers who have chosen U.S. production or sourcing over offshore.

- Bison Gear and Engineering Corp. moved production of electric motors and gears from China to St. Charles, IL, creating 10 jobs.
  - Reasons: Cost, quality, lead time and lean manufacturing
- Pequea Machine Inc. brought production from China to the U.S., bringing contract work to Buck Co. (PA foundry) and Circle Gear (IL machine shop), and creating up to 20 new future jobs (Ref. 1).
  - Reasons: Quality (25% of gear boxes from China failed due to substandard metals used); equivalent price (cost was about \$900 to produce gearboxes in the United States, and between \$800-\$900 in China); Total cost
- ZF Group, a Supplier for Chrysler, brought production from Germany to Gray Court, SC and Detroit, bringing 1,650 jobs in South Carolina, and some additional jobs in Michigan. ZF originally began building gearboxes for wind turbines in Gainesville, GA with a \$98 million investment, adding 250 jobs.
  - Reasons: Time to market, proximity to market
- Metem Corp., which makes gas turbines and aerospace industry products, is expanding its Parsippany, NJ plant over plants in Pennsylvania and Hungary. Metem's CEO on the company's growth: "One of the great things about gas turbines is that the U.S. really has a leadership position in that technology. We are seeing our custom-

ers bring turbine manufacturing back to the U.S. from other parts of the world."

– Reasons: Highly skilled workers, access to universities, advanced manufacturing

Conclusion

The Reshoring Initiative publishes data (Ref. 3) annually to show that the current trend in manufacturing for the United States market is to source domestically. With 3–4 million manufacturing jobs still offshore, we see huge potential for even more growth and hope this data will motivate more companies to reevaluate their sourcing and site selection decisions. Making better-informed decisions through the use of TCO and gaining a competitive advantage through sustainable strategies will enable U.S. companies to locate more manufacturing closer to home and strengthen the U.S. economy.

We would like to build on the reshoring momentum achieved at the AGMA meeting. We have outlined (Table 3) our tools and programs that you can use. The best way to accelerate the trend is to document and promote the successful cases. Therefore, we especially encourage you to report the cases where you reshored, where you directly replaced an imported gear source or where your customer brought back product assembly and sourced gears from you. Reports can be made on our Case Studies feature. The resulting PDFs will be posted on the Reshoring Initiative website, and you can post on your site. Case submitters also receive a *Manufacturing is Cool* T-shirt, made in the USA of U.S. cotton.

References

1. *www.themadeinamericamovement.com/uncategorized/pequea-machine-joins-the-reshoring-movement-reshores-part-production-for-better-quality/.*
2. *www.njbiz.com/article/20130130/NJBIZ01/130139989/Manufacturer's-expansion-in-Parsippany-expected-to-create-jobs-CEO-says.*
3. *www.reshorenow.org/content/pdf/2014_Data_Summary.pdf.*

Harry Moser founded the Reshoring Initiative to bring manufacturing jobs back to the United States after working for GF AgieCharmilles, starting as President in 1985 and retiring at the end of 2010 as Chairman Emeritus. Previously he worked for Disamatic U.S. for six years. Largely due to the success of the Reshoring Initiative, Harry was inducted into the Industry Week Manufacturing Hall of Fame 2010 and was named Quality Magazine's Quality Professional of the Year for 2012. Moser participated actively in President Obama's January 2012 Insourcing Forum at the White House, won the January 2013 The Economist debate on outsourcing and offshoring, and received the Manufacturing Leadership Council's Industry Advocacy Award in 2014. He received a bachelor's degree in mechanical engineering and a master's degree in engineering from MIT in 1967, and he earned an MBA from the University of Chicago in 1981.

For Related Articles Search

sourcing

at www.geartechnology.com

Index Bevel Gear Hobbing Package

PRODUCES GEARS WITH TOOTH HEIGHT IN A MODULE RANGE OF 0.6 TO 4 MM

Index recently developed a "bevel gear hobbing" package, which consists of a control cycle and four Index cutter heads with module-dependent inserts. Equipped with these features, the Index R200 and Index R300 turn-mill centers become gear cutting machines on which spiral bevel gears can be produced from bar stock, with front and rear end machining, complete in one setup or as a pure two-spindle gear cutting machine.

By hobbing using a continuous indexing method — which corresponds to the Klingelnberg Cyclo-Palloid method — spiral bevel gears can be produced with constant tooth height in a module range of 0.6 to 4 mm.

Compared to the conventional process chain with classic gear cutting machines, users can achieve shorter cycle times and better geometry and position tolerances. And it is designed to be more flexible.

"The starting point of the development by Index lies in its own manufacturing governed by the principle: quality-determining components are made in-house," said Dr. Volker Sellmeier, Index-Werke's head of technology development. "When the tool holder production was reorganized several years ago, the decision was made to produce the required bevel gears ourselves."

Due to their static, dynamic and thermal properties, the turn-mill centers of the Index R-series are suited to gear-cutting, provided they are equipped with the "bevel gear hobbing" technology package. The R machines' axis configuration with two milling spindles on Y-B-axes running in hydrostatic bearings makes it possible to machine on the main and counter spindle simultaneously in five axes.

The turn-mills' ability to complete gear-part machining on the front and rear ends simultaneously is meant to shorten total cycle times and lower cost per piece.

"When we machine typical bevel gears with module 1.15 mm and approximately 25 teeth for our tool holders completely from bar stock, we achieve a cycle time of less than 3 minutes," Sellmeier said. "The share of gear cutting amounts to about 30 seconds."

In a classical gear process chain, the workpiece has to be set up on several individual machines for turning, drilling, and milling, gear cutting and deburring. Index's approach is to run all operations on the turn-mill center. Bevel gears are turned, drilled, milled and finally cut on a single machine. Even brushes for deburring can be set up. The soft machining process is thus completely autonomous, according to Index with a process-reliable gear quality of IT5 (according to DIN 3965). This is then followed by hardening. A final finishing process is usually required only for the mounting distance and the polygonal shaft/hub connection.

In addition to bar stock machining, which is best primarily for small quantities, for series production the R machine can be used as a pure gear cutting machine, working on the main and counter spindles simultaneously.

"This requires the use of an automated workpiece-loading and unloading system that loads the blanks and removes the finished parts gently," Sellmeier said. "We offer a quadruple gripper with two stations on the main and counter spindle that picks up the finished parts, rotates and then loads new blanks. This way we use the machine as a kind of double-spindle machine, cutting the time per piece in half."

Two cutter heads are required per bevel gear. They differ slightly in their cutting circle radius in order to produce the longitudinal crowning. Index offers the cutter heads in four different sizes that can be fitted with up to six carbide inserts and feature internal cooling.

In contrast to the typical Cyclo-Palloid method with an interlocking cutter head, the Index method uses two separate cutter heads per bevel gear.

"The two cutter heads provide a larger number of cutting edges. This allows us to achieve a higher cutting performance," Sellmeier said. "We also have more freedom for flank modifications and correction of the contact pattern."

Index also offers a control cycle they have developed. The user enters the same parameters as on a conventional gear cutting machine. These include, for example, machine distance, eccentricity and auxiliary angle. The cycle translates these values into the movements of each axis so that at the end the same relative movements are effected as on a conventional gear cutting machine.

For more information:
Index Corporation
Phone: (317) 770-6300
www.indextraub.com

Bonfiglioli 300 Series Planetary Gearboxes

DESIGNED FOR HARSH APPLICATIONS

Bonfiglioli´s 300 Series is designed for harsh applications where shock loadings and impacts are common.

Bonfiglioli´s ongoing mission to improve its planetary gearboxes for industrial applications has led to two new features that result in an easier and safer assembling/disassembling of the drive to/from the application. The new FDK and FZP versions feature an output hollow shaft that will make the series more effective and suitable for shaft mount assembly.

The hollow shaft solutions reduce the time and effort for the disassembling of the drive from the customer´s machine shaft, due to the new solution with the axial locking ring. The new product solutions make mounting and commissioning easier and faster thanks to the smarter design and allow for easier and more accurate screw tightening.

The cutting-edge design of the shrink disk will improve and speed up setup and commissioning. The hollow shaft with the two keys at 120° will allow full-rated torque and max-torque transmissions. The axial locking ring with threaded holes completes the solution for an easier and more reliable shaft mounting. The keyed hollow shaft is available in smaller sizes, ranging from 300 to 310 and will be included in the designation of the series with the acronym FDK; when the FZP version is available it will come in larger sizes from 311 to 325.

Another design component of the new 300 series is the splined hollow shaft which meets the DIN 5480 standard and offers the same bearings available in the current FP version. It provides double centering for an aligned assembling of the solid shaft of the machine. Like the keyed hollow shaft, the splined hollow shaft also includes an axial locking key with threaded holes for easier mounting and grants full rated and max torque transmissions.

The new shrink disks prevent accidental mounting errors (even when dismounting and re-mounting the shrink disk) due to simpler design and visual-control of screw tightening torque. This design makes the 300 series now complete and effective for any shaft mounted requirements for all sizes and ratios. The series has a torque range of 1,000-1,287,000 Nm and gear ratios of 3.4-5,234.

For more information:
Bonfiglioli Riduttori S.P.A.
Phone: +39 051 647 3932
www.bonfiglioli.com

Schunk Tendo Platinum Toolholder

BALANCED TO G2.5 AT 25,000 RPM

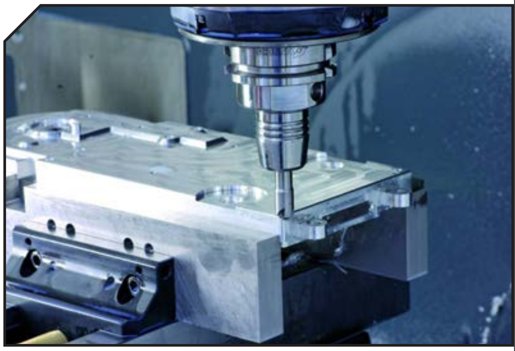

Schunk recently introduced the new Tendo Platinum toolholder. Tendo Platinum offers improved brazing technology by using a brazing and hardening process all in the same cycle.

The Tendo Platinum is balanced to G2.5 at 25,000 RPM. With improved vibration dampening and precise runout accuracy of less than 0.003 mm (0.0001") at 2.5× clamping diameter, the Tendo Platinum works in configuration with the machine spindle and the cutting tool, to reduce wear and damage.

Schunk offers three lengths with two precision ground taper sized: CAT40 — 2.5", 4", 6" / CAT50 — 81 mm, 4", 6".

Schunk also offer direct clamping in both metric and inch sizes to assure improved accuracy and vibration dampening.

For more information:
Schunk, Inc.
Phone: (919) 572-2818
www.schunk.com

Walter Blaxx F5038 Helical Mill

FEATURES TANGENTIAL, QUADRUPLE EDGE SYSTEM

The new Walter Blaxx F5038 helical milling cutter features the improved stability, including face and shoulder milling cutters. Stability is particularly important for helical cutters, and the Walter Blaxx F5038's provides a solid and stable body. In conjunction with the tangential, quadruple edge system of indexable inserts made of Tigertec

Silver, users of the new Walter Blaxx F5038 helical milling tool achieve top values in process reliability and cost efficiency. In comparison to conventional tool solutions of this type, machining times have been reduced by up to 30%. The accurately arranged, precision indexable inserts produce step-free shoulders.

For more information:
Walter USA, LLC
Phone: (800) 945-5554
www.walter-tools.com

Cimcool Cimperial 861 Metalworking Fluid

INCREASES TOOL LIFE AND PROVIDES SUPERIOR LUBRICITY

Cimcool recently announced the release of Cimperial 861 with InSol technology, a hybrid lubricity, semi-synthetic metalworking fluid, which recently received approval under Boeing BAC5008 RevU.

Cimperial 861 with InSol technology is designed for heavy-duty machining of non-ferrous and ferrous metals including 6,000 and 7,000 series aluminum, stainless steels, titanium and other exotic alloys. It can also be used for grinding and is formulated to deliver extended sump life. The product is designed to increase tool life and provide superior lubricity while remaining low foaming for today's demanding high-pressure applications. In addition, Cimperial 861 with InSol technology has low chemical odor and is mild to the skin.

"Cimcool Fluid Technology has developed a hybrid semi-synthetic to maximize tool life without the compromising part quality on aerospace alloys," Aerospace Product Manage Kyle Walker said. "The benefit will be one fluid that handles machining needs by delivering superior cooling and lubricity directly to the point of cut. Cimperial 861 with InSol technology is a great example of how we support customers in the aerospace industry using technology approved by Boeing. The hybrid combination of InSol Technology in a semi-synthetic metalworking fluid delivers superior performance when compared to other semi-synthetic or micro-soluble technology."

By design, Cimperial 861 with InSol technology is stain resistant when tested on 6,000 and 7,000 series aluminum, titanium and stainless steels alloys.

For more information:
Cimcool Fluid Technology
Phone: (888) 246-2665
www.cimcool.com

Dayton DayLube Grease

DESIGNED TO MAINTAIN VISCOSITY AFTER 100,000 STROKES

Dayton Lamina recently introduced their DayLube high-performance nano-ceramic grease. The grease is designed to maintain its original viscosity and adhesion after 100,000 production strokes. Nano-ceramic particles act as sub-microscopic ball bearings to provide continuous lubrication to steel surfaces.

DayLube is designed to have a lower coefficient of friction at all temperatures than traditional PTFE greases and to be chemically inert. DayLube is meant for industrial applications such as the protection of bearings, bushings cables, cams, chains, conveyors, gears, lifters, machine parts, robotics, slides, wear plates and more.

DayLube operates in temperature ranges from -40°F to 800°F, and the nano-ceramic particles remain intact up to 2500°F. It survived the ASTME 4-ball weld test with no weld and minimal damage to all ball bearings.

DayLube has high load-bearing properties, a low dielectric constant, does not contain metal or silicone and is resistant to steam, acids, and most chemical products.

"Customers using DayLube report significantly longer service life — up to 10-times longer — than traditional PTFE lubricants" said Dayton Progress Marketing Communications Manager Brian Marsh. "Even when compared to nanotechnology products, DayLube has a lower cost per ounce. When considering all factors there is not a better lubricating value than DayLube."

DayLube is available in 16-ounce tubes and 16-ounce jars, as well as 1-gallon and 5-gallon pails. DayLube is marketed mainly towards the aerospace, agricultural, automotive, can makers, consumer goods, food and beverage processing, general manufacturing, marine, material handling, medical/scientific, military/national defense, pharmaceutical, stamping & fabricating, and truck and bus industries.

For more information:
Dayton Lamina
Phone: (937) 859-5111
www.daytonprogress.com

Mitutoyo Legex 4 CNC Machine

PROVIDES HIGH-ACCURACY MEASUREMENTS

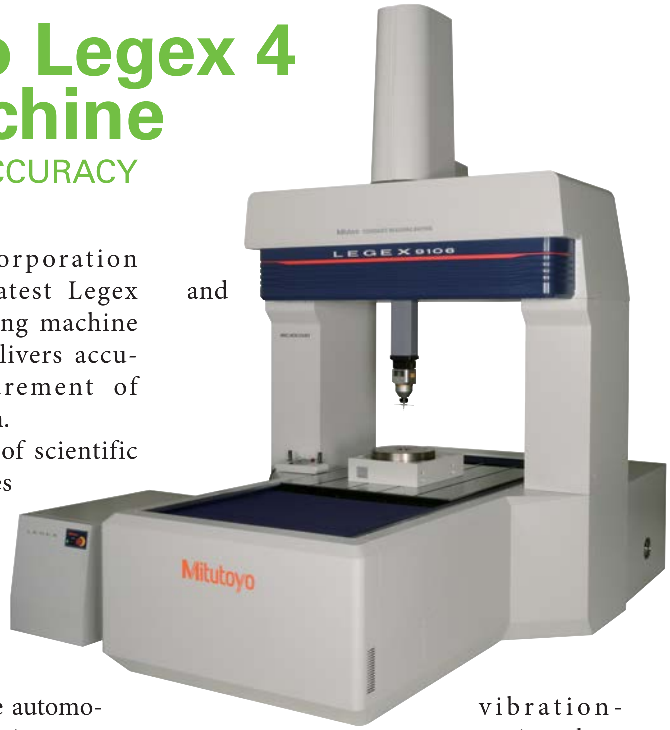

Mitutoyo America Corporation recently released the latest Legex CNC coordinate measuring machine (CMM). The Legex 4 delivers accuracy in length measurement of E0,MPE = (0.28 + L/1000) µm.

With the advancement of scientific and industrial technologies and driving demand for improvements in high-accuracy manufacturing, Mitutoyo Legex produces applications such as ultra-precise molds, components and aspherical lenses in the automotive, aviation and medical instrument industries, and calibration of master gages for research institutes. To meet these needs, Mitutoyo started from the elemental technology level and worked upward, with the aim of eliminating all possible sources of measurement error.

Key features include: sources of static and dynamic error minimized to realize measurement accuracy of 0.28 µm; fixed-bridge structure with moving table; base is made from spheroidal graphite (ductile) cast iron in a sealed-structure design to provide high rigidity and vibration-attenuating characteristics; high-rigidity structure and feed mechanisms increase accuracy and improve cycle times; thermally symmetric structure features full covers around the main body to reduce possible impact in ambient temperature changes; vibration-dampening unit is standard; an air server stabilizes the air temperature to 20°C±0.1°C.

For more information:
Mitutoyo America Corporation
Phone: (888) 6488-9696
www.mitutoyo.com

Mahr MarShaft Scope 250

MEASURES PARTS UP TO 250 MM IN LENGTH

Mahr Federal recently introduced a new addition to its growing family of optical shaft measurement systems. The MarShaft Scope 250 plus features an accurate matrix camera with four million pixels. The system measures parts up to 250 mm in length and 40 mm in diameter. It features an MPE (Maximum Permissible Error) of less than 1.5 microns + L/40 when measuring diameter and 3 microns + L/125 when measuring length.

"The MarShaft Scope 250 plus is a very compact, attractively designed system that provides out-of-the-box functionality," said Patrick N. Nugent, vice president of metrology systems for Mahr Federal. "It is extremely easy to use, and very fast. In our lab here in Providence,

we measured 28 features on a sample shaft in less than ten seconds, and a customer part with only seven required features in less than three seconds."

One key to the system's speed is the high-resolution CMOS matrix camera with a live image field of view of 40 × 24 mm, enabling it to capture an entire part diameter in a single view. With Z-axis positioning speeds of up to 200 mm/second and an image acquisition rate of over 120 images per second, measurements are performed faster than the blink of an eye. Zoom functions allow measurement of the smallest details such as chamfers and radii, which can be difficult and in some cases even impossible to test, with conventional measuring methods.

MarShaft Scope 250 plus can be operated entirely on the integrated touch screen, or via a keyboard and mouse if desired. *MarWin*-based *EasyShaft* software enables the precision measurement of diameters, lengths, contour features, and form and position tolerances in accordance with standards, and offers many new evaluation and documentation options. *EasyShaft* runs on the *Windows* operating system and is compatible with other *Windows* applications and printers.

For more information:
Mahr Federal, Inc.
Phone: (401) 784-3100
www.mahr.com

Dillon 1018 CR Steel Full Grip Jaws

REDUCE DISTORTION AND PROVIDE MORE FRICTION

Dillon Manufacturing recently introduced full grip jaws made of 1018 CR steel from 6" to 15" in diameter, with heights of 2", 4" and 6". These heat treatable and weldable steel jaws allow for complete gripping of the work piece - to maintain repetitive accuracy. This type of jaw reduces distortion and provides more friction for drives during turning operations.

With close tolerances and concentricity maintained, they are meant for applications such as valves, cylinders, specialty wheels and gears, housings and enclosures, adaptors and connectors, aluminum and steel shells, flanges, retainer rings, and other thin-walled parts such as automotive smog control air pump rotors, gas turbine parts, thin-wall tubing and cylinder liners for diesel engines and more.

For more information:
Dillon Manufacturing, Inc.
Phone: (800) 428-1133
www.dillonmfg.com

Siemens Sinumerik Blackline Panels

ENABLE RAPID INTERACTION WITH THE USER INTERFACE

The Sinumerik blackline panels OP 015 black and OP 019 black are a new generation of operator panels for the Sinumerik 840D sl CNC system and offer new options for machine operation. The inductive sensor technology enables rapid interaction with the user interface even when the operator is wearing gloves. Similarly, it prevents incorrect entries, for example caused by the heel of the operator‘s hand.

The 19-inch display of the OP 019 black can show all the entries made in widescreen format at a glance. The OP 015 black also features an alphanumerical keypad on the right that can be operated via touch control. This feature means that the 15-inch display is not restricted by the superimposed keypad during data entry, which ensures clear and efficient operation. Both blackline panels also have an integrated glass panel on the front side and are designed with IP65 (OP 019 black) and IP66 (OP 015 black) degrees of protection. They are resistant to liquids and dust and can be operated even under harsh industrial conditions. An integrated key lock helps safeguard against operating errors. The operator panel can provide a basic machine display, with three or four channels showing up to 13 axes.

The blackline panels also feature durable LED background lighting, providing 40 percent energy-savings compared to conventional neon lamps.

In combination with the Sinumerik 840D sl control, for use on high-end milling, turning, grinding and laser cutting machine tools, the blackline panels can be used as an operating and programming station for aerospace composite machining, power generation and medical part manufacturing, in addition to tool- and mold-making, rotary indexing machines and in shopfloor manufacturing.

For more information:

Phone: (800) 879-8079
www.usa.siemens.com

Birchwood Cold Presto Black Process

FORMS NON-DIMENSIONAL COATING THICKNESS OF 0.5 MICRON

Birchwood Technologies now offers three mini systems for use in small batch metal finishing at low temperatures. Mini systems are designed for manufacturers looking to add in house capabilities but do not have the necessary volume or space for a full sized process line. Birchwood Technologies offers these blackening solutions for the Presto Black and TruTemp processes for iron and steel parts, and the Lumiclad process for aluminum parts.

The cold Presto Black process forms a non-dimensional coating thickness of less than 0.5 micron thickness and is designed for components that require a black finish for visual appeal. Presto Black is a short fifteen-minute process that provides high corrosion resistance and is tested for up to 800 hours humidity exposure when sealed with appropriate rust preventive. The Presto Black process offers a friable crystal structure that serves as a sacrificial barrier on sliding surfaces to protect the underlying steel itself from galling and deformation.

The low temperature TruTemp process forms a durable satin black magnetite coating, 0.5 micron thick, with no effect on material hardness or tensile strength. The sealed finish withstands up to 100 hours of neutral salt spray or several hundred hours of humidity, and protects the metal surface during shipment & storage as well as in service. TruTemp black oxide operates effectively with alkaline chemistry that does not embrittle metal or create unsightly salt bloom in and around recessed part areas.

The Lumiclad process forms a non-dimensional black oxide finish on all aluminum surfaces that is durable, clean and tightly adherent to the metal substrate. The Lumiclad process develops a uniform coating thickness of 1.5 microns that will not close down hole diameters or change critical part dimensions. The smooth black finish has a slightly porous crystal structure that absorbs an optional topcoat such as a dry-to-touch sealant, light oil, or clear polymer.

All three processes utilize a conventional seven-tank immersion process line, and operate at low or room temperature, making the processes easy and safe to operate in-house. Mini systems are designed for short run sporadic production because the lines can be sealed and stored, with the chemicals in the buckets, for six to twelve months.

For more information:
Phone: (952) 937-7931
www.birchwoodtechnologies.com

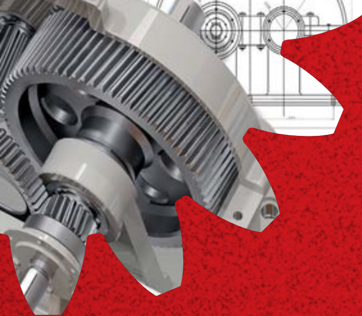

GEAR EXPO 2015

THE DRIVE TECHNOLOGY SHOW

POWERFUL CONNECTIONS

OCTOBER 20-22, 2015
DETROIT, MI
COBO CENTER

REGISTER TODAY

FOR THE DRIVE TECHNOLOGY SHOW OF THE YEAR!

GEAR EXPO 2015 brings together the full range of experts — design, manufacturing, application engineering — all in the same place — **Cobo Center, Detroit, October 20–22.**

From a single gear to complex drives, **GEAR EXPO** covers it all...

- **More exhibitors** — from gear making machines to systems integrators.
- **More education sessions** — from metallurgy and geometry to maximizing power density.
- **More attendees** — buyers and makers from automotive, construction, mining, agriculture — wherever high-performance drives are critical.
- **More solutions** — meet the experts and evaluate your capabilities.

GEAR EXPO 2015 is the place to be.

- Make powerful connections.
- See the latest technology in action.
- Get the inspiration you need to take your products to the next level.

Improved drive technology is critical to achieving higher efficiencies and longer service life. All the information and answers you need will be at **GEAR EXPO 2015**.

VISIT

www.gearexpo.com/GETECH

Use code **GETECH** when registering.

TDM Global Line Software

TAILORED TO INTERNATIONAL MANUFACTURERS WITH GLOBAL PRODUCTION SITES

TDM Systems recently launched its new software module, TDM Global Line. TDM Global Line is tailored to international manufacturers with global production sites. With new software architecture and data compression, all of the centrally defined tool data and graphics are available at each production facility with the click of a mouse. Customers of TDM Systems can expand their central application to other plants. TDM Global Line is compatible with the existing TDM database applications.

In addition to performance, TDM Systems placed an emphasis on user-friendly handling. For example, the Google-like tool search provides quick results that can be listed by item, tool assembly and tool list. The customer can also individually configure their information view on the screen using widgets, depending on their own requirements. A completely new and modern software design has been developed for TDM Global Line.

With the new software module, customers can manage user rights and mandates in one central location. When entering data, concurrent data validation also recognizes incorrect entries and forgotten mandatory fields. TDM customers can also use the initial booking functions that are already included in the first module 1.0. This allows the tool usage to be recorded in the connected plants.

For more information:
Phone: (847) 605-1269
www.tdmsystems.com

Mitutoyo MeasurLink 8.0

RE-INTRODUCES THE GAGE MANAGEMENT MODULE

Mitutoyo America Corporation recently announced the latest version of *MeasurLink* software with a variety of functional improvements. *MeasurLink 8.0* builds on the previous version, allowing an operator to collect data from most measuring instruments and analyze, monitor and manage the results in real-time.

The latest version of the data management software reintroduces the gage management module, along with support for managing multiple measurement specifications. The gage management module assists users in developing, maintaining, organizing and managing information about the gages, including service intervals, GR&R dates, recall dates and general gage event history.

MeasurLink is available with floating/concurrent license options for multi-seat packages. This is an option to include more users without purchasing additional seats. Upgrades can be integrated during installation or added to an existing installation.

For more information:
Mitutoyo America Corporation
Phone: (630) 820-9666
www.mitutoyo.com


GearScan 500
Be sure your gears are perfect
Grinding quality and heat treatment control by Barkhausen Noise
Residual stress measurement by X-ray diffraction
stresstech group
www.stresstechgroup.com

The Gear Industry's Family Reunion

Gear Expo 2015 to feature familiar faces, new exhibits

Erik Schmidt, Assistant Editor

When it came to picking a personal favorite booth at Gear Expo, AGMA Vice President of Marketing Jenny Blackford donned her proverbial TAG Heuer watch and embroidered silk apron and decided to keep her allegiance neutral.

"I'm going to play Switzerland," she says.

And really, can you blame her?

With approximately 200 total exhibitors and 55,000 square feet of showroom space, trying to crunch the robust numbers of the biennial event down into one bite-sized numeral can be a bit like ice skating uphill. And even if Blackford did have a favorite (not that we're alleging anything of the sort), it's unlikely she would ever fess up — you see, offending relatives isn't part of her MO.

"I've heard people refer to Gear Expo as a 'family reunion,'" Blackford says. "If you've been in the industry for a long time, you'll see a lot of people — both exhibitors and other people just walking the aisles –that you haven't seen in two years or even longer.

"It's a great place to touch base with people you already know in the industry, but even more importantly it's your opportunity to see the latest and greatest technologies, services and companies that are serving the industry. So there's sort of a level of enthusiasm that you get at [Gear Expo] that you don't get elsewhere."

The Players Come Together

Since 1986, Gear Expo — the "Drive Technology show" that consistently brings out an impressive throng of power transmission professionals — has rotated around the country every two years to industrial meccas like Indianapolis, Cincinnati, Columbus and Nashville. This year's show stops at Detroit's Cobo Center, a gleaming, glass-walled convention center featuring 623,000 square feet of contiguous exhibition space that's eternally guarded by a statue of the great Black Bottom slugger Joe Louis, who stands crouched and loaded, ready to throw one of his legendary "brown bombs" at unsuspecting passerby.

The three-day event hosted by AGMA takes place from October 20-22, giving attendees and exhibitors ample time to build relationships and absorb the latest industry information. Co-located with the ASM Heat Treating Society Conference & Exposition, Gear Expo promises to provide solutions to streamline workflow, reduce errors and increase productivity for attendees, according to Blackford.

"It's a place where all the players come together and just converse and see the latest innovations, technologies, features and processes," says Amir Aboutaleb, AGMA technical division vice president. "It's really a networking opportunity for the members and players within the gearing industry.

"The manufacturers are there; the designers are there; the engineers are there; buyers, sellers, makers — everybody is there. That's the biggest value of the show."

Attendees represent a large contingent of tangentially connected industries, including automotive, oil and gas, aerospace, off-highway, agriculture and construction, while exhibitors will display more than 750,000 pounds of machinery on the show floor.

On top of the general, meet-and-greet opportunities that Gear Expo provides, there will also be several returning components to the show's program.

"One of our most popular features is the Solutions Center," Blackford says. "It's an education space that's on the show floor, and exhibitors give presentations every half hour during the show. You have a chance, for free, to come hear the latest solutions people have to offer. Then you can ask questions to the presenter, and if it's a more involved question you can go back to their booth with them and find out more.

"Also at the Solutions Center, we have keynote presentations once a day that are on larger topics. They're on emerging technologies or business issues that speak to pretty much everybody that would attend the show."

Some of the educational course

All Photos by David Ropinski

This year's Gear Expo will display over 750,000 pounds of machinery.

For Related Articles Search
gear expo 2015
at www.geartechnology.com

GEAR EXPO 2015
THE DRIVE TECHNOLOGY SHOW
October 20-22 • Detroit • Cobo Center
Solutions: Gear Making & High Performance Drives

presentations include: "Gearbox Maintenance" (instructed by John B. Amendola, John B. Amendola III, Dereck Yatzook); "Lubrication of Gearing" (instructed by Richard Schrama, Tribological Services); "Taming Tooth Deflections" (instructed by Raymond Drago, Drive Systems Technology); "Materials Selection and Heat Treatment of Gears" (presented by AGMA and ASM International); "Why Bearings are Damaged" (presented by American Bearing Manufacturers Association); and "Cylindrical Gear Inspection: Chart Reading and Interpretation" (instructed by John Lange, Gleason Cutting Tools).

"The educational opportunities are great for newcomers as well as the [veterans]," Aboutaleb says. "The newcomers get to hang out with some of the [veter-

CEO Fred Young at Forest City Gear's booth in 2013

ans] and learn from their experiences. Just sitting in the class and listening to the lectures—it's part of the game—but the opportunity to speak with the guys who have 10, 15 years of experience and asking them questions is the biggest part."

Another popular aspect of the show that will return, according to Blackford, is the networking reception, which will take place on Wednesday, Oct. 21.

"It's a time to grab a drink and maybe a snack and huddle up with your fellow gear industry peers in a more casual environment," she says.

Also taking place on Wednesday is a unique aspect of the 2015 show: AGMA's centennial celebration kick-off. AGMA began in 1916 in Alexandria, VA and has grown into an association with about 430 member companies.

"Attendees will get to see the history of AGMA in exhibit form (throughout the three-day show) and on Wednesday, after the networking party, AGMA is holding a centennial dinner at Gear Expo that will be the kick-off event for the year," Blackford says.

With so many moving pieces, Blackford says she's always pleasantly surprised that everything seems to come together every two years when Gear Expo rotates back under the industry spotlight.

A presentation at the Solutions Center in 2013

And it was then (with absolutely no further coercion on our part, we swear), that Blackford finally decided on her favorite:

All of it.

"Putting together a trade show is amazing, because a little city is built in a matter of a couple of days," she says. "Just like the rest of the attendees, it's always great to see all the people you haven't seen in two years and just see everything that all these people have to offer."

For more information:
American Gear Manufacturers Association
Phone: (703) 684-0211
www.gearexpo.com

CUBITRON™ II

Register now for our Gear Technology Webinar.
3M.com/GearTechnologyWebinar

Up Your Average ...from **Incredible** to EXTREME!

Get closer to a **FREE TRIAL** of 3M™ Cubitron™ II Grinding Wheels today.

These kinds of improvements are made possible thanks to 3M's exclusive Precision Shaped Grain – a breakthrough abrasive technology that "slices" through metal, to cut faster, last longer and improve your average. Nothing else comes close!

Visit us at Gear Expo 2015, Booth 1622

Our customers' average improvements are **Incredible!***

- Up to 2.5x higher Q'_w removal rates
- Up to 50% cycle time reduction
- Up to 50% fewer dressings

And at times their improvements are **Extreme!***

- Up to 6x higher Q'_w removal rates, ID grind
- Up to 6.5x higher Q'_w removal rates, general grind
- Up to 60% cycle time reductions, Module 3 (70 teeth gear grinding)
- Up to 60% cycle time reductions, Module 10 (23 teeth gear grinding)
- Up to 80% longer dressing cycles

* Above test results included comparisons against wheels containing aluminum oxide, ceramic, and other grain varieties.

Learn more:
3M.com/EXTREMEPrecisionPowertrain
Or call our 3M Customer Helpline
1-866-279-1235

3M

GEAR EXPO 2015

2015 Fall Technical Meeting (FTM) and Presentations

Presented by: American Gear Manufacturers Association
Sunday, October 18 — Tuesday, October 22
8:00 a.m. — 5:00 p.m.

Anyone even remotely involved with the gear industry knows that Gear Expo is B-I-G. Every two years, it is an invaluable opportunity for buyers, sellers and just-lookers to come together and glorify gearing.

But one can't help wondering how many exhibitors and attendees even think about the two days that precede the show, i.e. — the Fall Technical Meeting. It must be important, because they convene this gathering *every* year — not every *other* year. And important it surely is — today more than ever. With the ongoing dearth of new and qualified workers for the gear industry, educating and re-educating the people we do have in our corner of the work world is paramount. With that in mind, let's see what's on offer for the 2015 Annual Fall Technical Meeting. (Go to *www.gearexpo.com/Detroit* for course pricing.)

Register for an education course and receive a complimentary pass to the exhibit hall. Bring colleagues along to qualify for group pricing and benefits. Monitor *www.gearexpo.com/Detroit* for upcoming information on group pricing.

AGMA's Fall Technical Meeting is a great opportunity for anyone in the gear industry who is interested in the latest research and technical developments in gearing. The 2015 FTM will have 25 presentations divided into five sessions over three days.

Authors and Abstracts

Session I — Materials & Heat Treatment

Influence of Surface Finishing on the Load Capacity of Coated and Uncoated Spur Gears

Philip Konowalczyk: M.Sc., Laboratory for Machine Tools and Production Engineering (WZL) of RWTH Aachen University

PVD/PECVD coatings have been proven to increase the pitting and scuffing resistance of materials. However, due to concerns that the application process of PVD/PECVD coatings leads to a reduction in tooth root strength, as well as high production costs, the use of these coatings have not been adopted by the gear industry. The aim of this work is to investigate and determine the influence of surface finishing processes — specifically, the impact of PVD/PECVD coatings applied using an optimized coating process on the pitting load capacity of gears.

Improved Materials and Enhanced Fatigue Resistance for Gear Components

Dr. Volker Heuer, ALD Vacuum Technologies

To answer the demand for fuel-efficient vehicles, modern gearboxes are built much lighter. Improving fatigue resistance is a key factor to allow for the design of thin components used in advanced transmissions. The choice of material and the applied heat treat process are of key importance to enhance the fatigue resistance of gear components. This presentation shows the latest progress in steel grades and case hardening technology for gear components.

Practical Approach to Determining Effective Case Depth of Gas Carburizing

March Li, Lufkin Industries, LLC

This presentation shows calculations of the effective case depth governed by carburizing temperature, time, carbon content of steel, and carbon potential of atmosphere. This method provides simple and practical guidance of optimized gas carburizing and has been applied to plant production.

Case-Hardening for Mass Production of Gears with Minimal Distortion and Maximum Repeatability

Maciej Korecki, Seco/Warwick

This presentation looks at the major causes of deformation during traditional heat treatment and methods of their control, correction, and elimination. A case-hardening system will be presented which allows individual adjustment to the size and shape of the particular gear, in order to minimize hardening distortion and ensures ideal repeatability of results throughout the gear series. Additionally, this presentation will discuss the operational aspects, the costs and productivity.

Innovative Steel Design and Gear Machining of Advanced Engineering Steel

Lily Kamjou, Ovako

This presentation will describe how shot peening may be eliminated in high cleanliness, as-carburized steel components using an alternative composition. The fatigue performance of such a solution is compared to conventional grades used today, both with and without shot peening. It will also deal with the production process, including quantitative machining trials and the importance of tooling selection.

Powder Metal Gear Technology: A Review of the State of the Art

Anders Flodin, Höganäs AB

Several hurdles had to be overcome to put powder metal gears into automotive transmissions, such as fatigue data generation on gears, verification of calculation methods, production technology, materials development, heat treatment recipes, design development, and cost studies. The advancements needed—and achieved—to overcome these hurdles will be discussed, and examples of current vehicles using powder metal gears in transmissions will be shown.

Session II — Manufacturing

Industry 4.0 and its Implication to Gear Manufacturing

Dr. Hermann J. Stadtfeld, The Gleason Works

This presentation will provide an overview of the Industry 4.0 initiative and discuss the four industrial periods from the viewpoint of gear manufacturing. It will discuss in depth the techniques and elements of the "cyber physical production systems" and how they will change the way of industrial manufacturing.

Proposed Pre-Finished Cylindrical Gear Quality Standard

Peter Chapin, The Gleason Works

Final gear quality can be vastly different from pre-finish quality. Using finished gear quality class such as ANSI/AGMA ISO 1328 is not recommended or even appropriate for pre-finish gear quality evaluation. This presentation will outline a proposed standard for pre-finished cylindrical gear quality for typical finishing operations. It proposes to only include the inspection elements that are important to properly evaluate pre-finished gear quality as it applies to the finishing operation.

Influence of Hobbing Tool Generating Scallops on Root Fillet Stress Concentrations

Benjamin Sheen and Matthew Glass, Eaton Corporation


This paper will discuss the specific example of parallel-sided splines manufactured with a finish hobbing process and the effects of generating root fillet stress concentrations. To estimate the value of the stress concentrations, finite element analysis was performed on the components for two unique hobbing tool designs. The FEA results were then correlated to actual components with known field service lives.

Selecting the Proper Disc Cutter Design for Milling of High Quality Parallel Axis, Cylindrical Gears and Splines

Brent Marsh, Sandvik Coromant

This presentation will provide a comprehensive view of topics such as tool selection, material selection, and surface finish requirements to assist the manufacturing engineer or process planner in successfully choosing the design of disc mill cutters, in order to make cost effective cylindrical gears to the appropriate quality.

Simulation of Hobbing and Generation Grinding to Solve Quality & Noise Problems

Prof. Dr.-Ing. Günther Gravel, Institute for Production Engineering, Hamburg University of Applied Sciences (HAW)

When deviations occur during generation manufacturing of gear teeth, it is not easy to pinpoint the causes due to the tool design and complex kinematics. A simulation tool has been developed to allow the simulation of typical faults that occur during hobbing and generation grinding to help solve quality and noise problems. This presentation will discuss practical examples to demonstrate applications for the simulation program.

Session III — Gear Application

Thermal Capacity of a Multi-stage Gearbox

Benny Wemekamp, SKF Engineering Research Centre

In many industrial gearbox applications, the thermal rating is a key factor in the practical utilization of the gearbox. A simulation tool that goes beyond traditional thermal estimation methods, such as those found in ISO/TR 14179, by calculating the interaction between heat losses, thermal expansions, and (bearing) pre-loading, has been used to understand the interaction between mechanical and thermal equilibrium.

Minimum Backlash of Helical Gear Pairs in Complex Shaft Gearbox Systems

Dr. Carlos Wink, Eaton Corporation - Vehicle Group

Increasingly, there has been pressure on gearbox designers to reduce the noise produced from a gearbox, especially in the truck market where engines are running at lower speeds to increase fuel efficiency. An analytical model was developed to determine the minimum backlash of each gear pair when not transmitting load, and thus susceptible to generating a noise, at lower transmission power paths.

New Refinements to the Use of AGMA Load Reversal and Reliability Factors

Ernie Reiter, P. Eng., Web Gear Services Ltd.

Information will be presented on two ways to calculate a load reversal factor, which will be material specific, based either on Modified Goodman or Gerber failure theories. This presentation will further provide a method of calculating the reliability factors which very closely match the tables found in ANSI/AGMA 2101-D04.

Harmonized Assessment of the Design Reliability of Wind Turbine Gearboxes

Douglas Guthrie, Vestas Wind Systems

This presentation posits a new approach for assessing design reliability of wind turbine gearboxes. The deterministic approach in prevailing standards does not allow designers to predict failure rates over time, but expresses strength by a safety factor for a given duty cycle. This paper suggests a harmonized method for assessing the design reliability of wind turbine gearboxes.

Homogeneous Geometry Calculation of Arbitrary Tooth Shapes—Mathematical Approach and Practical Applications

Dipl.-Ing. Maximilian Zimmer, Gear Research Centre (FZG), Technical University of Munich

This presentation will outline a mathematical framework, and its implementation, for calculating the tooth geometry of arbitrary gear types, based on the basic law of gear kinematics. The mathematical algorithms are summarized in implemented software modules for the particular gear types.

Rating for Asymmetric Tooth Gears

Dr. Alexander L. Kapelevich, AKGears, LLC

This presentation will describe a rating approach for asymmetric tooth gears by their bending and contact stress levels in comparison with equivalent symmetric tooth gears, whose rating is defined by standards. This approach applies FEA for bending stress definition and the Hertz equation for contact stress definition. It defines equivalency factors for practical asymmetric tooth gear design and rating.

Session IV—Lubrication, Efficiency, Noise & Vibration

Worm Gear Efficiency Estimation and Optimization

Massimiliano Turci, Studio Tecnico Turci

This presentation will outline the comparison of efficiencies and of transmissible torques of worm gear drives with center distance sized from 28 mm to 150 mm and single reduction from 5 to 100, calculated by several standards (AGMA, ISO, DIN, BS). It will also outline the experimental works required for the calibration of an analytical model, now used for bevel and cylindrical gears only, but ready to become suitable to predict worm gear drive efficiency too.

Investigations on the Efficiency of Worm Gear Drives

Dipl. Ing. Eva Maria Reitinger, Gear Research (FZG), Technical University of Munich

This presentation will examine the efficiency and the load carrying capacity of worm gears. The tests performed consisted of generally pairing a bronze worm wheel with a case hardened worm with center distances between a 65 and 315 mm. In the course of these investigations, overall gearbox efficiencies of up to $\eta = 96\%$ were achieved.

Polish Grinding Gears for Higher Transmission Efficiency

Walter Graf, Reishauer AG

This presentation introduces a new gear polish grinding process and describes its multiple benefits, especially to makers of automotive transmissions. The overall increase in efficiency realized through the new polish grinding process has been demonstrated through independent scientific studies and field trials. The production process and economic considerations of this new process will also be discussed.

Development of a New Class of Industrial Gear Oil

David B. Gray, Evonik Oil Additives

A new class of industrial gear lubricants, based on alternative synthetic materials, has been developed to satisfy the critical market performance expectations, ensure global supply chain security, and address both economic and performance challenges. This presentation will describe the technical aspects of the novel synthetic gear oil lubricant approach.

Noise Reduction in an EV Hub Drive Using a Full Test and Simulation Methodology

Dr. Owen Harris, Smart Manufacturing Technology, Ltd.

With the current trend towards electric vehicles more work is being conducted in the area of noise reduction specific to these vehicles. This presentation will outline a series of tests and simulations that have been performed to specifically look at noise reduction in an EV hub drive. A detailed methodology is presented, combining both a full series of tests and advanced simulation to troubleshoot and optimize an EV hub drive for noise reduction.

Tribological Coating Wear and Durability Performance Guideline for Gear Applications

Randy Kruse, The Timken Company

It is important to understand the performance enhancement limits of DLC tribological coatings so that gear and bearing engineers can accurately specify and predict system life. This presentation reports the results of testing a tungsten incorporated diamond-like carbon coating as applied to SAE4320 and AMS6308 gear materials using a ball on disk test machine under conditions that simulate the contact stresses and sliding velocities of gears.

Session V—Gear Wear & Failure

An Experimental Evaluation of the Procedures of the ISO TR 15144 Technical Report for the Prediction of Micropitting

Donald R. Houser, The Ohio State University

This presentation will provide practical information on some of the idiosyncrasies of using the ISO/TR 15144 micropitting prediction methodology. A review of the ISO methodologies is presented and its application in a spreadsheet analysis using contact stresses predicted from load distribution prediction is discussed.

Calculating the Risk of Micropitting Using ISO Technical Report 15144-1:2014 –Validation with Practical Applications

Dr. Burkhard Pinnekamp, RENK AG

This presentation describes the calculation method in ISO Technical Report 15144-1:2014 and its application to examples where micropitting has either occurred or not. The examples give evidence that the Technical Report reliably predicts the risk of micropitting where it is later found on the gear flanks, and it does not do so when the gears run without micropitting.

Wear: A New Approach for an 'Old' Failure Phenomenon of Gears

Dr. Ing. Ulrich Kissling, KISSsoft AG

This presentation outlines research conducted on gear wear and how it affects the performance of the gear over time. The progress of wear is calculated step by step because the tooth form changes as it becomes worn, and therefore the load distribution will change over the meshing. This new calculation method predicts the modification of the tooth contact area through wear and the consequences for the gear behavior.

Application of Advanced Mesh Analysis to Eliminate Pinion Field Failures

Terry Klaves, Power Transmission Solutions—Regal Beloit America, Inc.

This presentation will walk through a specific case study involving field macro pitting failures on production helical gearing. It will include evaluation of the pitting failures for root cause, review of gearing service factors, and application of advanced mesh analysis tools to define root cause of the failures.

Tooth Flank Fracture—Influence of Macro- and Micro-geometry

Dr. Stefan Beermann, KISSsoft AG

This presentation discusses the first results obtained from a systematic variation of gear parameters—both for the macro geometry, (mainly the pressure angle) and the micro geometry (with tip reliefs of various kinds and profile crowning)–to show the influence of these parameters as modeled by the method being developed by ISO/TC 60 Working Group 6.

In addition to the regular FTM presentations, AGMA is also offering a number of educational courses:

- Gearbox Maintenance
- Why Bearings are Damaged
- How to Specify a Gear System
- Lubrication of Gearing
- High Profile Contact Ratio Gearing: Concept, Advantages, Comparison & Cautions
- Design of Net Shape Gears using Plastic and Powder Metal Materials
- Basics of Gearing
- Counterfeit Bearings: What You Need to Know
- Taming Tooth Deflections: The Case for Profile Modifications
- Materials Selection and Heat Treatment of Gears
- Cylindrical Gear Inspection: Chart Reading and Interpretation

For a full list of course titles and descriptions, visit *www.gearexpo.com/education*

An Arena of Color, Light and Concepts

Get Poetic and Pragmatic at Gear Expo's sister show, Heat Treat 2015

Erik Schmidt, Assistant Editor

When you look at the floor plan for the Cobo Center (Detroit, MI) from Oct. 20-22, the names on the lineup really shouldn't come as a great surprise.

Gear Expo and the ASM Heat Treating Society Conference & Exposition are both present and accounted for, co-located in the same showroom like peas in a very large pod — two different shows cut from the same cloth (or, if you want to be more on the nose: a high-powered gear grinder).

The industries really do go hand-in-hand (no heat treating, no gears, after all), and so it makes a perfect sort of sense that their respective biennial shows would exist side-by-side, conjoined at the hip.

Gears and heat treating — well, it just seems to work doesn't it?

And for even more serendipitous symmetry, get this: The show's host, the ASM International Heat Treating Society (HTS), was founded in 1913 *in Detroit*.

"Heat Treat 2015 is the premiere event organized by the HTS, the world's largest network of heat treaters," said Kelly Thomas, CEM, CMP senior manager of global events and exhibit sales for ASM. "HTS members work to provide events and services to serve their worldwide membership of captive and commercial heat treaters, equipment manufacturers, researchers, governments and technicians. We are excited to bring our members back to [Detroit] for Heat Treat 2015."

According to Thomas, the 28th Heat Treat Expo will feature nearly 200 exhibitors and 5,500 attendees covering 100,000 gross square feet of show floor.

"The HTS Exposition is a fun and exciting place to be," said Professor Richard Sisson, chairperson of the Heat Treat 2015 Organizing Committee. "The exhibitors are presenting their latest and greatest products. This is a chance to meet with the experts and learn the latest developments and future products and services that are in the works. If you are looking to purchase a new system, service or even software, this is the place for one-stop shopping. I learn something new with every visit to the show floor.

The show floor at the ASM Heat Treat Society Conference & Exposition.

"There will be over 130 technical sessions where attendees can learn the latest research and development in their respective fields, highlighted by the returning 'master series', a comprehensive technical program with three special lectures: 'Martens & Osmond: Hardenite Past & Future', 'Bainite and the Bainite Controversy' and 'Holloman and Jaffe on Tempering'.

"The Organizing Committee has been hard at work putting together the programming for Heat Treat, and I think that attendees will respond positively to the quality and variety of our technical sessions. In addition to topics such as 'Advances in Heat Treating', 'Quenching and Cooling', 'Applied Energy' and 'Processes and Applications', we will offer a new 'Applied Technology' track for operators and technicians.

"Industry leaders will also present their view of the future direction of the industry during a special panel session, 'New Directions and Opportunities in Heat Treating'. There are more opportunities to learn and exchange ideas than ever before, so I encourage heat treat professionals at any level to attend this show."

Though Gear Expo and Heat Treat Expo share a great expanse of common ground, they certainly aren't without distinct differences. Both shows were described as being akin to a "family reunion" — highly educational, mind expanding family reunions, to be fair — but it was Robert J. Madeira, vice president of heat treating at Inductoheat, Inc, who took up his quill and parchment to paint Heat Treat Expo in a most Shakespearian light.

"The first impression of stepping onto the Heat Treating exhibition show floor is one of purpose," Madeira said. "The everyday work of one's job transforms into an arena of color, light and concepts. The feeling of one person, one job, leaves and an overwhelming feeling of being a part of an enormous family of dedicated people.

"With each step the mind focuses on what the visual and sounds mean to our own experiences. Then there is a draw that develops, freezing one moment in the experience, whether a concept worth investigating or maybe a machine that would make our daily duties better. First step by step, then stride by stride, the reality of your purpose and what brought you here in the first place takes root. The day ends with a host of new ideas, greetings among old acquaintances and security that you are part of the ASM Heat Treating family who stands to support you doing a job that matters."

It's a nice bit of fresh air to get such poetic musings in an industry stuffed to the brim with pragmatism, but then again, solving problems is the main objective of Heat Treat 2015 — not soliloquies or bawdy puns.


Many heat treaters will be displaying furnaces on the show floor.

Photo by David Ropinski

And on top of several returning educational programs, there will be a handful of new learning opportunities for attendees to gather information to apply to their businesses back home.

"This year, we are highlighting the work of the LIFT Consortium (Lightweight Innovations for Tomorrow) during a special plenary session with Dr. Alan Taub, LIFT chief technical officer," said Thomas. "Since the conference was in Detroit, we really wanted to highlight a local organization that is doing great work for the industry.

"We are also featuring live demos and workshops. Attendees can learn about the latest equipment and technology through live demos on the expo floor — for free. It's also important that we continue to encourage the younger generation to explore a career in materials science and engineering. With that in mind, we have put together a 'This is Heat Treat' student program, which will provide students with a unique opportunity to network with professionals in the industry and learn about all aspects of the field through technical programs."

So come and learn and listen and then depart on Oct. 22 with knowledge in your mind and poetry in your heart, leaving both Gear Expo and Heat Treat Expo behind until 2017, proclaiming to no one and everyone in eloquent tongue like the Bard of Avon:

Good night, good night! Parting is such sweet sorrow.

For more information:

ASM International
Phone: (440) 338-5151
www.asminternational.org

Gear Mathematics for Bevel & Hypoid Gears

Hermann J. Stadtfeld

Bevel Gear Technology

Chapter 2

This article is the third installment in *Gear Technology's* series of excerpts from Dr. Hermann J. Stadtfeld's book, *Gleason Bevel Gear Technology*. The first two excerpts can be found in our June 2015 and July 2015 issues.

The goal of the following sections is to develop a deeper understanding of the function, limits and possibly the not fully utilized possibilities of bevel and hypoid gears.

The gear mathematics developed by the author is based on a triangular vector model that presents a comprehensive tool for simple observations in the generating gear, up to complex three-dimensional developments. Many types of bevel and hypoid gears can be observed and manipulated with this model — without alteration of the notation. However, at the most complex level the lengths and directions of the vectors change according to higher-order functions, depending on the rotational position of the generating gear (Refs. 1–2).

The first chapter of this book — "Nomenclature and Definition of Symbols" — should help to avoid or minimize the interruption of the flow in the gear theoretical developments with definitions of formula symbols.

At the beginning of this chapter the development of a face-milled, conjugate spiral bevel gearset is conducted. Next, an analogue face-hobbed bevel gearset is derived that in a third step is converted to a non-generated (Formate) version. In step four an offset is added to the Formate spiral bevel gearset that results in a hypoid gearset. Consequences regarding the introduction of the hypoid offset and unique facts regarding general spatial transmissions are also discussed in this chapter. At the end of this chapter, length and profile crowning are added to the Formate bevel gearset that delivers a practical-use, angular transmission as it is used in industrial gear boxes; the reader will be able to apply the derivations to any other bevel and hypoid gearset. With the results of each calculation step, basic settings are computed as they are commonly used by modern CNC bevel gear generators in order to cut or grind real bevel gearsets. **—Hermann J. Stadtfeld**

Development of a Face-Milled Spiral Bevel Gearset

The following data are given for this example:

Method	single indexing with Gleason straddle cut	
Tooth depth along face width	parallel	
Shaft angle	Σ	$=90°$
Offset	$a=TTX$	$=0$ mm
Number of pinion teeth	z_1	$=13$
Number of ring gear teeth	z_2	$=35$
Outer ring gear pitch diameter	D_{02}	$=190$ mm
Face width	$b_1=b_2$	$=30$ mm
Mean spiral angle	$\beta_1=\beta_2$	$=30°$
Pinion hand of spiral	$HOSP_1$	= left-hand
Nominal cutter radius	R_w	$=76.2$ mm (6")
Pressure angle	$\alpha_C=\alpha_D$	$=20°$
Profile shift factor	$x=x_1=-x_2$	$=0$
Tooth depth factor	f_{Depth}	$=1$
Top-root-clearance factor	f_{CL}	$=0.2$
Profile side shift factor	$x_S=x_{S1}=-x_{S2}$	$=0$
Pinion addendum	$h_{K1}=(f_{Depth}+x)\times m_n$	$=1.0m_n$
Pinion dedendum	$h_{F1}=(f_{Depth}+f_{CL}-x)\times m_n$	$=1.2m_n$
Ring gear addendum	$h_{K2}=(f_{Depth}-x)\times m_n$	$=1.0m_n$
Ring gear dedendum	$h_{F2}=(f_{Depth}+f_{CL}+x)\times m_n$	$=1.2m_n$

Wanted are the design data of the pinion and ring gear blanks, as well as the cutter specifications and basic machine settings.

Calculation of Blank Data

The calculation begins with the computation of the ring gear blank data. The geometrically relevant parameters are shown in Figure 1. The position of the teeth relative to the blank coordinate system of a bevel gear blank is satisfactorily defined with the following data: *RAUR*; *RINR*; γ; *ZFKR*; *ZTKR*; and *ZKKR*. Those blank data are calculated from the given data as follows:

$$z_1/z_2=\sin\gamma_1/\sin\gamma_2 \tag{1}$$

(*Regarding Eq.1, see also Eq.'s 10–12, Chapter 1*)

The sum of the pitch angles of spiral bevel gears is equal to the shaft angle:

$$\gamma_1+\gamma_2=\Sigma \rightarrow \gamma_1=\Sigma-\gamma_2$$

In case of a 90° shaft angle the relationship will simplify to:

$$\gamma_1=\arctan(z_1/z_2)=20.38 \tag{2}$$

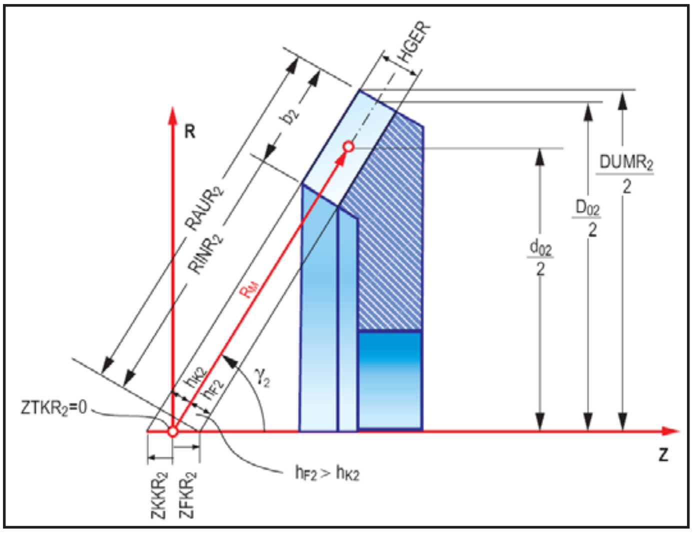

Figure 1 Graphical specification of ring gear blank.

$$\gamma_2 = 90° - \gamma_1 = 69.62° \quad (3)$$

Now the different cone distances, normal module, and mean pitch diameter can be calculated:

$$R_M = D_{02} / 2 / sin\gamma_2 - b_2 / 2 = 86.34\,\text{mm} \quad (4)$$

$$d_{02} = 2 \times R_M \times sin\gamma_2 = 161.87\,\text{mm} \quad (5)$$

$$m_f = d_{02} / z_2 = 4.63\,\text{mm} \quad (6)$$

$$m_n = m_f \times cos\beta_2 = 4.00\,\text{mm} \quad (7)$$

$$h_{K2} = 1.0 \times \text{m}_\text{n} = 4.00\,\text{mm} \quad (8)$$

$$h_{F2} = 1.2 \times \text{m}_\text{n} = 4.80\,\text{mm} \quad (9)$$

$$\boldsymbol{RINR_2} = R_M - b_2/2 - h_{F2} / tan\gamma_2 = 69.56\,\text{mm} \quad (10)$$

$$\boldsymbol{RAUR_2} = RINR_2 + b_2 = 99.56\,\text{mm} \quad (11)$$

The positions of the cone apexes, the whole depth and the maximal ring gear diameter are:

$$\boldsymbol{ZFKR_2} = +h_{F2} / sin\gamma_2 = 5.12\,\text{mm} \quad (12)$$

$$\boldsymbol{ZKKR_2} = -h_{K2} / sin\gamma_2 = -4.27\,\text{mm} \quad (13)$$

$$\boldsymbol{ZTKR_2} = 0.00\,\text{mm} \quad (14)$$

$$\text{HGER} = h_{K2} + h_{F2} = 8.80\,\text{mm} \quad (15)$$

$$DUMR_2 = 2(RAUR_2 \times sin\gamma_2 + HGER \times cos\gamma_2) = 192.78\,\text{mm} \quad (16)$$

Pinion pitch angle and mean cone distance *RM* (which is equal for pinion and gear) have already been calculated in the course of the gear blank calculations. Only the inner and outer cone distance — as well as the cone apex positions — remain in the pinion blank calculation (Fig. 2). The value for addendum and dedendum is equal to the ring gear values, since no profile shift was applied to the present example:

$$h_{K1} = 1.0 \times m_n = 4.00\,\text{mm} \quad (17)$$

$$h_{F1} = 1.2 \times m_n = 4.80\,\text{mm} \quad (18)$$

$$\boldsymbol{RINR_1} = R_M - b_1/2 - h_{F1} / tan\gamma_1 = 58.42\,\text{mm} \quad (19)$$

$$\boldsymbol{RAUR_1} = RINR_1 + b_1 = 88.42\,\text{mm} \quad (20)$$

The positions of the pinion cone apexes are:

$$\boldsymbol{ZFKR_1} = + h_{F1} / sin\gamma_1 = 13.78\,\text{mm} \quad (21)$$

$$\boldsymbol{ZKKR_1} = -h_{K1} / sin\gamma_1 = -11.49\,\text{mm} \quad (22)$$

$$\boldsymbol{ZTKR_1} = 0.00\,\text{mm} \quad (23)$$

All bold-printed parameters in this section are required for the definition of the toothed cones relative to the remaining pinion and gear blank. Those design data are summarized in Tables 1 and 2.

Calculation of Cutter Head Geometry

The nominal cutter radius was chosen a little bit smaller than the mean cone distance R_M. This seems to be a good choice for a face-milled (single indexing process) bevel gearset if large load-affected deformations are anticipated.

Although the nominal cutter radius is already given, the actual radii of inside and outside blades for gear and pinion cutter head have to be calculated depending on the chosen cut-

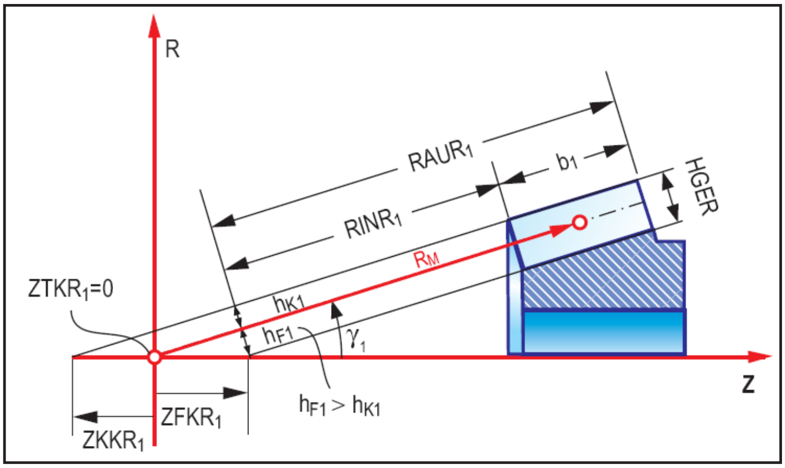

Figure 2 Pinion blank specification.

Table 1 Numerical ring gear blank specifications

Ring Gear - Blank Data			
Variable	**Explanation**	**Value**	**Dimension**
z_2	number of ring gear teeth	35	-
$RINR_2$	inner cone distance (along root line)	69.56	mm
$RAUR_2$	outer cone distance (along root line)	99.56	mm
$GATR_2 = \gamma_2$	pitch angle	69.62	°
$GAKR_2$	face angle	69.62	°
$GAFR_2$	root angle	69.62	°
$ZTKR_2$	pitch apex to crossing point	0.00	mm
$ZKKR_2$	face apex to crossing point	–4.27	mm
$ZFKR_2$	root apex to crossing point	5.12	mm
$DOMR_2 = mf_2$	face module	4.63	mm
HGER	whole depth of teeth	8.80	mm

Table 2 Numerical pinion blank specifications

Pinion - Blank Data			
Variable	**Explanation**	**Value**	**Dimension**
z_1	number of teeth pinion	13	-
$RINR_1$	inner cone distance (along root line)	58.42	mm
$RAUR_1$	outer cone distance (along root line)	88.42	mm
$GATR_1 = \gamma_1$	pitch angle	20.38	°
$GAKR_1$	face angle	20.38	°
$GAFR_1$	root angle	20.38	°
$ZTKR_1$	pitch apex to crossing point	0.00	mm
$ZKKR_1$	face apex to crossing point	–11.49	mm
$ZFKR_1$	root apex to crossing point	13.78	mm
$DOMR_1 = mf_1$	face module	4.63	mm
HGER	whole depth of teeth	8.80	mm

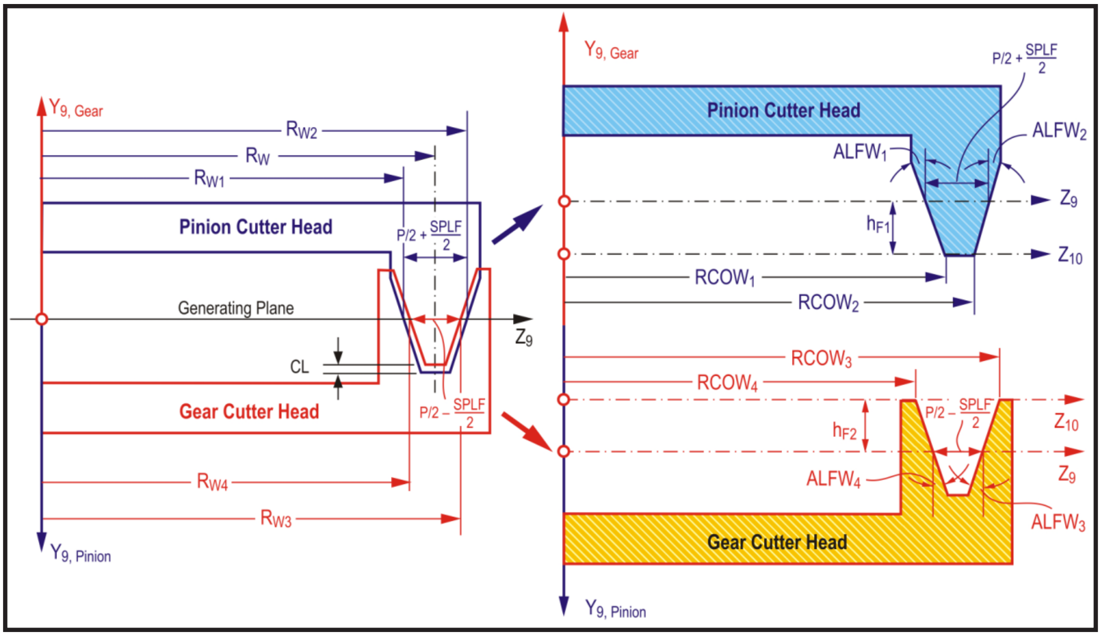

Figure 3 Pinion and ring gear blade geometry.

ting method. Since the method is Gleason straddle cut, the pinion blades cut a tooth slot while the gear blades are cutting a tooth — i.e., two proceeding "half-slots."

Figure 3 shows (left) the corresponding blades of pinion and ring gear (*see also Figs. 12–15, Chap. 1, Part II, July* Gear Technology). The generating plane intersects with the blades at the height of the calculation point. In order to generate the correct tooth thickness, the distance from the calculation point on the inside blade to the calculation point on the outside blade has to be equal to one-half of the normal pitch, plus one-half of the normal backlash. The blade tips extend about the tooth dedendum (h_F) — beyond the generating plane (blade dedendum). The blade contours in Figure 3 are therefore not exactly congruent to each other, but by the backlash values different on the flanks and by the clearance values different at the roots (tips).

Table 3 Cutter head and blade specifications

Cutter Head and Blade Data			
Variable	**Explanation**	**Value**	**Dimension**
$S8901_{1,2}$	reference point to blade tip pinion	4.80	mm
$S8903_{3,4}$	reference point to blade tip gear	4.80	mm
$WAME_1$	blade phase angle pinion convex	0.00	°
$WAME_2$	blade phase angle pinion concave	0.00	°
$WAME_3$	blade phase angle ring gear convex	0.00	°
$WAME_4$	blade phase angle ring gear concave	0.00	°
$XSME_{1,2}$	blade offset in pinion cutter head	0.00	mm
$XSME_{3,4}$	blade offset in ring gear cutter head	0.00	mm
$RCOW_1$	cutter point radius pinion inside blade	74.80	mm
$RCOW_2$	cutter point radius pinion outside blade	77.59	mm
$RCOW_3$	cutter point radius ring gear inside blade	81.09	mm
$RCOW_4$	cutter point radius ring gear outside blade	71.31	mm
$ALFW_1$	blade angle pinion inside blade	20.00	°
$ALFW_2$	blade angle pinion outside blade	20.00	°
$ALFW_3$	blade angle ring gear inside blade	20.00	°
$ALFW_4$	blade angle ring gear outside blade	20.00	°

Since the aim in this first flank generating example is to achieve a conjugate pair, it seems appropriate to set the backlash SPLF for this example to zero.

As a result the following calculations will sufficiently determine the required cutter head and blade parameters:

$$t_B = \pi \times m_n = 12.57\,\text{mm} \tag{24}$$

$$SPLF = 0.00\,\text{mm} \tag{25}$$

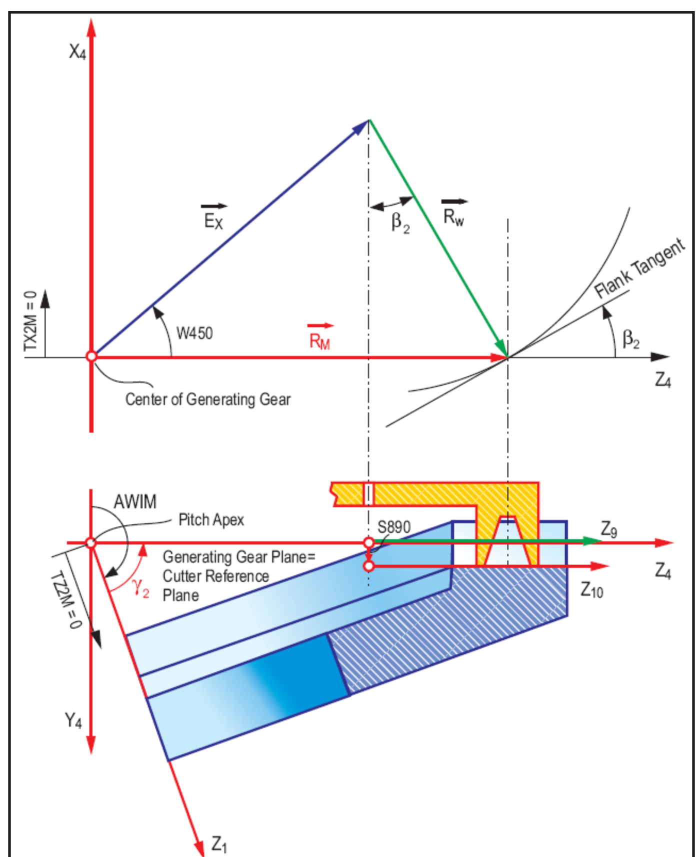

Figure 4 Ring gear, basic machine model: upper graphic — front view; lower graphic — top view.

$$ALFW_1 = ALFW_2 = ALFW_3 = ALFW_4 = \alpha = 20.00° \tag{26}$$

$$RCOW_1 = R_W - t_B/4 - SPLF/4 + h_{F1} \times tanALFW_1 = 74.80\,mm \tag{27}$$

$$RCOW_2 = R_W + t_B/4 + SPLF/4 - h_{F1} \times tanALFW_2 = 77.59\,mm \tag{28}$$

$$RCOW_3 = R_W + t_B/4 - SPLF/4 + h_{F2} \times tanALFW_3 = 81.09\,mm \tag{29}$$

$$RCOW_4 = R_W - t_B/4 + SPLF/4 - h_{F2} \times tanALFW_4 = 71.31\,mm \tag{30}$$

$$S890_1 = S890_2 = h_{F1} = 4.80\,mm \tag{31}$$

$$S890_3 = S890_4 = h_{F2} = 4.80\,mm \tag{32}$$

All parameters printed in bold are required for the definition of the pinion and ring gear cutter heads required. Those results are summarized in Table 3.

Calculation of Basic Settings for the Cutting Machine

The basic machine, as defined by Weck and Schriefer (Ref. 3), follows a clear systematic with 10 coupled Cartesian coordinate systems, beginning with system 1, which defines the work gear position via system 4 which defines the generating gear plane with its axes axis X_4–Z_4 and the generating gear axis with its axis Y_4 to system 10, which defines the cutter head axis with Y_{10} and the position of the blade origin (blade tip) with Z_{10}.

Figure 4 only includes the systems 1, 4, 9 and 10—which are required for the basic bevel gear calculation covered in this chapter.

The observations and machine setting calculation are first conducted for the ring gear and then the pinion. First we observe the generating gear plane X_4–Z_4 (Fig. 4), in which the mean cone distance R_M is drawn from the origin of the coordinate system along the positive Z_4 axis. At the tip of the R_M vector, the mean face position is located, which is the point of a curved tooth, where the spiral angle β has to be equal 30°. The spiral direction shown in Figure 4 is consistent with a right-hand ring gear that has a mating pinion with a left-hand spiral direction (the view in Figure 4 is directed to the back-side of the ring gear). The spiral angle in each point of a flank is the angle in the generating gear plane between the flank tangent and the connecting line to the generating gear axis. In Figure 4 it is the angle β between flank tangent and Z_4 axis. This now allows the positioning of the cutter radius vector R_W with its tip perpendicular to the flank tangent. The solution vector in this observation is the eccentricity vector E_X, which already includes a number of machine settings.

$$\vec{E}_X = \vec{R}_M - \vec{R}_W \tag{33}$$

$$\text{With:} \vec{R}_M = \{0., 0., R_M\} = \{0., 0., 86.34\} \tag{34}$$

$$\vec{R}_W = R_W\{-cos\,\beta, 0., sin\,\beta\} \tag{35}$$

$$\vec{R}_W = \{-R_W cos\,\beta, 0., R_W sin\,\beta\} = \{-65.99, 0., 38.10\} \tag{36}$$

$$\text{Resulting in:} \vec{E}_X = \{65.99, 0., 48.24\} \tag{37}$$

Utilizing the E_X vector, the following machine settings can be calculated:

$$\text{Center roll position: } W450_{3,4} = arctan\,(E_{XX}/E_{XZ}) = 53.83° \tag{38}$$

$$\text{Radial distance: } TZMM_{3,4} = \sqrt{E_{XX}^2 + E_{XZ}^2} = 81.74\,mm \tag{39}$$

$$\text{Sliding base: } TYMM_{3,4} = E_{XY} = 0.00\,mm \tag{40}$$

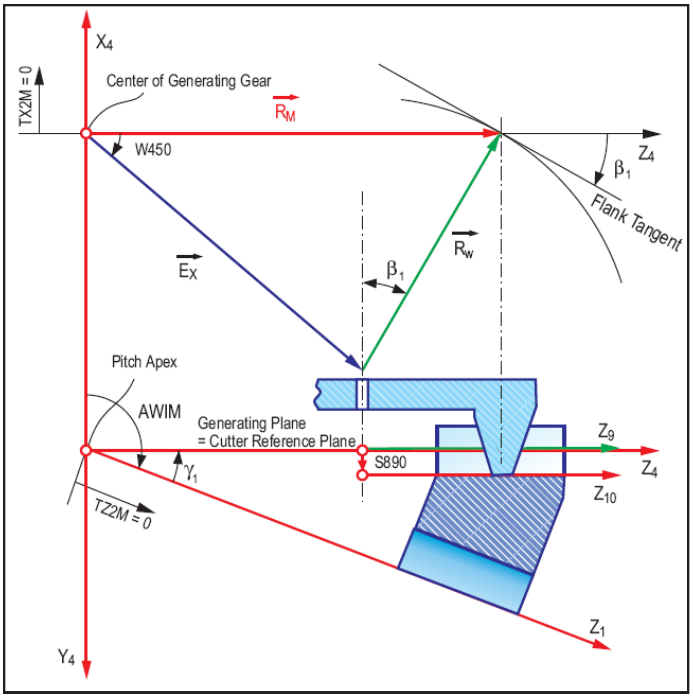

Figure 5 Pinion basic machine model: upper graphic—front view; lower graphic—top view.

Additional machine settings can be found from the graphical relationship in Figure 4:

$$\text{Machine root angle: } AWIM_{3,4} = -90° - \gamma_2 = -159.62° \tag{41}$$

$$\text{Machine center to crossing point: } TZ2M_{3,4} = 0.00\,mm \tag{42}$$

$$\text{Offset in the machine: } TX2M_{3,4} = 0.00\,mm \tag{43}$$

Further values such as cutter head tilt $WXMM_{3,4}$ and tilt orientation $WYMM_{3,4}$ are also zero in the observed conjugate design.

For the exact definition of the ring gear to be generated, the ratio of roll between generating gear and work gear is still missing. Using (Chapter 1, Part II, July *Gear Technology*) Equations 11 and 12, the ratio of roll can be computed with:

$$UDIF_{3,4} = sin\gamma_2 = 0.937404 \tag{44}$$

The ratio of roll number requires at least a mantissa with 6 digits, since the influence onto the gear geometry is correspondingly sensitive.

The second part of the machine setting calculations, the demonstrated gear calculations are repeated analogous for the pinion. At first, we observe the generating gear plane X_4–Z_4 (Fig. 5) in which the mean cone distance R_M is plotted from the coordinate origin along the positive Z_4 axis.

At the tip of the R_M vector, the mean face position of a curved tooth is located whose tangent in this point should show a spiral angle β of 30°. The spiral direction shown in Figure 5 is consistent with a left-hand pinion (in Fig. 5 (top) the view is directed from the back to the pinion). The spiral angle in each point of a flank is the angle in the generating gear plane between the flank tangent and the connecting line to the generating gear axis. In Figure 5 it is the angle β between flank tangent and Z_4 axis. This allows now the positioning of the cutter radius vector R_W with its tip perpendicular to the flank tangent. The solution vector

Table 4 Geometrical and kinematical machine settings

Variable	Explanation	Value	Dimension
Machine Basic Settings			
$WXMM_{1,2}$	cutter head tilt pinion	0.00	°
$WXMM_{3,4}$	cutter head tilt ring gear	0.00	°
$WYMM_{1,2}$	swivel angle pinion	0.00	°
$WYMM_{3,4}$	swivel angle ring gear	0.00	°
$W450_{1,2}$	center of roll position pinion	–53.83	°
$W450_{3,4}$	center of roll position ring rear	53.83	°
$TYMM_{1,2}$	sliding base position pinion	0.00	mm
$TYMM_{3,4}$	sliding base position ring gear	0.00	mm
$TZMM_{1,2}$	radial distance pinion	81.74	mm
$TZMM_{3,4}$	radial distance ring gear	81.74	mm
$AWIM_{1,2}$	machine root angle pinion	–110.38	°
$AWIM_{3,4}$	machine root angle ring gear	–159.62	°
$TX2M_{1,2}$	pinion offset in the machine	0.00	mm
$TX2M_{3,4}$	ring gear offset in the machine	0.00	mm
$TZ2M_{1,2}$	machine center to crossing point pinion	0.00	mm
$TZ2M_{3,4}$	machine center to crossing point gear	0.00	mm
$UTEI_{1,2}$	indexing ratio of pinion cutting	0.00	-
$UTEI_{3,4}$	indexing ratio of ring gear cutting	0.00	-
$UDIF_{1,2}$	ratio of roll for pinion cutting	0.348245	-
$UDIF_{3,4}$	ratio of roll for gear cutting	0.937404	-

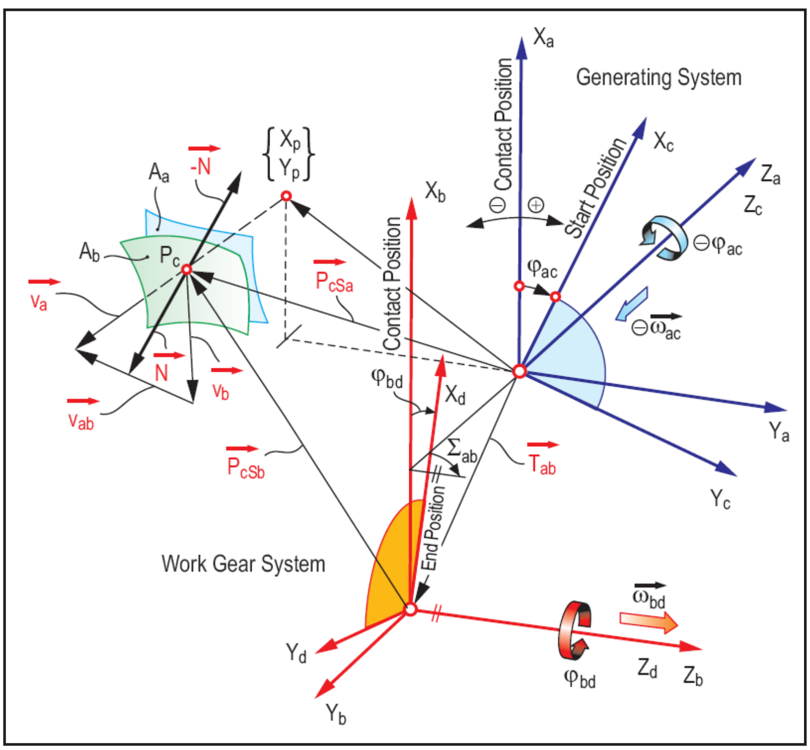

Figure 6 Kinematical relationships to solve gearing law equation.

in this observation is the eccentricity vector E_X, which already includes a number of machine settings.

$$\text{With:}\ \vec{R}_W = \{R_W \cos\beta, 0., R_W \sin\beta\} = \{65.99, 0., 38.10\} \tag{45}$$

$$\text{Resulting in:}\ \vec{E}_X = \{-65.99, 0., 48.24\} \tag{46}$$

By means of the E_X vector the following machine settings can be calculated:

$$\text{Center of roll: } \boldsymbol{W450_{1,2}} = \arctan\,(E_{XX}/E_{XZ}) = -53.83° \tag{47}$$

$$\text{Radial distance: } \boldsymbol{TZMM_{1,2}} = \sqrt{E_{XX}^2 + E_{XZ}^2} = 81.74\,\text{mm} \tag{48}$$

$$\text{Sliding base: } \boldsymbol{TYMM_{1,2}} = E_{XY} = 0.00\,\text{mm} \tag{49}$$

Additional machine settings can be found from the graphical relationship in Figure 5:

$$\text{Machine root angle: } \boldsymbol{AWIM_{1,2}} = -90° - \gamma_1 = -110.38° \tag{50}$$

$$\text{Machine center to crossing point: } \boldsymbol{TZ2M_{1,2}} = 0.00\,\text{mm} \tag{51}$$

$$\text{Offset in the machine: } \boldsymbol{TX2M_{1,2}} = 0.00\,\text{mm} \tag{52}$$

Further values, such as cutter head tilt $\boldsymbol{XMM_{1,2}}$ and tilt orientation $\boldsymbol{WYMM_{1,2}}$ are also zero in the observed conjugate design.

For the exact definition of the pinion to be generated, the ratio of roll between generating gear and work gear is still missing. From (Chap. 1, Part II, July *Gear Technology*) Equations 11 and 12, the ratio of roll can be computed with:

$$\boldsymbol{UDIF_{1,2}} = \sin\gamma_{12} = 0.348245 \tag{53}$$

All bold-printed values calculated in this section are input values for a bevel gear cutting simulation program, whose functionality is discussed in the next section. The machine settings are summarized in Table 4.

Simulation of the Gear Cutting Process and Tooth Contact Analysis of Face-Milled Spiral Bevel Gearset Example

A typical example of a simulation program is the FVA *Bevel-Gear-Chain*, which was developed at the Machine Tool Laboratory of the University of Aachen (Ref. 3). Some of today's commercially available software systems for bevel gear calculation and optimization have been developed on the basis of this universal software tool. The analysis and experimentation, introduced in the following chapters, are also based on an advanced version of the FVA *Bevel-Gear-Chain*. This software utilizes the same data as is used in modern free-form bevel gear cutting and grinding machines for the manufacture of real bevel gear sets. The core of this program is a flank generating module that applies the coordinate systems of Figures 4 and 5 to model a generating gear.

In the generating gear system X_c–Y_c–Z_c (system S_c) in Figure 6, a generating gear flank point is given by position vector P_{cSa} and normal vector N. The application of the gearing law (*Chap. 1, Eq. 1, June* Gear Technology) delivers the rotation angle φ_{ac} into the contact position (system S_a), in which the solution point P_c and the solution normal vector $-N$ is found in a coordinate system X_b–Y_b–Z_b (system S_b) as position vector P_{cSb}. In order to find a comprehensive flank as a result of computing a larger amount of individual points, which are necessary in order to define an entire flank (symbolized with surface A_b), the solution point has to be rotated "back" in its final position (system S_d). The angle φ_{bd} between the contact position and the final position is found by multiplication of the rotation angle φ_{ac} (in the generating gear system) with the ratio of roll. Figure 6 also shows that in the contact position the relative velocities $v_{ab} = v_a - v_b$ — and therefore the sliding and rolling velocities — can be determined rather easily.

The cutting edges, which are defined in the input data as lines, are treated in the flank surface generation program as a summation of discrete points; the rotation of the cutter head delivers a velocity vector in the respective cutting edge point. The vector product between the velocity vector and the cutting edge tangential vector results in a normal vector, which together with the cutting edge point, by solving the gearing law (as explained in Fig. 6), delivers a point and a normal vector of the work gear flank that is subject to the generating process. In a do loop the given number of cutting edge points — *YP*10 — are processed for each angular cutter head position (Fig. 7).

The result is the so-called "natural flank grid," which ends at the root fillet but extends beyond the tooth boundaries in all other directions. It becomes evident from Figure 7 that the distortions of the natural flank grid are caused by the changing generating conditions. In order to achieve a flank grid — which fits the real tooth boundaries — the desired flank grid, known until now only in the *YRI-ZRI* plane, is correlated to the natural grid (projected into the *YRI-ZRI* plane). The distance of a respective point of the flank grid to the closest point of the natural grid leads to new given cutter head angle $\varphi 89Y$ and cutting edge point *YP*10. The generating process with this new point will reduce the distance between the desired flank point and the actual generated point. This procedure is repeated in a semblance of an iteration until the distance lies within an iteration limit of usually 0.0002 mm. Flank surface points calculated with this method show an accuracy of 10^{-5} mm. The normal directions within the flank working area without undercut have deviations below half an angular minute.

The resulting flank surfaces are interpolated with bi-cubical spines in order to provide any in-between point with high accuracy during the following roll simulation between pinion and gear.

For the roll simulation the pinion flanks with their coordinate system *XRI-YRI-ZRI* are located in the correct position relative to the ring gear flanks with their coordinate system *XRA-YRA-ZRA*. This relative position is defined by the shaft offset vector *TT* and the shaft angle Σ. The signified blanks of pinion and ring gear are shown in Figure 8. In the present example the shaft angle is 90° and the

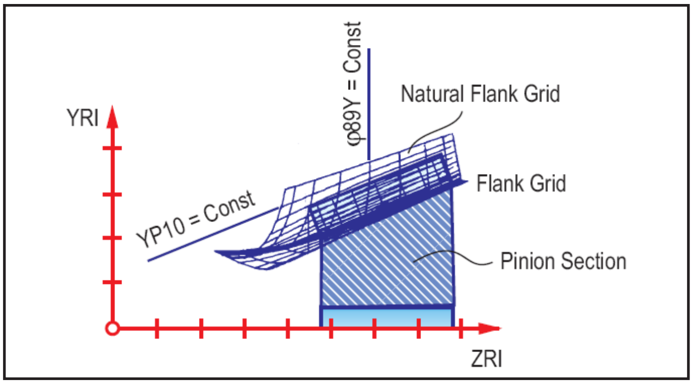

Figure 7 Flank grid and natural flank grid.

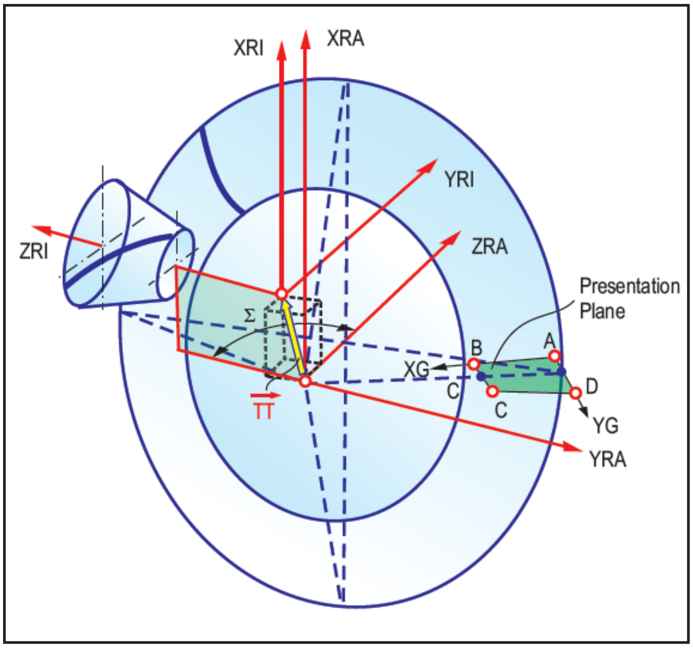

Figure 8 Arrangement of pinion and ring gear for roll simulation.

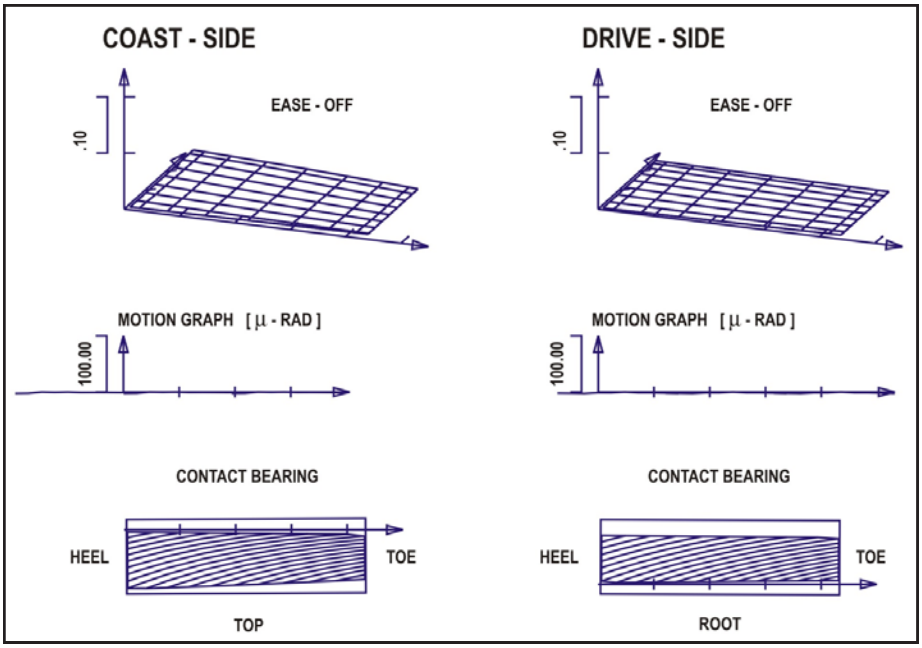

Figure 9 Graphical results of roll simulation (TCA) of face-milled gearset.

TT vector is zero — which defines a spiral bevel gearset without hypoid offset. In order to evaluate the properties of the gearset under load with deflected gear box housing, it is possible to use shaft angles that deviate from 90° together with any offset vector *TT*. The results of a roll simulation are Ease-Off, tooth contact pattern, and motion transmission error. In order to correlate those results in a meaningful way with the tooth flanks of the evaluated gearset, the flank projection into the plane *ZRA-YRA* (points *A, B, C* and *D*) is defined as presentation plane (Fig. 8). The Ease-Off is a three-dimensional graphic of the flank deviations from a conjugate pair; it is calculated by rolling the pinion flank "into" the gear coordinate system according to the gearing law, resulting in a virtual gear flank that is conjugate to the actual pinion flank. This conjugate gear flank will then be compared to the present gear flank, where all differences in arc length are plotted point-by-point in ordinate direction into the Ease-Off graphic.

If both mating bevel gears have conjugate manufacturing data, then the Ease-Off graphic has no deviations in ordinate direction. Also, if the pinion flanks and gear flanks have spiral angle errors of equal amounts, the Ease-Off graphic will not show any deviation. And although the individual gears are considered incorrect in this case, they will roll conjugate with each other, which subsequently leads to an Ease-Off without any ordinate values. Further explanations regarding roll simulation and tooth contact analysis results are presented in Chapter 4 (*Nov.-Dec. Gear Technology*).

The roll simulation analyses results of the bevel gearset calculated in this chapter (in its theoretical zero position) can be observed in Figure 9. In the left column the results of the coast-side are shown, which is the combination of the convex pinion flank and the concave ring gear flank. In the right column the results of the drive-side are shown, which is the combination of the concave pinion flanks and the convex ring rear flanks. The drive-side is the preferred flank combination; the reasons for the superior rolling conditions of the drive-side are discussed in Chapter 4.

Just like the theoretical goal, a conjugate gear pair with zero Ease-Off was created. The motion graphs in the middle section of Figure 9 only show some "numerical noise" along the abscissa of the diagrams, meaning there is no transmission error in any of the roll positions. The contact bearings in the lower section of Figure 9 show contact lines, which extend inside the entire flank working areas.

The flank working area is the common surface between the active pinion flank that is rolled with the active ring gear flank. For a better understanding of the flank working area, the previously mentioned rolling of the pinion flank into the ring gears coordinate system can be employed. If the resulting conjugate ring gear flank is projected into the presentation plane (rotational projection) where it overlays the area of the actual ring gear flank (which is already projected into the presentation plane), then the working area is defined as the area where both the conjugate gear flank and the real gear flank exist. It seems obvious that no flank contact or correct rolling outside of this area is possible. On the heel and toe borders only "air" is present outside of the working area of one of the two flanks (or both). At top and root either the rolled on top edge of the one flank, or the border to the root fillet of the other flank is the limitation. Caution is required if the root fillet border is the limitation. In many cases this leads to interferences that can cause noise and surface damage. The flank working areas in Figure 9 end along the horizontal coordinate axis (coast-side on the top, drive-side on the bottom) that represent the transition line between flank and ring gear root fillet.

On the opposite sides (coast-side on the bottom, drive-side on the top) exists a non-working area between ring gear face edge and tooth contact zone, pointing to a "pulled-up" pinion root transition that migrates into undercut in the toe region. A pulled-up pinion root transition is more dangerous than undercut, since interferences can occur that can lead to flank surface damage, as mentioned above. The result in many cases is the population of pitting and even tooth fracture. Intentionally, no profile shift was applied in the present example in order to demonstrate the motivation to introduce a profile shift. In a simplified observation a negative ring gear profile shift with a magnitude equal to the white zone at the top of the ring gear tooth is required (app. 1.75 mm).

Profile shift:

$$\Delta h = x_2 \times m_n = x_2 \times 4.00\,\text{mm} = -1.75\,\text{mm} \tag{54}$$

$$x_2 = -0.448 \tag{55}$$

In bevel and hypoid gears, generally the *V*0 system is applied, which allows determination of the pinion profile shift as:

$$V0 \equiv x_1 + x_2 = 0.00 -> x_1 = -x_2 = 0.448 \tag{56}$$

This will shorten the gear addendum and lengthen the gear dedendum, which will result in a match between the common flank area and the active flank working area. The region with incorrect roll conditions along the pinion root will be eliminated by using the optimal part of the involute. The white region along the ring gear top will now be filled with contact lines and the active flank working area will be maximized.

Dr. Hermann J. Stadtfeld received in 1978 his B.S. and in 1982 his M.S. degrees in mechanical engineering at the Technical University in Aachen, Germany; upon receiving his Doctorate, he remained as a research scientist at the University's Machine Tool Laboratory. In 1987, he accepted the position of head of engineering and R&D of the Bevel Gear Machine Tool Division of Oerlikon Buehrle AG in Zurich and, in 1992, returned to academia as visiting professor at the Rochester Institute of Technology. Dr. Stadtfeld returned to the commercial workplace in 1994 — joining The Gleason Works — also in Rochester — first as director of R&D, and, in 1996, as vice president R&D. During a three-year hiatus (2002–2005) from Gleason, he established a gear research company in Germany while simultaneously accepting a professorship to teach gear technology courses at the University of Ilmenau. Stadtfeld subsequently returned to the Gleason Corporation in 2005, where he currently holds the position of vice president, bevel gear technology and R&D. A prolific author (and frequent contributor to Gear Technology), Dr. Stadtfeld has published more than 200 technical papers and 10 books on bevel gear technology; he also controls more than 50 international patents on gear design, gear process, tools and machinery.


GoldENgineering
Gear Up with Ingersoll!
Your most experienced source in the design & manufacture of ICI gear machining tools
Gear Shapers
• Roughing at three to four times faster than conventional methods
Gear Gashers
• Custom indexable roughing & finishing cutters
• Designed to your specific tooth profile
Hobbing Cutters
• Segmented designs with angled screw holes for simple, accurate indexing
• Single, double and even triple-start designs
Member IMC Group
Ingersoll
Cutting Tools
845 South Lyford Rd · Rockford, IL 61108-2749 · 866/690-1859 · Fax: 815/387-6968 · www.ingersoll-imc.com

Tooth Flank Fracture – Basic Principles and Calculation Model for a Sub-Surface-Initiated Fatigue Failure Mode of Case-Hardened Gears

Dipl.-Ing. I. Boiadjiev, Dr.-Ing. J. Witzig, Dr.-Ing. T. Tobie
and Prof. Dr.-Ing. K. Stahl

Cracks initiated at the surface of case-hardened gears may lead to typical life-limiting fatigue failure modes such as pitting and tooth root breakage. Furthermore, the contact load on the flank surface induces stresses in greater material depth that may lead to crack initiation below the surface if the local material strength is exceeded. Over time the sub-surface crack propagation may lead to gear failure referred to as "tooth flank fracture" (also referred to as "tooth flank breakage"). This paper explains the mechanism of this subsurface fatigue failure mode and its decisive influence factors, and presents an overview of a newly developed calculation model.

Introduction

Case-hardened gears are highly loaded machine elements used for power transmission in many field applications. But one factor that can limit the life cycle of such highly loaded gears is load-carrying capacity. To ensure safe operation of these gears, reliable calculation and test methods are needed. With a variation in material type and heat treatment parameters, it is possible to influence the flank load-carrying capacity. Extensive theoretical and experimental investigations have been carried out in order to derive calculation methods and an optimized heat treatment — mostly for the fatigue failure pitting mode that occurs as a result of cracks initiated at or just below the flank surface. What is more, in many field applications of highly loaded, case-hardened gears, failures also occur due to primary crack initiation deep below the material surface. Affected are not only case-hardened cylindrical gears but also bevel and hypoid gears for different applications. Such failures were also found in nitrided and induction-hardened gears. The consequence of such failures with crack initiation below the flank surface is, in almost all cases, the spontaneous and complete loss of drive of the affected gear set. Because the crack propagates below the surface, it is almost impossible to detect at an early stage with visual inspections. Whether a failure occurs at the surface or at greater material depth, it is influenced by local contact load that depends on the gear flank geometry — in particular the equivalent radius of curvature — and by the local material strength. The in-depth strength of the material results primarily due to heat treatment. To predict a failure, the load curve has to be set in relation to the strength curve over the material depth. On gear sets with relatively small equivalent radius of curvature, the maximum Hertzian stress occurs relatively near the surface. Furthermore, the influences of oil and surface roughness should be taken into account, as they can lead to a substantial increase of the local loads in this area. Under the condition of constant Hertzian stress, a larger equivalent radius of curvature results in shifting the maximum Hertzian stress towards a larger material depth

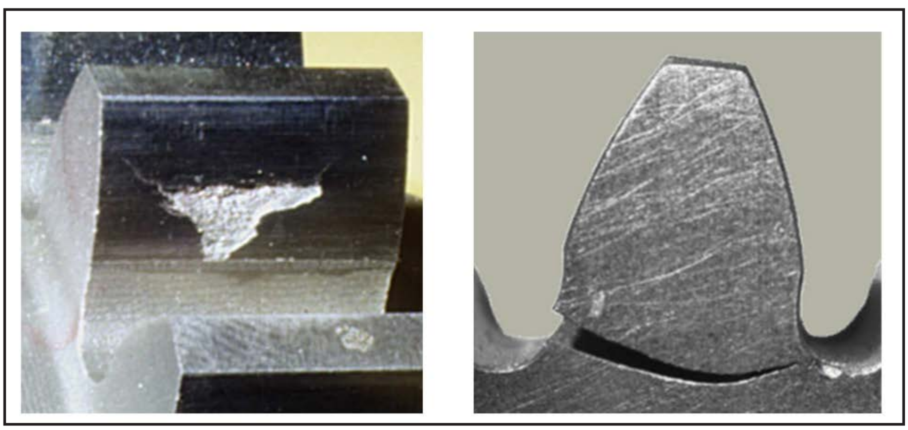

Figure 1 Typical surface gear failure examples – pitting (left) and tooth root breakage (right)

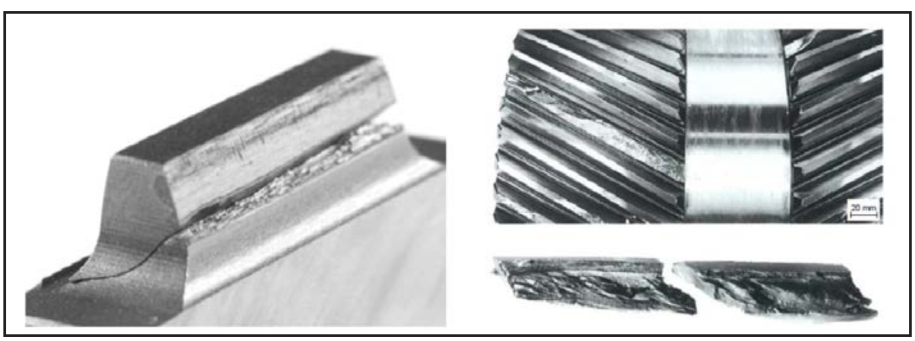

Figure 2 Examples of tooth flank fracture – test gear from (19) (left), turbine gear from (2) (right)

This paper was originally presented at the 2014 International Gear Conference, Lyon Villeurbanne, France and is republished here with the authors' permission.

and a flatter load curve beneath the surface. This leads to higher stresses in greater material depth, whereas the influences on the flank surface remain nearly the same. If the material strength below the surface is exceeded due to these shifted stresses, a crack can be initiated in this area. With time the crack propagation through the material may result in a gear failure sometimes referred to as "tooth internal fatigue fracture" (TIFF), tooth flank fracture or subsurface fatigue that can eventually lead to the total damage of the gear set. Such sub-surface fatigue failures were observed — even at loads below the rated allowable ones based on standard calculation procedures for pitting and bending strength. This fact indicates a different failure mechanism. There was so far basically no common understanding about the failure mechanism and its influence factors. Furthermore, due to lack of consequent investigations, there was no adequate calculation method present, so the risk of tooth flank fracture could not be quantified. For this reason, investigations in the field of subsurface fatigue were of a great importance.

In recent years extensive theoretical and experimental investigations have been conducted in order to achieve a better understanding of the failure mechanism and to isolate the decisive influence factors on the failure mode of tooth flank fracture. From the results of these investigations a calculation method was derived that allows the evaluation of the material exposure — not only at the loaded flank surface — but also in greater material depth. The model sets the in-depth shear stress, resulting from the Hertzian load on the flank surface in relation to the local material strength, which is directly derived from the local hardness profile. In this way a local material exposure for every volume element below the surface can be calculated. Based on gear geometry, operating conditions, and material properties — which also include the residual stresses as a decisive influence parameter — the risk of sub-surface fatigue failure can be determined.

Failure Mechanism of Tooth Flank Fracture

Gears with tooth flank fracture show characteristic features that differentiate them from gears that failed due to pitting, micropitting or tooth root breakage. For example, Figure 1 shows two gears that failed due to pitting and tooth root breakage, which have in common the fact that the crack was initiated at or close to the surface. Figure 2 shows two example gears — a test and a turbine gear — with tooth flank fracture. These are only two examples, among many others, showing that sub-surface fatigue failures, such as tooth flank fracture, can occur in almost every field application. Failures due to tooth flank fracture are reported in wind and steam turbines, truck gearboxes, bevel gears for heavy machinery, and test gearboxes. Typical failure mode for tooth flank fracture is that the crack initiation is normally located below the flank surface in an approximate depth of the case-core transition (Fig. 3a and b) in the active flank area. The primary crack is often initiated at non-metallic inclusions that have significantly different Young's modulus compared to the normal material structure. Such imperfections below the surface act as stress risers during the roll off of the flank because of the notch effect. If the material strength is locally exceeded, a crack with growth potential could be initiated in the material that can lead to tooth flank fracture later.

After a crack has been initiated below the surface, it slowly propagates during operation in an angle of 40° to 50° relative to the flank surface — but without direct connection to the surface. During the crack propagation a so called "fish eye" can occur due to relative microscopic movement of the cracked surfaces. The primary crack propagates from the crack starter towards the surface of the loaded flank, and into the tooth core towards the opposite tooth root section. The crack propagation rate towards the loaded flank is smaller in comparison to the core, due to the higher hardness. After the primary crack has grown enough so the tooth stiffness is reduced, secondary cracks may occur under load. A distinctive feature of these cracks is that they normally start at the flank surface and propagate parallel to the tooth tip into the material. As shown in Figure 3a) and b), after the secondary crack meets the primary one, particles from the active flank might break out. As the main crack reaches the

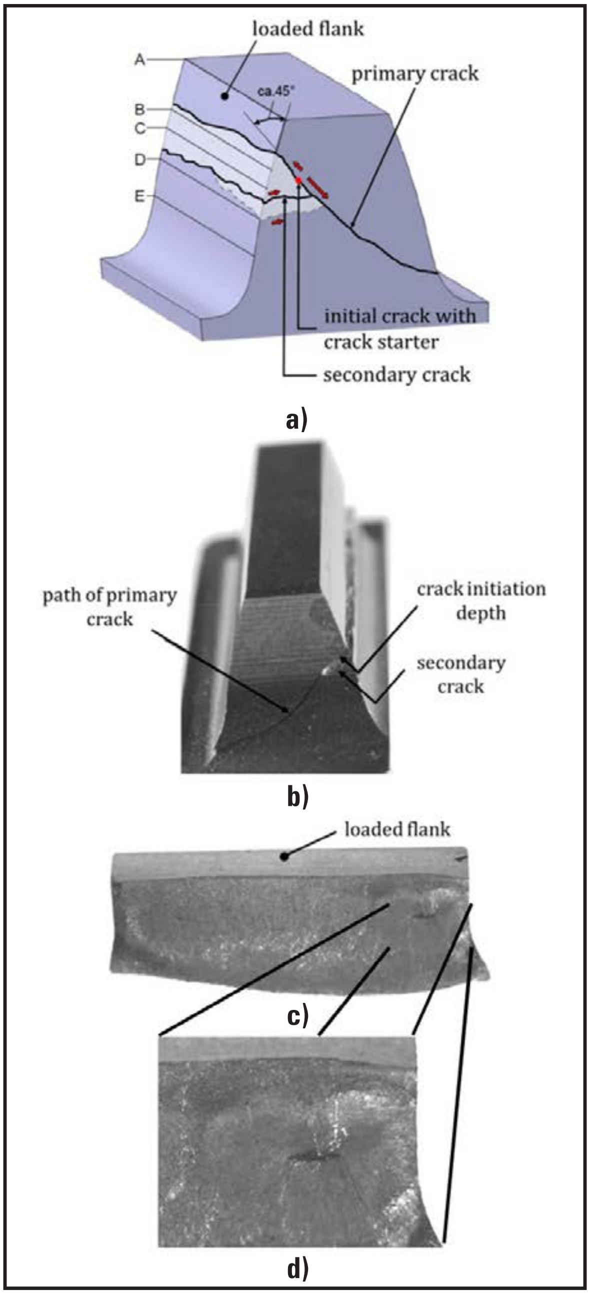

Figure 3 Characteristic features of tooth flank fracture (19)

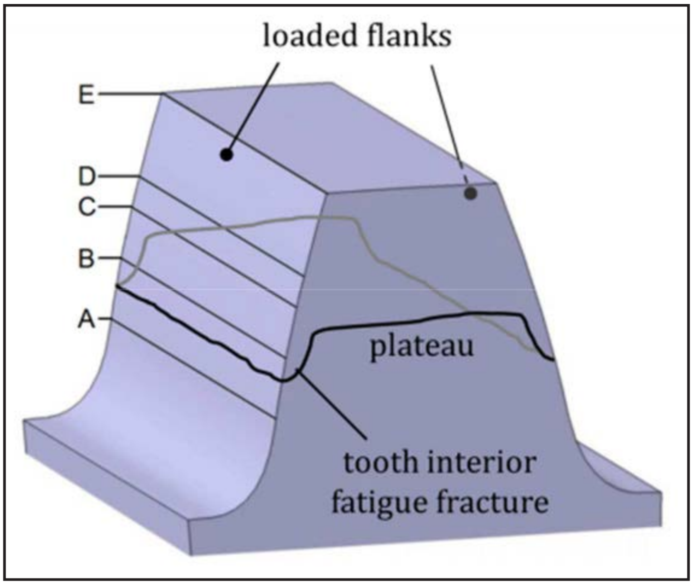

Figure 4 **Schematic visualization of tooth interior fatigue fracture (TIFF).**

loaded flank surface the remaining cross section of the tooth that carries the load is rapidly decreased. When a critical cross-section is reached, the upper tooth piece is separated from the gear. The final breakage of the tooth is due to overload breakage (Fig. 3c). On the fracture area, a typically shiny crack lens around the crack starter and a zone of rough overload breakage can be observed (Fig. 3c and 3d). Due to the given characteristics, the failure type of tooth flank fracture can be differentiated from other failure types such as tooth root breakage and tooth interior fatigue fracture (TIFF) that show a crack progression over the tooth cross-section as well. The failure type of tooth root breakage is characterized by a crack in the 30°-tangent area on the tooth root fillet. According to (Ref. 3) the load on the tooth leads to a complex, multi-axial stress condition. The bending stress in the tooth root changes over time when the load on the flank moves towards the tooth tip or the tooth root, respectively. Due to the bending moment, stresses in the tooth root cross-section are induced, which are tensile on the loaded and compressive on the unloaded flank side. These stresses have their maximum at the surface, so the risk of a crack initiation is greatest there. The two main differences between the failure modes of tooth flank and tooth root breakage are location of the failure in tooth height direction and location of the initial crack. The typical endangered area for tooth flank fracture can be found at half tooth height of the active flank, whereas tooth root breakage normally occurs below the active flank in the 30°-tangent area on the tooth fillet. Furthermore, the crack initiation of the tooth root breakage happens mostly at, or just below the surface, and not in greater material depth like the initial crack of the tooth flank fracture. The failure type of tooth interior fatigue fracture is most common on gears with alternating loads, where both tooth flanks are used to transmit torque. A characteristic feature of TIFF (Fig. 4) is that the crack propagation path runs nearly parallel to the tooth tip surface with small drops near the surface. The causes for TIFF are not only the alternating loads on both sides on the tooth, but also the tensile residual stresses in the tooth core resulting from the heat treatment. Also typical for TIFF is that the upper tooth segment is normally separated along a plateau at half tooth height.

Influence Factors on the Failure Type Tooth Flank Fracture

General stress conditions in the tooth. The induced stresses inside the loaded tooth are shown in Figure 5. Considering an ideal, smooth flank surface, the general stress condition inside the tooth is composed of following components:

- Stresses due to the normal force resulting from the transmitted torque
- Shear stresses on the flank surface due to friction
- Thermal stresses caused by the thermal gradient
- Bending stresses and shear stresses due to shear load caused by the normal force
- Residual stresses

Figure 5 shows the stress components acting in a considered element below the surface. In Figure 5a) the stress distribution due to the normal force is shown, where the contact stress can be described according to the Hertzian theory. The effects of the relative sliding between the two gear flanks are considered with the friction force. Figure 5b illustrates the bending stress distribution over the tooth cross-section. Due to the normal force, tensile stress is induced on the side of the loaded flank and compressive stress on the back flank. In comparison to the bending stress, which is nearly linear over the tooth cross-section, the stresses due to shear load can be approximated by a parabolic distribution with a maximum at the middle of the tooth. In Figure 5d the residual stresses are shown. As a result of the heat treatment, compressive stresses normally occur in the case area, and are compensated by tensile stresses in the tooth core. Unlike the stresses in 5a, b and c, the residual stresses are load-independent and constant over time if the load is not too high. The residual stresses and the load induced stresses can be superimposed if the different time dependence of the stress components is considered.

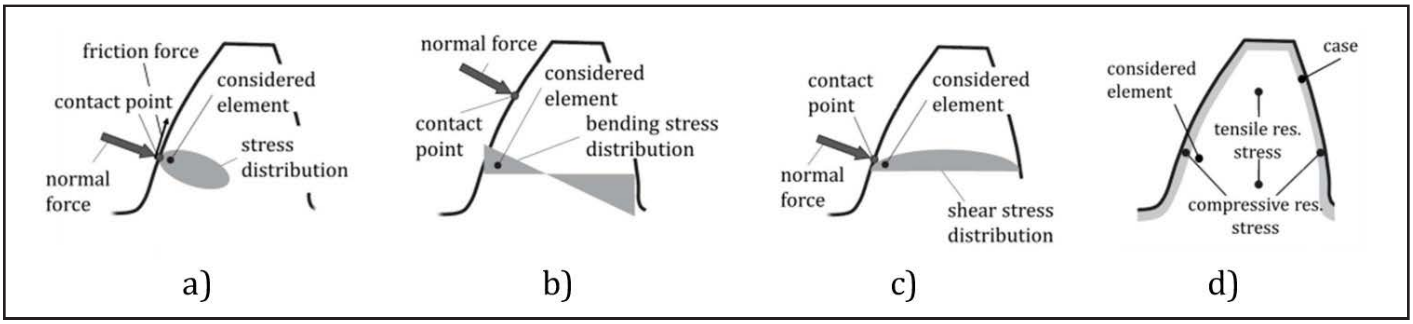

Figure 5 **Stress conditions inside the tooth (19).**

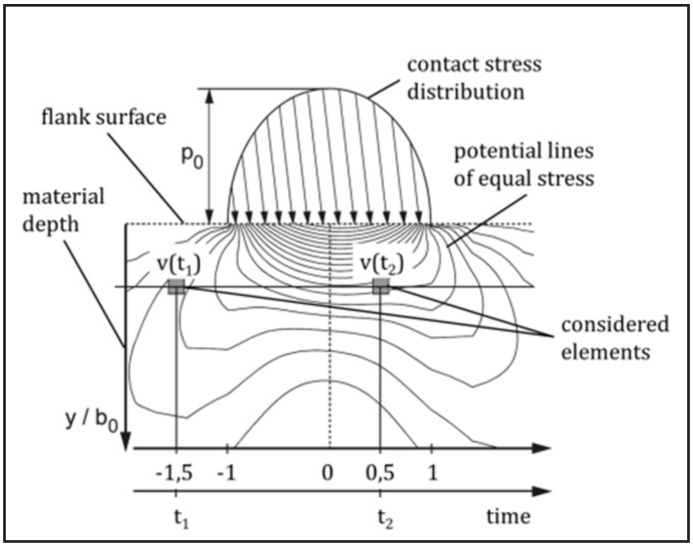

Figure 6 **Time-dependent stress in the rolling contact (7).**

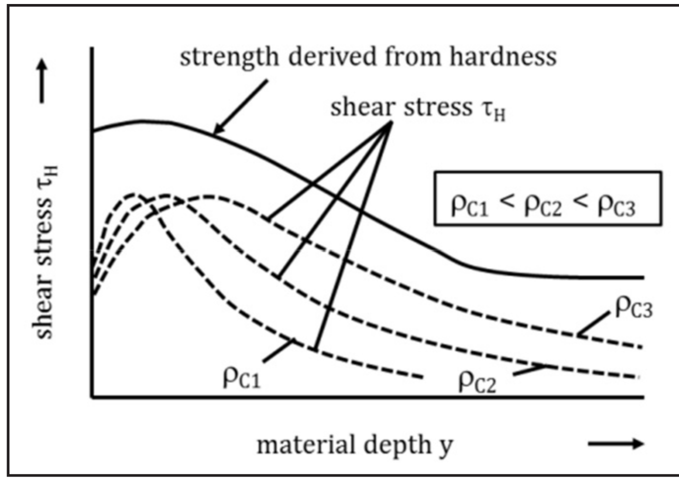

Figure 7 **Influence of the equivalent radius of curvature on the shear stress below the surface (19).**

Stress conditions in the rolling contact. On a loaded tooth flank the rolling direction × can also be seen as the time axis. For each considered element in the material the stress conditions change due to the relative motion of the mating tooth flanks. Figure 6 illustrates schematically the rolling contact with the induced stress (one component of the 3-axis stress condition) below the surface. Under the assumption of constant equivalent radius of curvature and normal force, all volume elements in the same material depth are exposed to equal stresses, but at different times during the roll-over process. Furthermore, a single volume element is subjected to different stresses at different times, so when the material exposure is calculated in a considered element below the surface, the stresses have to be considered over the whole time axis (*x*-axis). However, the difficulty in this observation is the turning of the principal coordinate system during the rolling contact, resulting in a variation of the absolute stress values as well as the direction of the principal stresses for each volume element. The stress distribution over the material depth is mainly influenced by the maximum Hertzian pressure p_0 resulting from the Hertzian contact load and the local equivalent radius of curvature ρc. As shown in Figure 7, the shear stress τ_H below the surface increases with an increasing equivalent radius of curvature ρc — even if the maximum contact pressure p_0 and maximum shear stress τ_H remain the same. Because the relative radius of curvature increases not only with increasing center distance, but also with increasing pressure angle or increasing addendum modification factor, an increased shear stress τ_H below the surface can be expected in these gear configurations. Furthermore, based on the fact that the local strength profile derived from the hardness profile remains constant, the remaining strength reserve erodes and the risk of a crack initiation below the surface increases.

Multi-axial stress conditions are commonly described by means of equivalent stresses. Theoretical investigations in (Ref. 7) have shown that many of the common equivalent stress hypotheses, such as the distortion energy hypothesis, shear stress hypothesis and alternating shear stress hypothesis, are not suitable for alternating stresses and stress conditions with a rotating principal coordinate system. In (Ref. 7) various hypotheses are discussed to their applicability for rating the material exposure in rolling contacts. In (Ref. 7) it could be shown that the so called shear stress intensity hypothesis (SIH) is applicable to loaded rolling contacts. The shear stress intensity τ_{eff} can be calculated according to Equation 1; it considers all maximum shear stresses $\tau_{\gamma\alpha}$ in each sectional plane γα of the considered volume element.

$$\tau_{eff}=\sqrt{\frac{1}{4\pi}\int_{\gamma=0}^{\pi}\int_{\alpha=0}^{2\pi}\tau_{\gamma\alpha}^{2}\sin\gamma\, d\alpha\, d\gamma} \tag{1}$$

Local material strength. Another decisive influence factor, beside the stress conditions in the rolling contact, is the local material strength limiting the load carrying capacity. Tooth flank fracture can occur if the material strength below the surface is exceeded. According to (Ref. 7) the material strength can be determined based on material-physically relations where the local strength values are calculated out of the local Vickers hardness. An alternative, simpler method is used in (Refs. 6; 12–14; 16; 19) where the material strength is assumed to be directly proportional to the local hardness. Further influences due to grain size and segregation cannot be considered by the actual state of the art.

Calculation Model

Basic formulae. A calculation model was developed at FZG to determine the risk of tooth flank fracture. The model considers different volume elements below the surface to determine the local material exposure as a comparison of the local occurring equivalent stress and the local strength that is derived from the hardness profile. Using Equation 2, the occurring local stress based on the equivalent stress according to the shear stress intensity hypothesis (SIH) can be calculated:

$$\tau_{eff,\,DA}=\tau_{eff,\,Last,\,ES}-\tau_{eff,\,ES} \tag{2}$$

Both $\tau_{eff,\,Last,\,ES}$ and $\tau_{eff,\,ES}$ can be calculated using Equation 1. However, different stress components are considered. For the calculation of $\tau_{eff,\,Last,\,ES}$ all stress components due to external loads as well as components due to residual stresses are used, whereas the determination of $\tau_{eff,\,ES}$ is done only with the quasi-static residual

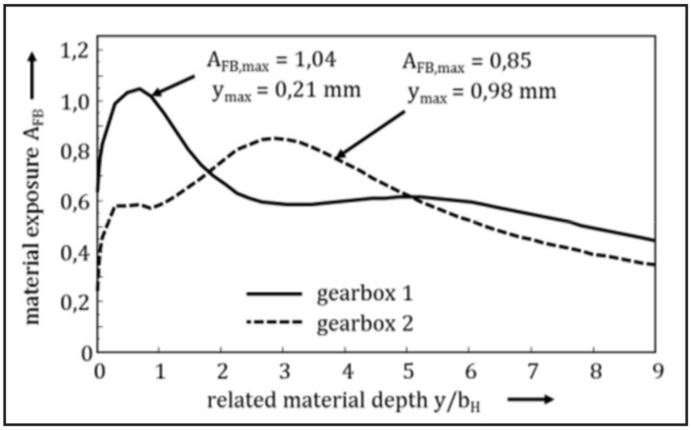

Figure 8 Comparison of the calculated material exposure curves for two example gearboxes (19).

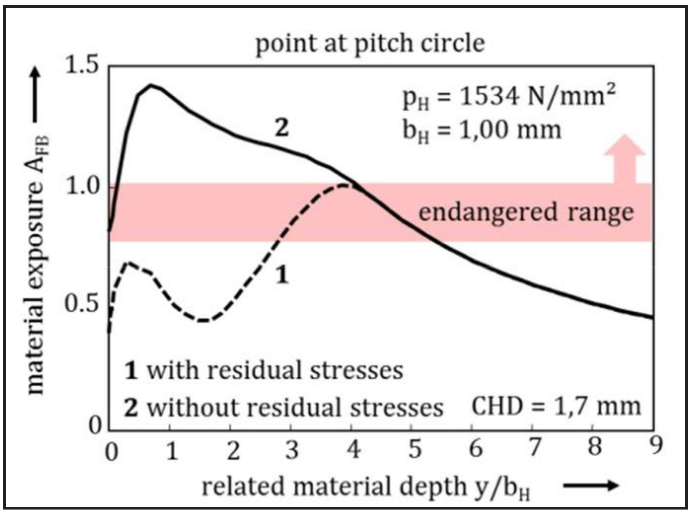

Figure 9 Material exposure curve for one contact point calculated with and without residual stresses (19).

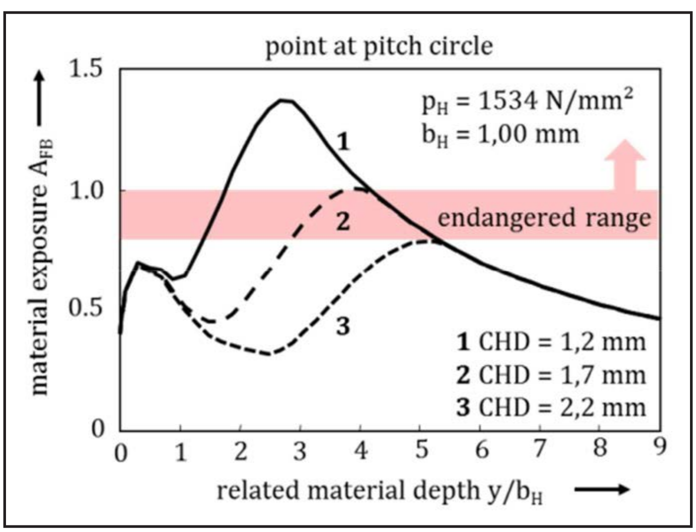

Figure 10 Influence of the CHD on the calculated material exposure (19).

stresses. Basically the decisive equivalent stress $\tau_{eff,\,DA}$ can be taken as an oscillating stress with the double amplitude (Eq. 2). For the calculation of the material exposure besides the occurring local stress, the local strength derived from the hardness profile below the surface is required:

$$\tau_{zul}(y) = K_{\tau zul} \cdot HV(y) \tag{3}$$

Although there is no generally valid relation between the permissible shear strength and the local hardness, simplified it can be assumed that the material strength, especially on case-hardened gears, is directly proportional to the local hardness. The factor describing the linear relation between the Vickers hardness and material strength has a constant value of 0.4, which was derived from gear running tests and results from industry gearboxes. This value is valid for case-carburized gears made of typical case-hardening steels and with adequate heat treatment. With $\tau_{eff,\,DA}$ and τ_{zul} the material exposure A_{FB} for each volume element below the surface can be determined according to (Ref. 19) using Equation 4:

$$A_{FB} = \frac{\tau_{eff,\,DA}}{\tau_{zul}} \tag{4}$$

With the calculation of the material exposure A_{FB} over the material depth at different points from the tooth root towards the tooth tip the risk of tooth flank fracture can be evaluated for different mesh positions considering the local equivalent radius of curvature, the local contact pressure and the local hardness. The limit for the material exposure A_{FB}, above which tooth flank fracture should be expected, was set to 0.8. This critical value was derived from gear running tests on test gears and recalculation of gearboxes from different industry applications.

Figure 8 shows the comparison of two calculated material exposure curves for two example gearboxes. The material exposure maximum $A_{FB,\,max}$ for gearbox 1 is reached near the surface, whereas the maximum exposure $A_{FB,\,max}$ for gearbox 2 can be observed in greater material depth. The location of the peak is mainly influenced by the equivalent radius of curvature, by the occurring contact loads and by the heat treatment parameters. Depending on the location of the maximum material exposure, the failure type can be predicted. High material exposure values at the surface indicate pitting whereas material exposure peaks in greater depth can be interpreted as at high risk of tooth flank fracture. Figure 9 shows a variation calculation of the material exposure for one contact point with and without consideration of the compressive residual stresses near the surface. By neglecting the compressive residual stresses in the case their positive effect on the material exposure is lost, which always leads to a maximal exposure close to the surface. By using the reduced calculation model without consideration of the residual stresses the tooth flank fracture failure, which has its initial crack in greater material depth, cannot be reproduced. This indicates a decisive influence of the residual stresses on the calculation results. Thus fatigue failures due to tooth flank fracture can only be evaluated correctly if the residual stresses are considered during the calculation. As shown in Figure 10 the reduction of the case-hardening depth (curve 1) leads to an increase of the maximum material exposure in greater material depth, whereas the local maximum near the surface remains almost unchanged. Furthermore the maximum of the material exposure shifts towards the surface. Because of the reduced CHD, the core hardness is already achieved in smaller material depth while the hardness near the surface remains the same. An increase of the CHD has the effect that the maximum value of the material exposure is decreased and shifted towards greater depth. All three curves indicate a strong influence of the case hardening depth on the maximum material exposure and its location below the surface. The local peak near the surface is not significantly changed by the CHD variation.

The presented calculation model has the following features and capabilities:

- Check if the maximum material exposure occurs near the surface of the loaded flank or in greater material depth;
- Check if the maximum material exposure is exceeded;
- Predict how deep below the surface an initial crack may occur and consequently which type of failure can be expected;
- Evaluate the risk of tooth flank fracture;

The most decisive influence factors that can be optimized in order to reduce the risk of tooth flank fracture are the gear geometry, represented by the local equivalent radius of curvature, the gear external loads, and the heat treatment.

Validation of the calculation model with test results. A number of tests with test gears especially designed to fail due to tooth flank fracture were carried out in order to prove the applicability of the calculation model, and to verify the critical value of 0.8 of the material exposure. On these test gears the failure of tooth flank fracture was dominant, as it could be reproduced repeatedly during the tests. All failed gears had a maximum material exposure in material depth which was higher than the limit of 0.8. Examinations of the fracture area showed that in almost all cases the initial crack occurred in the case-core transition at non-metallic inclusions, such as aluminum-oxides and/or manganese-sulfides, in an approximate material depth between 0.8 and 1.9 mm. Hereby, the different operating conditions and case-hardening depths of the test gears have to be considered.

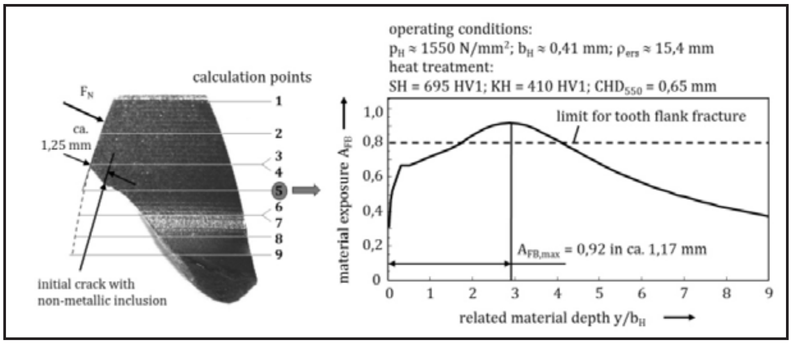

Figure 11 **Comparison of test result and calculated material exposure (example for tooth flank fracture).**

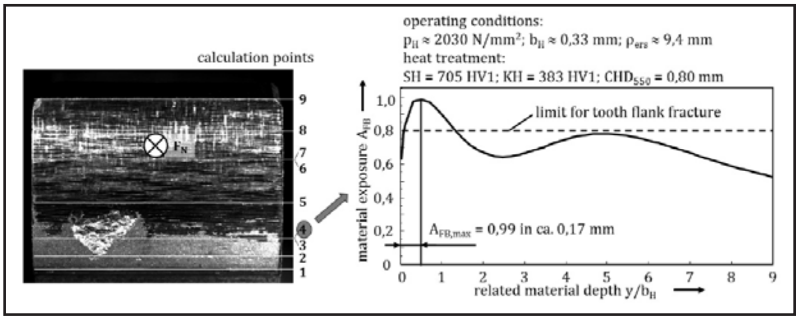

Figure 12 **Comparison of test result and calculated material exposure (example for pitting).**

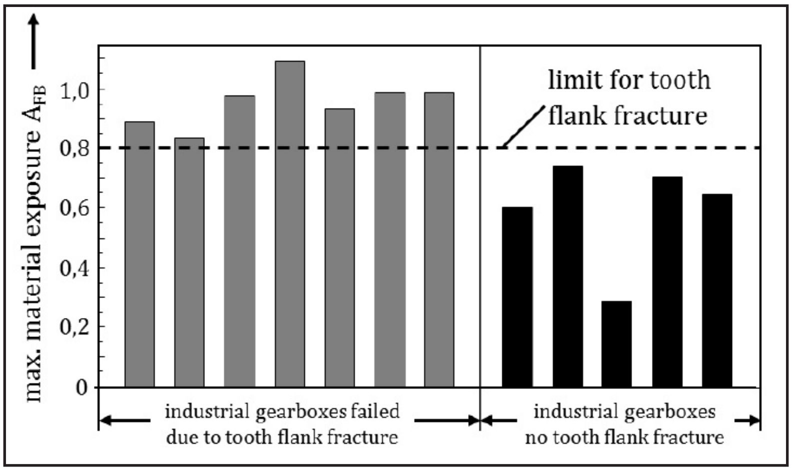

Figure 13 **Calculated maximum material exposure for different industrial applications (19).**

Figure 11 shows example comparison between test result from the gear running tests and the corresponding calculated material exposure. Because of characteristic features, the failure could be identified as tooth flank fracture (Fig. 11, left). The initial crack occurred at flank mid-height in a depth of ca. 1.25 mm below the loaded flank surface, which equals nearly twice the case hardening depth. In Figure 11, right, the calculated material exposure curve for mesh position 5 is plotted over the material depth. The maximum value of $A_{FB,\,max} = 0.92$ occurring in a depth of 1.17 mm exceeds the limit of 0.8 and therefore indicates a significant risk of tooth flank fracture. The critical material depth derived from the gear test was very well represented by the calculation as well.

For comparison, a test gear used for pitting investigations ($m_n = 5$ mm, $a = 91.5$ mm, $z_{1.2} = 17/18$) is shown in Figure 12. The pitting failure, as illustrated on the left, occurred during the test run near the tooth root at mesh position 4. The maximum material exposure of $A_{FB,\,max} = 0.99$ in this position is found just below the loaded flank surface, while the material exposure in greater material depth is slightly below the limit for tooth flank fracture of 0.8 and therefore still non-critical regarding tooth flank fracture. Consequently a good correlation between the test and the calculation results is present.

Figure 13 summarizes the results from calculation studies regarding tooth flank fracture, including gearboxes from different applications such as wind turbines, water turbines, high-speed gearboxes and roller mills. For all examined gearboxes the calculated global maximal material exposure is given. The gearboxes on the left failed due to tooth flank fracture and for all gearboxes on the right side no damage or failures due to flank breakage were reported. A good correlation can be found between the calculated maximum material exposures and the observations of the different industrial gearboxes. The comparison confirms tooth flank fracture failures when the critical value of 0.8 of the material exposure is exceeded. All other gearboxes, where no flank breakage occurred, lie beneath 0.8. In general a good applicability of the calculation method could be observed.

Conclusions

Tooth flank fracture is a sub-surface fatigue failure mode observed on case hardened gears. One characteristic feature of tooth flank fracture is that in comparison to pitting and tooth root breakage, the initial crack can be found below the loaded surface, in greater material depth. Tooth flank fracture leads in almost all cases to the complete breakdown of the gear set. Due to the fact that the crack is propagating inside the material, the failure occurs spontaneously and often without any indications. Standardized calculation methods for pitting and tooth root breakage according to ISO 6336 do not cover this kind of failure. Because of the different failure mechanism, systematic investigations and the development of a new calculation method were of a great importance. The risk of tooth flank fracture can be described with the so called material exposure, which is defined as a relation of the local equivalent shear stress and the local material strength in each volume element in material depth. One distinctive feature of tooth flank fracture is that the crack initiation is normally located below the flank surface in an approximate depth of the case-core transition due to high material exposure — mostly at stress risers like non-metallic inclusions. With time the initiated crack propagates bi-directionally towards the loaded flank and the tooth fillet of the unloaded flank. When the primary crack reaches the surface, the upper tooth part is separated within a short time due to overload breakage. Both the crack propagation and the overload breakage can be observed on the fracture area — typical for tooth flank fracture. Extensive experimental investigations have shown that the gear geometry, operating conditions, gear material and heat treatment are the decisive factors that influence the risk of tooth flank fracture. A new calculation method was developed in order to calculate the material exposure below the flank surface. It enables the evaluation of the risk of tooth flank fracture and the optimization of the gear design considering all important influence parameters. The validation of the new calculation method shows good correlation with the results from gear running tests and from industrial gear boxes. Because of the fact that tooth flank fracture is a sub-surface fatigue failure that can occur in any application of highly loaded case-hardened gears, the risk should always be considered during the gear design. The new calculation model based on the material exposure below the surface enables the prediction of tooth flank fracture and the optimization of the geometry, material and heat treatment so the risk of a failure can be reduced significantly. Although the newly developed calculation method is based on simplified approaches and assumptions, it allows the evaluation of the tooth flank fracture risk and stays in good correlation with experiences from the field. Goals of future studies are the investigation of further influence factors and their numerical quantification.

References

1. Bauer, E. "Beispiele für Verzahnungsschäden, Ausgehend von Innenliegenden Fehlstellen," *Allianz Report* 68, Heft 6, 1995, S. 230–238.
2. Bauer, E. "Flankenbrüche bei Hochleistungsgetrieben," *Allianz Report* 2, 1998, S. 79-87.
3. Bretl, N., T. Tobie and P. Oster. "Load Carrying Capacity of Nitrided Gears: Mechanical Properties, Main Influencing Factors and Critical Evaluation of the Application in Gear Transmissions," Tagung Nitrieren und Nitrocarburieren, Aachen, 2010.
4. (4) DIN 3990: Teil 1-5, Berlin, Beuth Verlag, 1987, *Tragfähigkeitsberechnung von Stirnrädern.*
5. (5) DNV: Tooth Interior Fatigue Fracture for Case Hardened Gear Wheels & Pinion, *Technical Information Newsletter* No. 01/2009.
6. (6) Elkholy, A. "Case Depth Requirements in Carburized Gears," *Wear* 88, 1983.
7. (7) Hertter, T. "Rechnerischer Festigkeitsnachweis der Ermüdungstragfähigkeit Vergüteter und Einsatzgehärteter Zahnräder," Dissertation TU München, 2003.
8. (8) ISO 6336: Calculation of Load Capacity of Spur and Helical Gears, Teil 1-5, Genf, 2003.
9. (9) Lang, O.R. "Berechnung und Auslegung induktiv gehärteter Bauteile," Berichtsband zur AWT-Tagung, Induktives Randschichthärten, Darmstadt, 1989.
10. Mack Aldener, M. "Tooth Interior Fatigue Fracture and Robustness of Gears," Dissertation KTH Stockholm, 2001.
11. Oster, P. "Beanspruchung der Zahnflanken unter Bedingungen der Elastohydrodynamik," Dissertation, TU München, 1982.
12. Pederson, R. and R.L. Rice. "Case Crushing of Carburized and Hardened Gears," *Trans. SAE*, 1961.
13. Sandberg, E. "A Calcualtion Method for Sub-Surface Fatigue," *International Symposium on Gearing and Power Transmissions*, Tokyo, Volume 1, 1981.
14. Sharma, V.K., D.H. Breen and G.H. Walter. "An Analytical Approach for Establishing Case Depth Requirements in Carburized and Hardened Gears," *Trans. of ASME*, *DETC*, Chicago, 1977.
15. Tobie, T., B.-R. Höhn and K. Stahl. "Tooth Flank Breakage — Influences on Subsurface Initiated Fatigue Failures of Case Hardened Gears," *Proceedings of the ASME 2013 International Design Engineering Technical Conferences and Computers and Information in Engineering Conference*, Oregon, 2013.
16. Tobie, T. Zur Grübchen- und Zahnfußtragfähigkeit Einsatzgehärteter Zahnräder, Einflüsse aus Einsatzhärtungstiefe, Wärmebehandlung und Fertigung bei unterschiedlicher Baugröße, Dissertation, TU München, 2001.
17. Wirth, C., B.-R. Höhn and C. Braykoff. "New Methods for the Calculation of the Load Capacity of Bevel and Hypoid Gears," AGMA Technical Paper 12FTM15, 2012.
18. Witzig, J. Entwicklung eines erweiterten Berechnungsverfahrens zur Ermittlung optimaler Zahnflankentragfähigkeit bis in den Bereich großer Werkstofftiefen, FVA Forschungsheft Nr. 1000, Frankfurt a. M.: Forschungsvereinigung Antriebstechnik e.V., 2011.
19. Witzig, J. "Flankenbruch. Eine Grenze der Zahnradtragfähigkeit in der Werkstofftiefe," Dissertation TU München, 2012.

Gear Noise Prediction in Automotive Transmissions

J. Bihr, Dr. M. Heider, Dr. M. Otto, Prof. K. Stahl, T. Kume and M. Kato

Due to increasing requirements regarding the vibrational behavior of automotive transmissions, it is necessary to develop reliable methods for noise evaluation and design optimization. Continuous research led to the development of an elaborate method for gear noise evaluation. The presented methodology enables the gear engineer to optimize the microgeometry with respect to robust manufacturing.

Nomenclature

$x_{TE}(t)$	mm	mesh deflection
F	N	mesh force in the direction of line of action
$C_{zi}(t)$	$\frac{N}{mm}$	local tooth stiffness for the contact point i at the time t
$X_{fi}(t)$	mm	deviation from the ideal involute for the contact point i at the time t
$\underline{\underline{C}}$	$\frac{Nm}{rad}$	Stiffness matrix including nonlinear gear stiffness
$\underline{\underline{M}}$	kgm^2	mass matrix
$\underline{\underline{K}}$	$\frac{Nsm}{rad}$	damping matrix
$\underline{F}$	Nm	torque vector
$\underline{X}$	m	displacement vector

Introduction

Because of success in the reduction of engine and wind noise, gear noise has become even more important. For an efficient design process, it is necessary to have calculational methods for gear noise prediction.

The main cause of gear noise is the mesh excitation resulting from the time-variant mesh stiffness and deviations from the ideal involute. Deviations are distinguished by design flank modifications and arbitrary manufacturing errors. The resulting flank topology is a complex geometry. The gear mesh excitation results in structure-borne noise from shafts, bearings and housing. Primary action to reduce gear noise is to reduce mesh excitation. A common way regarding mesh excitation is to calculate transmission error (Refs. 2, 8 and 5). A more detailed way regarding the dynamic behavior of the surrounding parts of gears is to calculate dynamic tooth force; in most of the literature only the nominal flank deviations are regarded.

At the Gear Research Center (FZG), ongoing investigation leads to a computer-based method for calculating transmission error and dynamic tooth force based on measured flank topology (Ref. 4); this method is used in a comparison with noise measurement for automotive transmissions. The presented methodology enables the gear engineer to optimize the microgeometry with respect to robust manufacturing.

Method for Gear Noise Evaluation

The fundament of all mesh calculations is the accurate calculation of mesh stiffnesses in the mesh contact. According to Weber/Banaschek (Ref. 9) and Schmidt (Ref. 7), this stiffness can be calculated based on elastic beam and plate theory. In Figure 1 the abstract models are shown. For a special mesh position at the time t the points of contact are determined in a geometrical model (Fig. 1(a)). The line of contact is discretized to several calculation points with the index i. The model is then transferred into the mechanical substitute model in Figure 1(b), where the analytical plate deformation theory can be applied to solve the problem in form of a calculational model in Figure 1(c). The result of this calculation is the local tooth stiffness $C_{zi}(t)$ for all points i on a line of contact at time t. Alternatively there are several other methods to determine the mesh stiffness (e.g. FEM (Ref. 1)), but the shown theory is well proved within more than 50 years of gear calculation and experimental testing. This theory is very fast and has been implemented in special software programs. For the assessment of the excitation behavior of gears based on the stiffness calculations, several methods are used to determine the excitation characteristics. The most important methods are the calculation of transmission error (static: $n \Rightarrow 0$) and dynamic calculations. For all these methods it is necessary to calculate the mesh condition in the full field of action with a sufficient

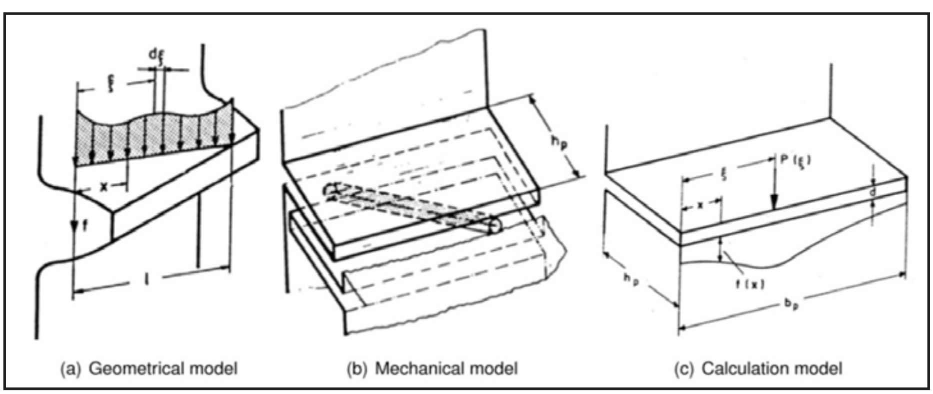

Figure 1 Models for determination of local mesh stiffnessess Czi at the contact point (*i*=1…*n*) for one special mesh position at the time *t* (acc. Weber/Banaschek (Ref. 9) and Schmidt (Ref. 7)).

This paper was originally presented at the 2014 International Gear Conference, Lyon Villeurbanne, France and is republished here with the authors' permission.

resolution. In this case we calculated with at least 18 points on the line of contact for 60 different mesh positions-per-pitch for the static calculations and with about 150 to 250 different mesh positions-per-pitch for the dynamic cases.

Static calculation of mesh excitation. The transmission error is the variation of the deflection in the path of contact between pinion and wheel under load. It is calculated under static conditions for several meshing positions ($n \Rightarrow 0$). Therefore the transmission error does not contain dynamic effects and is independent of the dynamic behavior of the surrounding system. The transmission error $x_{TE}(t)$ as shown in Equation 1 can be calculated by using the local mesh stiffnesses $C_{zi}(t)$ at the points i and all flank deviations at the points $x_{fi}(t)$. In the deviations, the flank corrections, the deviations of manufacturing and the deflection of all shafts, bearings and housing were considered.

$$x_{TE} = \frac{F - \sum_i [c_{zi}(t) \cdot x_{fi}(t)]}{\sum_i c_{zi}(t)} \tag{1}$$

Dynamic tooth force calculation. The excitation from gear mesh can be optimized by flank corrections. The influence of load on the excitation can be calculated quickly. But the dynamic behavior of the gear box also depends on the rotational speed. To consider the influence of natural vibrations in the presented methodology lumped-mass torsional vibration systems are used. Because of the nonlinear gear stiffness function the equations of motion have to be solved by numerical integration. For each integration step the gear stiffness has to be calculated and the stiffness matrix C has to be built. Equation 2 represents the system of the equations of motion. It is a system of nonlinear differential equations of the second order; the damping of the gear mesh is also calculated. According to Gerber (Ref. 6), it is dependent on center distance, oil viscosity and speed.

$$\underline{M} \cdot \underline{\ddot{x}}(t) + \underline{K} \cdot \underline{\dot{x}}(t) + \underline{C}(t) \cdot \underline{x}(t) = \underline{f} \tag{2}$$

Use of the Presented Method to Predict Gear Noise for Automotive Transmissions

Description of examined gear boxes. Two similar gearboxes have been analyzed with the aim of comparing and improving gear noise excitation. Both gearboxes (A and B) are automatic transmissions for vehicles with transverse motor configuration. One gear stage that is permanently engaged and critical in terms of mesh excitation has been analyzed in detail. Note that parts of the automated transmission, torque converter, planetary gear sets and several clutches, are not examined in this project. The power is transmitted by two stages, which are always engaged. These two stages are called counter gear stage and differential gear stage. In this project only the effect of counter gear stage is considered, as mentioned above.

Modelling of shafts, bearings and housing. For the gear noise calculation, it is important to capture the elastic environment of the gear wheels. The FVA Program *RIKOR* (Ref. 3), which provides load capacity calculations, considers the:
- shafts
- bearings
- housing

for static deformation analysis.

Among other calculation results, *RIKOR* calculates the load distribution. For the integrated bearing calculation in *RIKOR*, the geometrical data of the bearings are used (e.g., ball diameter, angle of taper, etc.). The load distribution between the rolling elements and race way in the bearing is calculated. Then the data are provided for other calculations, such as the mesh calculation used in this project.

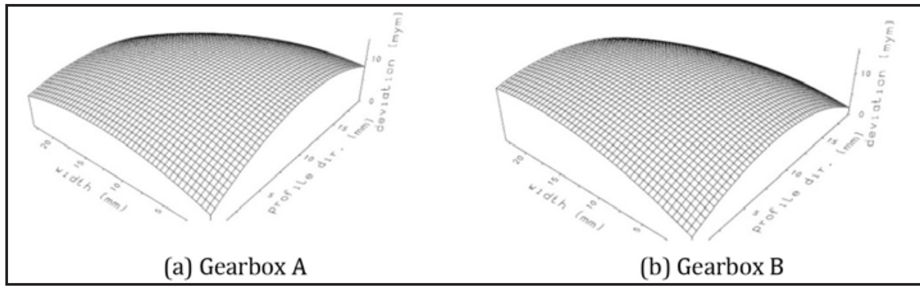

Figure 2 **Nominal microgeometry of counter drive gear.**

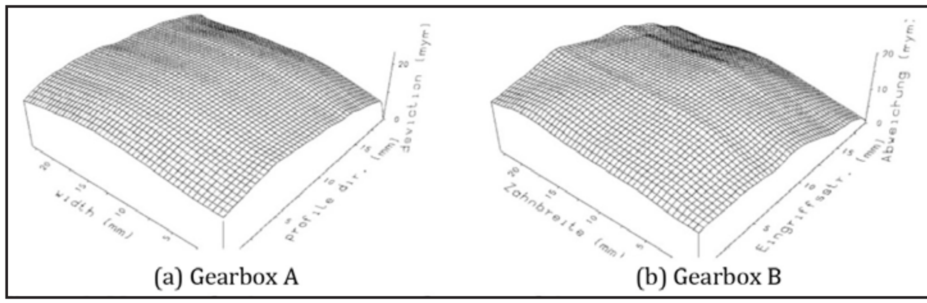

Figure 3 **Measured microgeometry of counter drive gear.**

Comparison of mesh excitation for designed and measured microgeometry — determination of microgeometry. The microgeometry is one of the most important influence parameters on vibration excitation of gears. Therefore it is necessary to model gear microgeometry as accurately as possible. Since the designed microgeometry is often not sufficient, the microgeometry has to be measured topologically. All teeth on both flanks were measured topologically with 30 points in face width direction and 30 points in tooth profile direction using a Klingelnberg P40 measuring center. This topological data was converted for use as microgeometry in the calculation program.

Figure 2 shows the designed microgeometry of the two examined drive gears. In Figure 3 the averaged microgeometry of the examined drive gear from topological measurement in the whole field of action is shown. There are some differences between the designed microgeometry and the measured microgeometry — which could influence the excitation. Since the deviation of individual teeth is even greater than the averaged microgeometry, the influence on excitation can be increased additionally.

Transmission error. The calculation of transmission error has been done for both designed and measured microgeometry; the time-dependent curves were transformed into the frequency domain. In the generated spectra the exciting characteristics of the mesh could be analyzed properly. In Figures 4 and

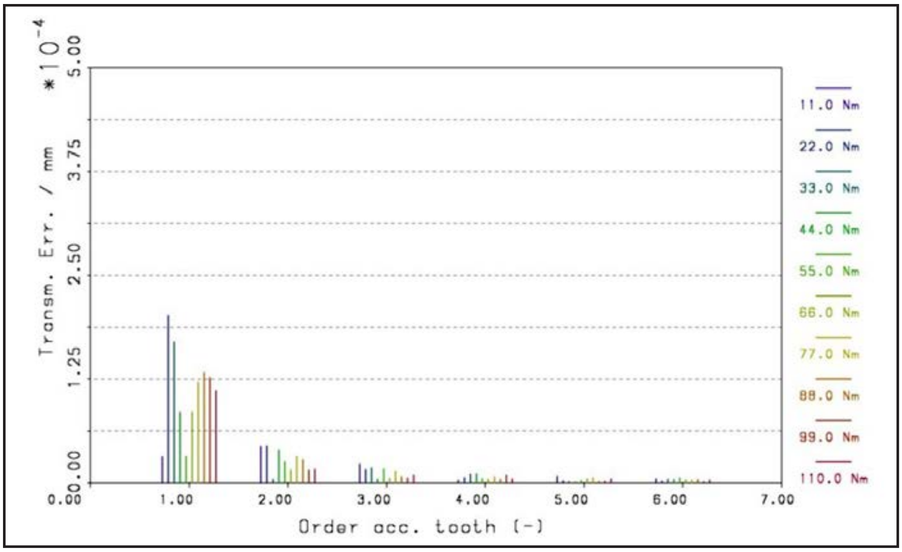

Figure 4 **Transmission error with the designed microgeometry for gearbox A counter drive stage at different load.**

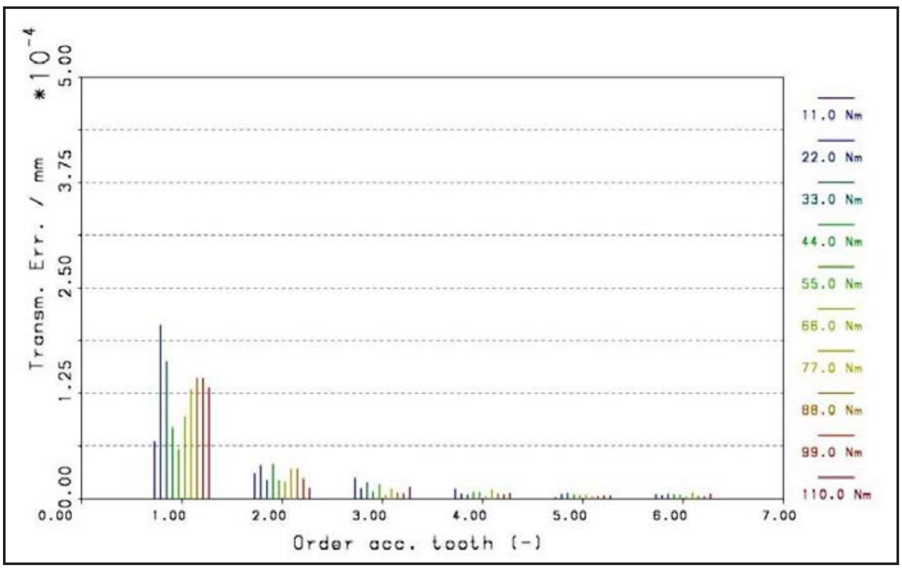

Figure 5 **Transmission error with the designed microgeometry for gearbox B counter drive-stage at different load.**

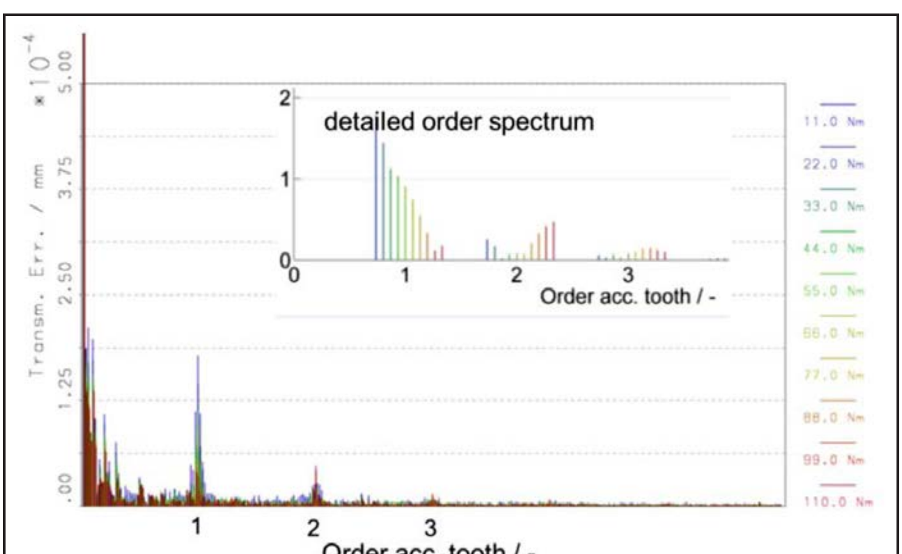

Figure 6 **Transmission error with the measured microgeometry for gearbox A counter drive-stage at different load.**

5 the results are shown for the design microgeometry. Both gearboxes show comparable exciting characteristics. The amplitudes of transmission error are very low level from 0.03 µ*m* to 0.2 µ*m* for 1st order. The results of the transmission error calculation with measured microgeometry are shown in Figures 6 and 7; the calculation was done with the individual measured flank geometry for each tooth (no averaging). Because every tooth is different in this calculation, more orders are visible — not only integer orders. Therefore in the pictures of full order spectra (Figs. 6 and 7) there is shown only the shape of amplitudes, but no development of amplitudes of TE with increasing load (different colors). For this reason the details of the spectra are displayed in Figures 6 and 7. When comparing the transmission error with designed microgeometry and measured microgeometry, there are different statements between the gearbox A and B. Regarding gearbox A, the excitation of tooth order and its harmonics decreases down to 50% of the amplitudes at design microgeometry for high loads (see Figs. 4 and 6 details). Regarding gearbox B the excitation of tooth order and its harmonics increases to 150% of the amplitudes of design microgeometry (see Figs. 5 and 7 details). The amplitudes of transmission error with amounts of around 0.1 µm are very small and the manufacturing of the real gears will change the transmission error only by 0.1 µm to 0.2 µm. But in analyzing lower frequency excitation there can be seen some additional excitation due to manufacturing errors. This additional excitation at low frequencies is typical for calculation with measured microgeometry data. In this case the amplitudes of mesh excitation for very low order increase up to 3 times the value of 1st order of mesh excitation, and even the 0.3 mesh order gets an amount of 2 times 1st order amplitude. This effect leads to the assumption that manufacturing errors probably have significant influence on excitation and will excite some frequencies that are not in tooth frequency.

Dynamic tooth force. Since the geometry of shafts for gearbox A and B are very similar, it is possible to perform dynamic calculations for both with the same dynamic model. It consists of eight rotational degrees-of-freedom. The gear mesh stiffness is calculated internally by *DZP* (Ref. 4) for every integration step. For comparison, the resonance curves of dynamic tooth force factor K_v have been calculated. The dynamic tooth force factor K_v with measured microgeometry for gearbox A is clearly lower at resonance frequency (2,400 rpm) than K_v with the designed microgeometry. Looking at gearbox B, the dynamic tooth force factor at resonance frequency is higher for the calculation with measured microgeometry in comparison to the calculation with nominal microgeometry; these results match the transmission error results.

All in all, calculation with design microgeometry shows comparable noise excitation of gearbox A and B. But regarding measured microgeometry, noise excitation of gearbox B is higher than noise excitation of gearbox A.

Noise measurement results. In the production facility, 100 gearboxes have been tested on their airborne noise behavior. Then the gearbox with the highest noise level was measured on the same test bench. The result of each type is shown in Figure 12. Gearbox A (Fig. 12(a)) has a broad frequency range of high noise behavior between 2,000 Hz and 2,500 Hz. For the gearbox B (Fig. 12(b)) there is shown a constant increasing noise behavior with higher frequency. Comparing the curves, the noise of gearbox B is ultimately higher than in gearbox A. This could be reproduced by calculations with the presented calculational method with the program *DZP* (Ref. 4). It can be shown that highly optimized design needs much effort in manufacturing because small deviations may have a big impact on noise excitation.

Conclusion

In this paper a method for gear noise prediction is presented. This method is used in a comparison between the measurement and calculation of gear noise excitation for two automotive gearboxes. After modelling the gear meshes with their nominal main and microgeometry, transmission error and dynamic tooth force were calculated. In the first step the mesh excitation of nominal and topologically measured microgeometry was compared. As a result the difference between

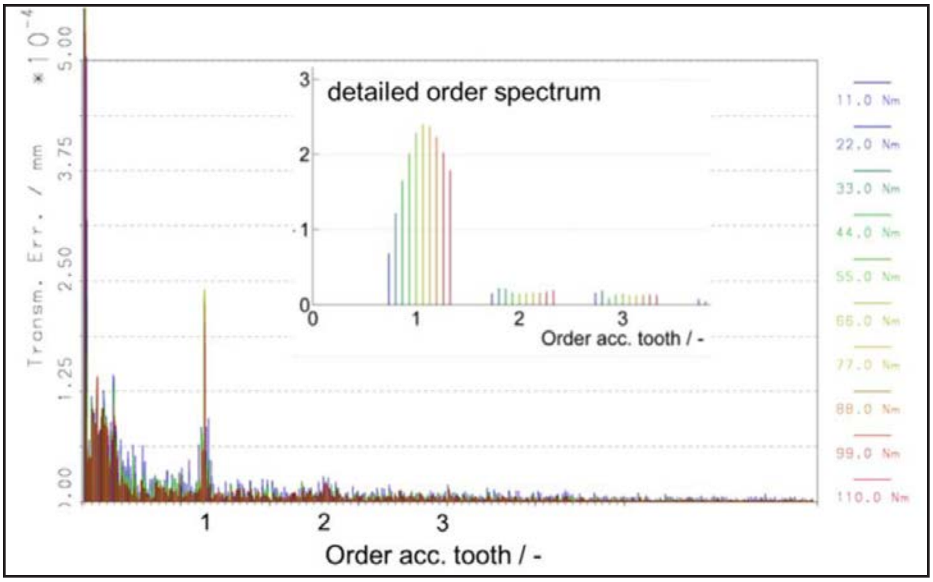

Figure 7 **Transmission error with the measured microgeometry for gearbox B counter drive-stage at different load.**

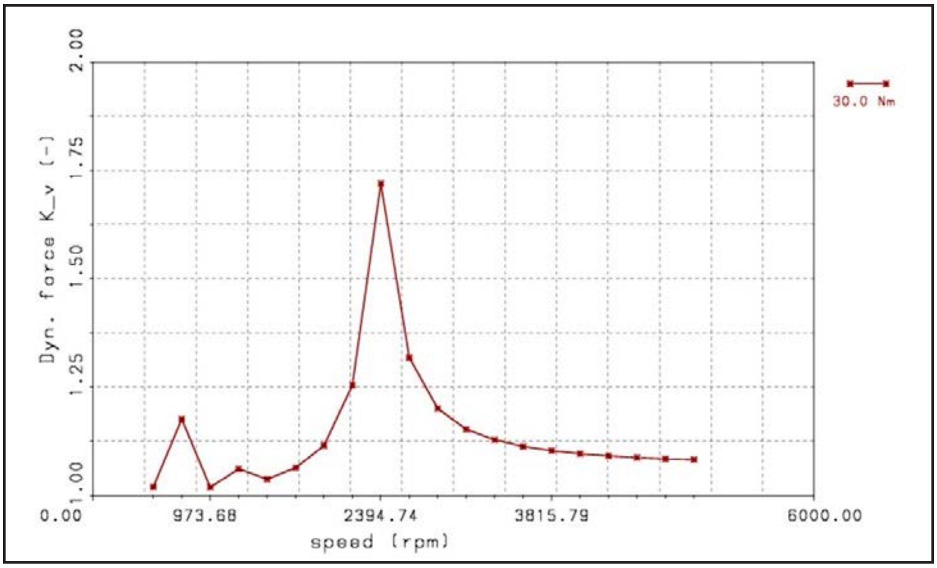

Figure 8 **Resonance curve with designed microgeometry for gearbox A.**

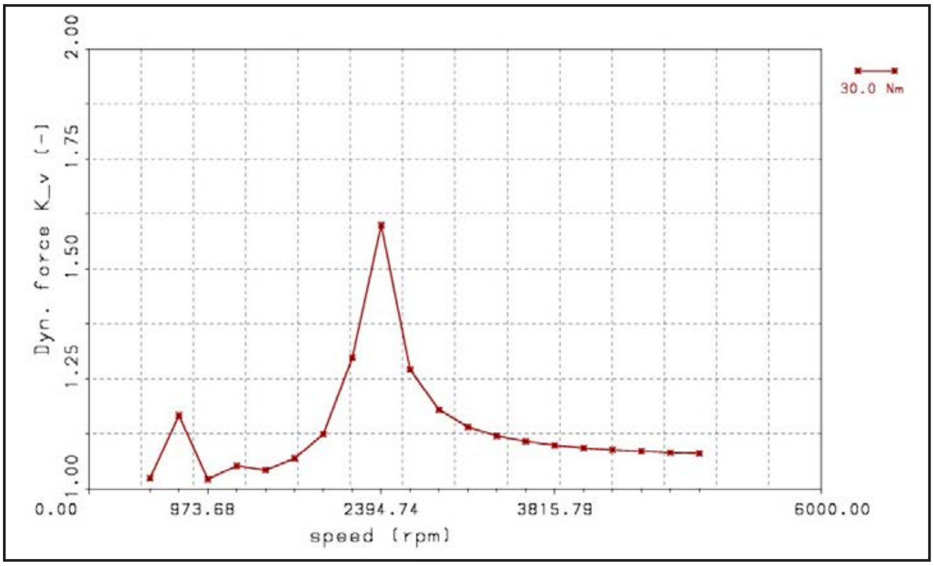

Figure 9 **Resonance curve with designed microgeometry for gearbox B.**

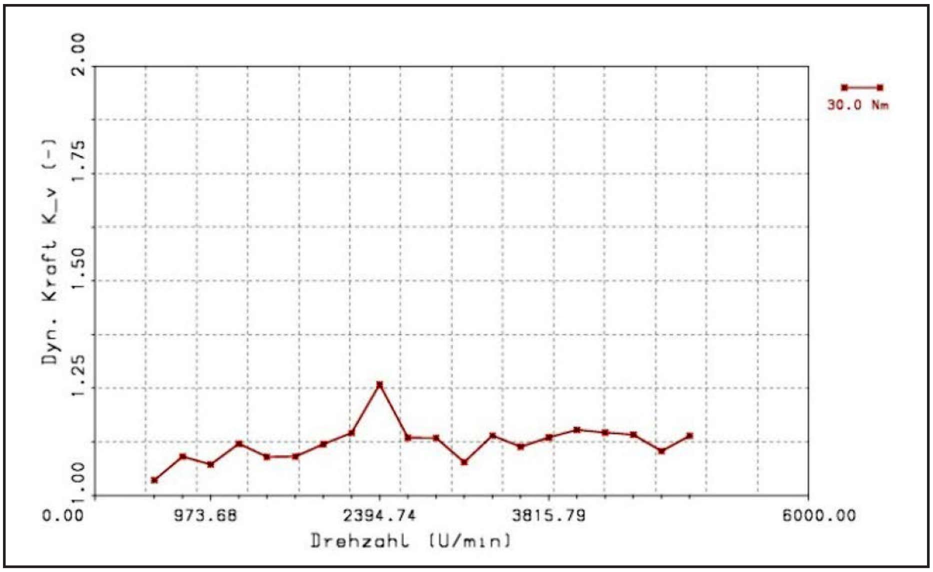

Figure 10 Resonance curve with measured microgeometry for gearbox A.

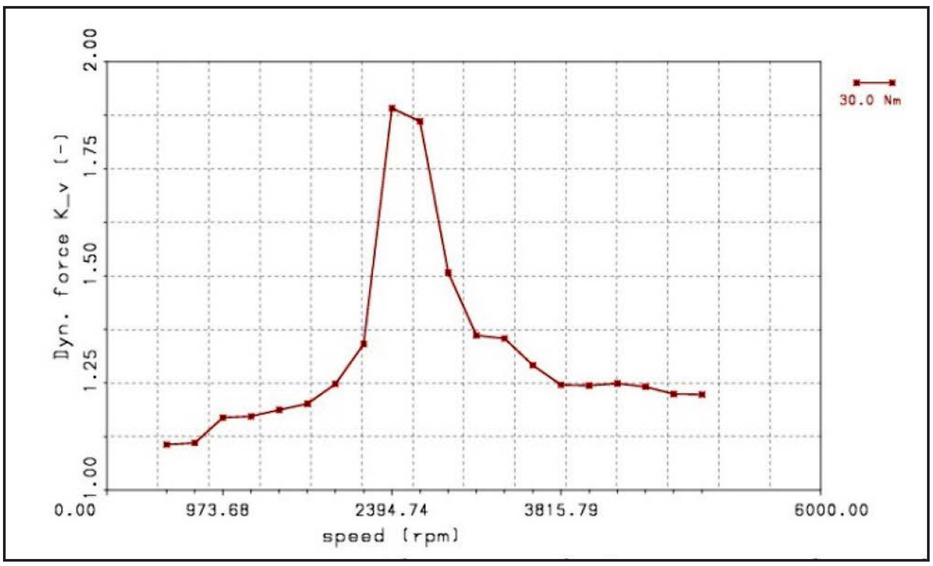

Figure 11 Resonance curve with measured microgeometry for gearbox B.

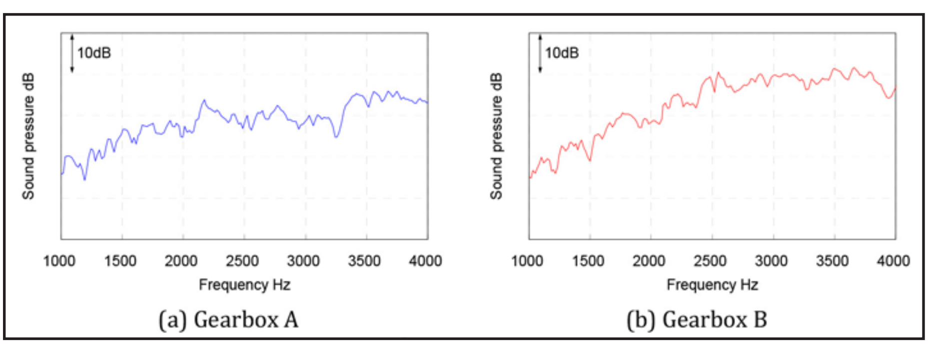

Figure 12 Noise measurement result.

nominal and measured microgeometry had a significant impact on the excitation behavior. In particular, highly optimized microgeometry design needs much effort in manufacturing because small deviations in manufacturing may result in major changes in noise excitation; noise measurement results confirmed the calculation. Additionally, the dynamic behavior of shafts, bearings and housing was addressed. The presented methodology enables the gear engineer to optimize the microgeometry of gears with respect to their robust manufacturing.

References

1. Cooley, C., R. Parker and S. Vijayakar. "An Efficient Finite Element Solution for Gear Dynamics," In: IOP Conf. Series: *Materials Science and Engineering*, DOI:10.1088/1757-899x/10/1/012150, 2010.
2. Davoli, P., C. Gorla, F. Rossa, F. Rossi and G. Boni. "Transmission Error and Noise Excitation of Spur Gears," In: *Proceedings of the ASME 2007 10th International Power Transnmisson and Gearing Conference*, Las Vegas-DETC2007-34099, 2007.
3. *Forschungsvereinigung Antriebstechnik E.V. (FVA) (Hrsg.): FVA-Heft Nr. 914: Ritzelkorrektur (Rikor), Version I. Rikor I*, 2009.
4. *Forschungsvereinigung Antriebstechnik E.V. (FVA) (Hrsg.): FVA-Heft Nr. 937: DZP, Version 5.0 und DZPopt, Version 2.0*, 2010.
5. Heider, M. "Schwingungsverhalten von Zahnradgetrieben," TU München, Diss. 2012.
6. Gerber, H. "Innere Dynamische Zusatzkräfte bei Stirnradgetrieben," TU München, Diss., 1984.
7. Schmidt, G. "Berechnung der Wälzpressung Schrägverzahnter Stirnräder unter Berücksichtigung der Lastverteilung," TU München, Diss., 1973.
8. Velex, P., J. Bruyère and D.R. Houser. "Some Analytical Results on Transmission Errors in Narrow-Faced Spur and Helical Gears — Influence of Profile Modifications," *Journal of Mechanical Design*, Vol. 133, No. 3, (March 2011), p. 11, ISSN: 1050-0472.
9. Weber, C. and K. Banaschek. "Formänderung und Profilrücknahme bei Gerad und Schrägverzahnten Rädern," Bd. 11, Schriftenreihe Antriebstechnik, Braunschweig: Vieweg Verlag, 1955.

For Related Articles Search
noise
at www.geartechnology.com

Ralf-Georg Eitel (left) and Bernd Rothenberger

DVS Group

LAUNCHES AMERICAN DIVISION

"Wherever gears, engines and drivetrains for passenger cars and commercial vehicles are produced around the world, our technicians for service, technology and sales provide support for our customers," says Bernd Rothenberger, Chief Sales Officer of the DVS Group.

"Local presence, competent communication, an understanding for custom requirements and direct access to the DVS development departments form the basis for successful collaboration," Rothenberger says.

For these reasons, the group has founded DVS Technology America Inc. in Michigan. The new company will bring together the group affiliates Buderus, Diskus, Präwema, Pittler, WMZ and Naxos to serve the automotive industry in North America.

The German DVS Group is a supplier of machine tools, automation solutions and tools for machining drivetrain components. DVS is an acronym stemming from the German words drehen (turning), verzahnen (gear cutting) and schleifen (grinding), describing the comprehensive range of know-how within the machine tool construction group.

Under the management of Ralf-Georg Eitel, the company will continue to expand its presence in North America, in cooperation with the sales and service partners already established in the United States.

Timken Company Researchers

RECEIVE 2015 WILBUR DEUTSCH MEMORIAL AWARD

Research conducted by The Timken Company to address a critical issue for wind turbine operators received the 2015 Wilbur Deutsch Memorial Award from the Society of Tribologists and Lubrication Engineers (STLE). Timken researchers used their technological expertise to solve customer problems in the wind energy sector and underscored the value of Timken wear-resistant bearings in helping to prevent smearing damage to turbine gearbox bearings.

Dr. Ryan Evans, manager of engineering fundamentals and physical testing at Timken, led a team of researchers in investigating the root cause of smearing damage to turbine gearbox bearings manufactured by various companies. It was known that lightly-loaded, high-speed shaft bearings (usually cylindrical roller bearings, or CRBs) in turbine gearboxes sometimes exhibited smearing damage in bands across various surface areas. These smeared areas can be initiation points for much more severe damage over the service life of a bearing.

The specific bearing assembly dynamics that caused the smearing were not well understood, and other researchers had been unable to reproduce the damage on full-size CRBs in a laboratory.

"It took us a few months and some creative test-rig settings and instrumentation to determine how to generate the smearing damage. In addition, we recognized the importance and value of measuring key bearing dynamic attributes like cage slip in real time," Evans said. "We took it a step further and were able to model the test conditions using the Timken CAGEDYN dynamic model, which led to a proposed 'smearing criterion' that can be used to assess smearing risk in other bearings and

dynamic situations.

"As that was the only way we could reproduce the damage in a laboratory, others outside Timken increasingly point to the same mechanism as an explanation for not only smearing, but other types of bearing damage in real wind turbines."

Comet Solutions

PARTNERS WITH BRIAN WILSON

Comet Solutions, Inc. recently announced a partnership with **Brian Wilson** of Advanced Drivetrain Engineering & Technology (ADET). This partnership is expected to strengthen Comet's commitment to providing solutions to designers and manufacturers of transmissions, axles, industrial gearboxes, and other power transmission products.

Wilson brings to Comet over 25 years of experience in the design, testing and analysis of rotating machinery. His experience includes Romax Technology, Inc. where he served as chief technology officer, Ford Motor Company where he held the position of NVH technical specialist and work as a consultant for SDRC (now Siemens PLM). He currently serves as vice-chair on the AGMA Sound & Vibration Committee and sits on ASME's Power and Transmission Gearing Committee.

Wilson will focus on expanding the market for Comet's existing drivetrain-related SimApps and guiding Comet product line expansion in order to broaden coverage of drivetrain engineering. In addition, the partnership delivers technical support and service for Comet customers to receive the most impact from their investment in Comet.

"We are excited that Brian will join our team and add his credentials to Comet's list of expert resources," said Dan Meyer, Comet Solution president and CEO. "Leveraging Brian's CAE software, test systems, and consulting expertise further advances Comet's commitment to deliver innovation within practical applications. Brian is a natural fit for our organization and vision, and we look forward to the many benefits he brings to our growing customer base."

"Comet is emerging as a key player within the world of simulation-led new product development," Wilson added. "After a thorough investigation of Comet's unique approach to CAE engineering, it was apparent to me that we share a common interest of putting advanced tools and technology in the hands of designers and analysts. I am excited to add my experience with that of Comet to further automate and streamline drivetrain-development processes."

Joel Radner

NAMED SALES MANAGER OF SECO'S ROUND TOOL DIVISION

Seco Tools, LLC recently named **Joel Radner** sales manager for its round tools division in North America. Radner brings more than seven years of Seco experience to the position, having previously served as the company's market segment specialist for aerospace and power generation.

In his new role, Radner will be responsible for all North American sales activities as they pertain to the company's solid round tool product offerings, which include items from the Jabro and Niagara Cutter lines.

His primary directives involve establishing realistic sales goals, maximizing sales revenues and managing sales personnel — all while following "The Seco Way," principles that guide how the company applies global resources to help customers overcome unique machining challenges.

Radner began his Seco career in April 2008, as a technical specialist responsible for the application and sale of indexable solid carbide cutting tools in the Northeastern portion of the United States.

According to Mike Parker, director of national sales for Seco Tools, LLC, Radner's proven performance record along with his industry expertise will allow Seco to continue moving forward with its aggressive market share growth plan.

"Joel has always been a valued member of the Seco team," said Parker. "He easily identifies with our customers and has a successful track record when it comes to establishing win-win relationships. I am confident he will put us in the best possible position to better serve our customers and take our round tool sales to the next level."

Roger Jones

RECEIVES 2015 HTS GEORGE H. BODEEN HEAT TREATING ACHIEVEMENT AWARD

Roger Jones, corporate president of Solar Atmospheres, Inc., Souderton, PA, was recently named the recipient of the 2015 George H. Bodeen Heat Treating Achievement Award.

Established in 1996, the award recognizes distinguished and significant contributions to the field of heat treating through leadership, management, or engineering development of substantial commercial impact. Jones was recognized "for advancing the thermal processing industry through technological developments in fixturing materials, methods, and the application of partial pressure atmospheres in vacuum furnaces for ferrous, stainless steels, and brass alloys."

After graduating from Hocking Technical College, Jones joined ABAR Corp. in 1975. In 1978, he joined Vacuum Furnace Systems Corp., founded by his father William R. Jones, FASM. In 1983, he helped found Solar Atmospheres, Inc., serving as vice president. He became president in 1993 and became corporate president in 2001. He has been a member of the Metal Treating Institute since 1983, serving on the Board of Trustees (1998-2004, and 2009-present), and as president (2004-2005).

Roger has been a member of the ASM Philadelphia Liberty Bell Chapter since 1983, and served as chapter chair from 1993-1994. He was chair of the ASM Heat Treating Society (HTS) Immediate Needs Committee and the HTS Education Committee, served on the Nominating Committee for two terms, and is a member of the HTS Technology & Programming Committee. He was elected to the HTS Board in 2005, served as vice president (2011-2013) and is the current president of HTS. He received the chapter's William Hunt Eisenman Award in 2001 and Distinguished Service Award in 2004. Under his leadership, Solar Atmospheres received the chapter's "Outstanding Company Support Award" in 1996 and 2006.

The Bodeen award will be presented at the HTS General Membership Meeting on Oct. 21, at the ASM Heat Treating Society Conference and Exposition in Detroit.

Gary Hulian

NAMED EMCO MAIER/MECOF PRESIDENT

EMCO Maier/EMCO Mecof Corporation (Novi, MI) recently named **Gary Hulihan** its new president, according to Dr. Stefan Hansch, EMCO Group CEO.

Hulihan has held key positions with German-based machinery manufacturers including EMAG, Ex-Cell-O and Eldec.

Hulihan said the chief company goal is to continue the EMCO Maier/Mecof tradition of serving their customers with cost-effective manufacturing solutions and world class service support. EMCO Maier/Mecof has supplied CNC milling, turning and multitasking machines for a wide span of industries, including educational, die/mold, mechanical components, automotive, aerospace, medical, hydraulic, power generation and more.

"We have a solid core group of highly competent associates and dealers and we will continue to work hard to exceed the expectations of our customers with the highest quality machine tools and professional competence in applications engineering and service," Hulihan said.

Scott Shea

NAMED NEW CHIEF OPERATING OFFICER OF CRP INDUSTRIES

CRP Industries Inc. recently named **Scott Shea** its new chief operating officer (COO). Daniel N. Schildge, CEO of CRP Industries Inc., noted that this was a newly created executive role in the company. As COO, Shea will be responsible for supply chain management, operations, the CRP Industrial Group and CRP de Mexico.

"We are positioning CRP Industries for long term growth and the potential for integrating future business opportunities," Schildge said. "Scott Shea will play a key role in helping us to not only continue the momentum that we have built here at CRP, but also help us to achieve our goals for growth and expansion. Scott brings us a wealth of experience and expertise in leading high performing, medium-size companies serving mass market and independent retailers, wholesale distributors, and end users."

Shea comes to CRP Industries after serving as the chief operating officer for Astriva, LLC since 2010. Prior to that, Shea worked for CSS Industries, Inc., serving as the divisional president for Berwick Offray, LLC. Before joining CSS Industries, Shea spent 14 years at E.I. DuPont where he held several management and engineering positions.

Shea holds a B.S. in mechanical engineering from Michigan State University. Shea is also a current member of the Board of Trustees for the Berwick Hospital Center (Berwick, PA) and the Berwick YMCA (Berwick, PA).

ABB Robotics

TO BECOME FIRST GLOBAL INDUSTRIAL ROBOTICS COMPANY TO MANUFACTURE ROBOTS IN THE UNITED STATES

ABB recently announced that it is to start producing robots in the United States, making it the first global industrial robotics company to fully commit and invest in a North American robotics manufacturing footprint. The company made the announcement at the opening of a new robotics plant at its facility in Auburn Hills, MI. Production is to commence immediately.

The new plant is ABB's third robotics production facility, alongside Shanghai, China, and Västerås, Sweden, and will manufacture ABB robots and related equipment for the North American market.

The United States is ABB's largest market with $7.5 billion in sales. The company has invested more than $10 billion in local R&D, capital expenditure and acquisitions since 2010, taking local employment from 11,500 to 26,300.

August 10-12—MPIF's Basic PM Short Course Penn Stater Conference Center Hotel, State College, PA. This intensive 3-day course is designed especially for you, if you are starting out in the field and looking for an introduction to powder metallurgy (PM); updating your knowledge of recent developments in PM; seeking to expand your current knowledge of the PM industry; a user of PM parts or are considering PM. This course is designed for engineers, tool designers, metallurgists, supervisors and technicians. For more information, visit *www.mpif.org*.

September 13-15—TECHINDIA 2015 Bombay Exhibition Centre, Mumbai, India. TECHINDIA will be the ultimate facilitator for b2b cooperation between manufacturers and consumers of all hues connected to the engineering, machinery and manufacturing industry. This leading business event is co-located with five other industry events to make it an extended platform for metal, engineering, manufacturing and machine tools industry: World of Metal – International Exhibition on Metal Producing, Metal Processing and Metal Working Industry; CWE – International Exhibition on Cutting and Welding Equipment; IMEX – International Exhibition on Machine Tools and Engineering Products; UMEX – International Exhibition on Used Machineries; Hand Tools and Fasteners Expo – International Exhibition on Hand Tools and Fasteners. The co-location of industry events will maximize business opportunities for industry professionals. For more information, visit *techindiaexpo.com*.

September 21-23—Gear Failure Analysis Big Sky Resort, Big Sky, MT. Explore gear failure analysis in this hands-on seminar where students not only see slides of failed gears but can hold and examine those same field samples close up. Experience the use of microscope and take your own contact pattern from field samples. Cost is $1,600 for members and $2,100 for non-members. For more information, visit *www.agma.org.*

September 29-October 1—2015 Gear Manufacturing Seminar Hyatt Regency, Rochester, NY. This seminar provides the gear design engineer with a broad understanding of the methods used to manufacture and inspect gears and how the resultant information can be applied and interpreted in the design process. Following this seminar, participants will be able to identify methods of manufacturing external and internal spur, single and double helical, and bevel and worm gears, describe the methodology ad underlying theory for basic manufacture and inspection of each, and much more. Cost is $1,430 for member and $1,930 for non-members. For more information, visit *www.agma.org*.

October 4-7—Euro PM2015 Congress & Exhibition Reims Congress Centre, Reims, France. Europe's annual powder metallurgy congress and exhibition, organized and sponsored by the European Powder Metallurgy Association, will return to France in 2015. The combination of a world class technical program and state-of-the art exhibition will provide the ideal networking opportunity for suppliers, producers and end-users. The program of plenary and keynote addresses, oral and poster presentations and special interest seminars will focus on: additive manufacturing; hard materials and diamond tools; hot isostatic pressing; new materials and applications; and more. Alongside the technical sessions the Euro PM2015 Exhibition will be an excellent opportunity for international suppliers to the PM industry to network with new and existing customers from the powder metallurgy and associated sectors. For more information, visit *www.europm2015.com*.

October 7-8—Design & Manufacturing Philadelphia Pennsylvania Convention Center, Philadelphia, PA. As the United States' first major industrial city, Philadelphia continues to grow into a leading design and manufacturing hub across a wide variety of industries. With manufactured goods exports increasing twice as fast as the overall stateSeconomy, accounting for 87.8% of all state total exports, now is the time to bring everyone within this community to one dedicated design and manufacturing event to spark new ideas and partnerships. See the newest technologies, equipment, products, and services and get real time answers to your questions from industry experts. The educational offerings bring you the latest in manufacturing trends and applications with comprehensive full day conferences across both days of Design & Manufacturing Philadelphia. For more information, visit *www.dmphilly.designnews.com*.

October 20-22—Gear Expo 2015 Cobo Center, Detroit, MI. Gear Expo was recognized by Trade Show Executive magazine as one the 50 fastest-growing shows in 2013. For more than two decades, power transmission professionals—including CEOs, owners, presidents, engineers, marketing and sales managers, consultants and other executives have come to Gear Expo to learn the latest industry information and see firsthand technology, products, and services that help them expand and streamline their business. Attendees represent a variety of industries including off-highway, industrial applications, automotive, and oil and gas as well as aerospace, agriculture and construction. They come from around the United States, international manufacturing hubs, and emerging markets to conduct profitable business transactions and collaborate on the innovations that make their operations more streamlined. Exhibitors have the opportunity to meet face-to-face with attendees. For more information, visit *www.gearexpo.com*.

October 27-29—Modern Furnace Brazing School Brazing Engineering Center, Wall Colmonoy Aerobraze Division, Cincinnati, OH. The late Robert Peaslee's tradition continues with the return of the brazing school. The Brazing Engineering Center provides engineering services and training, as well as offering new practical experience on the shop floor. For over 60 years, Wall Colmonoy engineers have gained practical experience on actual problems in brazing plants around the world. Knowledge and practical application will be taught by industry-leading brazing experts. In 1950, Peaslee developed the first nickel-based brazing filler metal, Nicrobraz. Modern Furnace Brazing School will allow you to apply workable solutions to your brazing needs. For more information or to register, contact *brazingschool@wallcolmonoy.com*.

October 27-29—Discover 2015 Florence, KY. Mazak Corporation encourages those involved in the metalworking industry to attend its Discover 2015 technology and education event. Here, the machine tool builder plans to spotlight new technologies and trends that will change how part manufacturers operate, including unconventional ways to drive operational efficiency via additive manufacturing, CNC technology and the Industrial Internet of Things (IIoT) concept. Additive manufacturing is creating a shift in the way engineers and designers think about product development, and Mazak is leading the way with its additive-capable Integrex i-400AM. The Hybrid Multi-Tasking machine will make its North American debut at Discover 2015. For more information, visit *www.MazakUSA.com/DISCOVER2015*.

ad index

CORRECTION

In the July issue of *Gear Technology* we incorrectly attributed a photo of a batch furnace on page 34 of the article "Don't Get Burned" to Applied Process, Inc. The photo should have been attributed to AFC Holcroft. *Gear Technology* regrets this error.

CORRECTION

In the July issue feature, "New Transmissions Make the Grass Greener," the company name — Ricardo Incorporated — was mistakenly listed. *Gear Technology* sincerely regrets the error.


QUALITY CUSTOM GEARING!
Documented
Quality Control Program
Inspection Lab
including Complete
Gear Tooth Diagnostics
Tooth Cutting, Grinding & Shaving Services Available
All Sizes & Configurations
• Reverse Engineering
• Design Analysis
• Complete Machine Shop Including CNC Machining
CIRCLE GEAR CO
Circle Gear and Machine
Quality Custom Gearing Since 1951
1501 South 55th Ct. • Cicero, IL 60804
Ph: 708-652-1000 • Fax: 708-652-1100
Please email your inquiries to sales@circlegear.com • www.circlegear.com


Dry Lube Coating
• WS_2
• MoS_2
• PTFE
Call on MicroSurface
for unbeatable prices!
CALL: (408) 723-0700
info@ws2coating.com
MICRO SURFACE
CORPORATION


PHOENIX
TOOL & THREAD GRINDING
• CNC External Thread Grinding Specialists
• Emergency Service Available
• Any thread form
• Any lead
• Multiple starts
4760 Briar Rd, Cleveland, OH 44135
Phone: 216-433-7008 Fax: 216-433-7067
Phoenixgrinding@gmail.com
www.PhoenixThreadGrinding.com

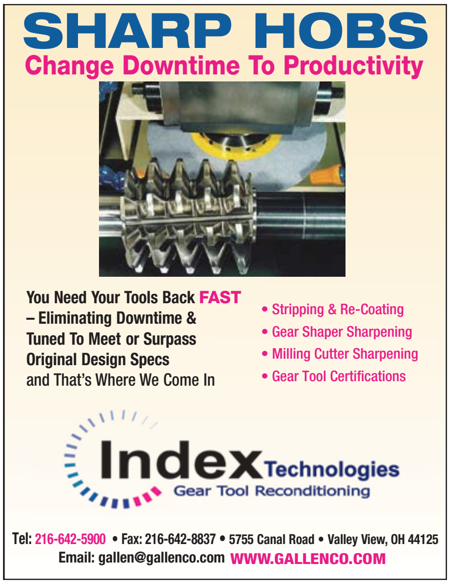
SHARP HOBS
Change Downtime To Productivity
You Need Your Tools Back FAST
– Eliminating Downtime &
Tuned To Meet or Surpass
Original Design Specs
and That's Where We Come In
• Stripping & Re-Coating
• Gear Shaper Sharpening
• Milling Cutter Sharpening
• Gear Tool Certifications
Index Technologies
Gear Tool Reconditioning
Tel: 216-642-5900 • Fax: 216-642-8837 • 5755 Canal Road • Valley View, OH 44125
Email: gallen@gallenco.com WWW.GALLENCO.COM


Sharpening Service
for hobs, milling cutters, shaper cutters,
shaving cutters and broaches
Service locations in:
• Hoffman Estates, IL
Tel: 847.649.1450 Fax: 847.649.0112
• East Tawas, MI
Tel: 989.362.0414 Fax: 989.362.2720
• Querétaro, México
Tel: 52 442 217 34 45
Fax: 52 442 217 34 46
Star SU
sales@star-su.com
www.star-su.com


For the Highest Quality
Gear Heat Treating
The Endocarb System from
The Heavy Carbon Co. LLC
• Carburize 30% Faster
• 50% Less energy
• Retrofit on existing furnace
Effective case depth
Standard Carburizing
140 hours = .263 ECD
Endocarb
100 hours = .262 ECD
See for yourself and send us your
gears to test!
See us at the ASM Heat Treat
Detroit Show – Booth 114
Co-located with Gear Expo
www.HeavyCarbon.com
Heavycarbon@frontiernet.net


KORO for Quality
Hob Sharpening Service
♦ Quick Turnaround 2 Day Service
♦ Spur Shaper Cutter Sharpening
♦ HSS & Carbide Hob with center hole
and straight flutes
♦ Thin Film Coatings
♦ Length up to 7 inches
♦ Diameter up
to 5 Inches
♦ Precise rake
and spacing guaranteed
to AGMA standards
♦ RUSH SERVICE AVAILABLE
Koro Sharpening Service
9530 85th Ave North
Maple Grove, MN 55369
763-425-5247
info@koroind.com

A GEAR IS A GEAR IS A GEAR, EXCEPT WHEN IT ISN'T

ALEX CANNELLA

Copper mace head, 200 B.C - A.D. 200, from the Vicus culture of Peru. Photo courtesy of the Metropolitan Museum of Art (Bequest of Jane Costello Goldberg, from the Collection of Arnold I. Goldberg, 1986).

Look at that picture right over there on the right. That's one of the Bronze Wheels of Peru. Looks like a gear, doesn't it? If you knew nothing about it or the culture it sprang from and just happened to see it on the street, you'd probably label it as such. So many people have had that same thought, in fact, that the set has picked up another name: the Bronze Gears of Peru.

Here's the thing: they aren't gears. Despite appearances, the Bronze Wheels of Peru are actually mace heads.

Much like with our own modern culture, everything is connected to everything in the ancient civilizations archaeologists study. The issue, and the reason that myths like these "gears" pop up, is that the archaeologists know enough to put those connections together, while the laymen just look at the Bronze Wheels and dub them gears.

Here's where things get even dicier. If the Bronze Wheels were, in fact, gears, they would be what people call an "out-of-place artifact." Out-of-place artifacts are basically archaeological "finds" that, according to the years of study and evidence that forms our understanding of conventional archaeology, just plain shouldn't exist. The Bronze Wheels of Peru, for example, were created in a time and place where gears aren't recorded existing.

The problem is that out-of-place artifacts aren't exactly scientific. They're basically fodder for every conceivable form of pseudoscience and conspiracy theory you can think of, from aliens giving us technology in ancient times to the actual, literal existence (or rather, former existence) of Atlantis. The reason many out-of-place artifacts "shouldn't exist" isn't because we've never found any of them before, but because there's a wealth of evidence actively pointing out that, in fact, they shouldn't. Often, these artifacts are touted about as incredible new discoveries that will revolutionize our view of an entire culture, but the reason they go against the grain is usually because one person screwed up and made a faulty leap of logic rather than because all of generally accepted archaeology is wrong.

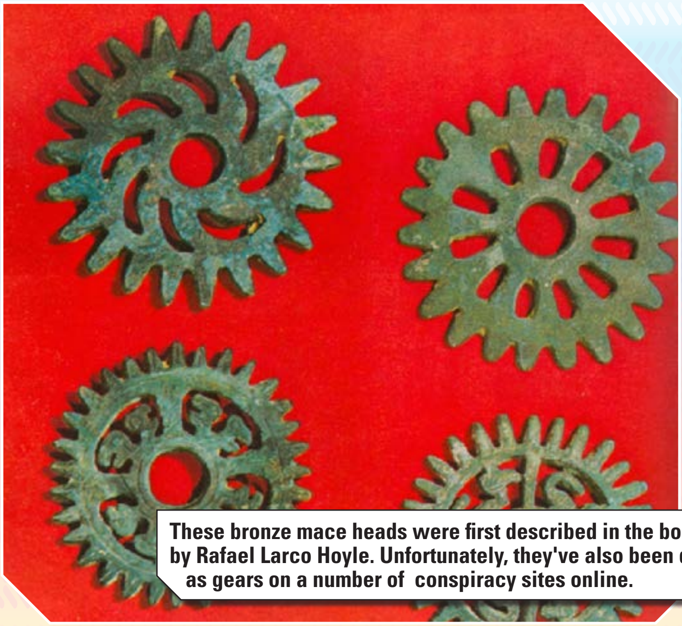

These bronze mace heads were first described in the book *Peru*, by Rafael Larco Hoyle. Unfortunately, they've also been described as gears on a number of conspiracy sites online.

People sensationalize and cling to these artifacts for the same reason that sci-fi in almost every form of media loves to drop the line "Einstein was wrong!" It's exciting! It fundamentally changes something about the way the world works! And unless you dig deeper than that enthusiastic Facebook post, it makes perfect sense! When looking at the logic behind the Bronze Wheels of Peru and other out of place artifacts as a wholly insular bubble, it holds up solely because there's nothing to contradict it.

In the Bronze Wheels' case, yes, they look like gears. This is how archaeologists and regular people alike jump to incorrect conclusions. But remember: In archaeology, as with any other culture, everything informs everything, and in the case of the Bronze Wheels, everything else points to a different explanation.

Everywhere the Bronze Wheels are referred to as gears, the name Rafael Larco Hoyle also comes up. Hoyle was a professor and museum curator who lived in the 20th century. His book, "*Peru*," is one of the first sources to ever mention the Wheels. The only problem with conspiracy theorists that name drop Hoyle is that he has never, at any point, referred to them as gears. In fact, he states in his book that they are mace heads belonging to the pre-Columbian Vicus culture, putting him in agreement with conventional archaeologists.

The moral of the story? Don't trust everything you find on the Internet, and always dig a little deeper than just a single post. Otherwise, you might get caught up in a conspiracy theory about aliens giving us gears.